Local-Scale Drivers of Spatial Patterns and Demographic Rates of Conifer Species in a Forest Chronosequence in Coastal British Columbia

by

Kaitlyn Dawn Schurmann

A thesis submitted in partial fulfillment of the requirements for the degree of

Master of Science

in

Conservation Biology

Department of Renewable Resources
University of Alberta

Abstract

Growth, mortality and recruitment are the fundamental demographic processes driving changes in forest structure and dynamics. Rapid changes observed in many forests globally have imposed serious threats to ecosystem services such as carbon sequestration, biodiversity and hydrology, emphasizing the importance of understanding the underlying mechanisms. In this thesis, I collected spatial and inventory data from five 1-hectare forest plots in a chronosequence on southern Vancouver Island, B.C. I used spatial point pattern analysis and regression modeling to determine the effects of competition and climate on tree spatial patterns and demographic rates of Douglas fir, western hemlock and western redcedar over a 17-year census period. Douglas fir growth and mortality were strongly influenced by negative density-dependent (competition) processes in all plots of the chronosequence with the species becoming more regularly distributed in older stands. Western hemlock and western redcedar growth was negatively influenced by competition, while facilitative processes may promote tree survival of these two shade-tolerant species in most stands. Recruitment of all three species occurred most often in close proximity to adult trees. Growth of the study species was also driven by tree size and climate. Summer precipitation was the most important climate variable, negatively affecting growth for all study species. Other temperature and precipitation variables were significant for the focal species, but the direction of the growth response was not consistent. Species-specific responses to climate highlight the difficultly in predicting stand-level changes under altered climate regimes. The results of this study underscore the importance of competition and climate in driving forest structure and dynamics in all ages of stands, necessitating the inclusion of both sets of variables in analyzing demographic rates. Knowledge of competition and climate as drivers of forest dynamics and structure can be incorporated into forestry and conservation management decision-making, and findings from this study provide a better understanding of the processes driving dynamics of forest succession, and can be used for anticipating stand structure in the future.

Acknowledgements

I would like to thank my supervisor, Dr. Fangliang He, for the opportunity to be a member of his lab group, and for the expertise and advice that supported me through my master's program. Thank you for the opportunity to travel to Guangzhou, China for the experience of attending a working group meeting and for the privilege of completing my research on beautiful Vancouver Island.

I would like to thank my committee member, Dr. Phil Comeau, for his knowledge of forest ecology and silviculture, and suggestions and feedback in directing my research. I would also like to thank Dr. Tony Trofymow for advising and supporting my fieldwork financially and logistically, providing additional guidance throughout my studies, and acting as the external examiner.

This project would not have been possible without funding provided by NSERC and Alberta Innovates research grants awarded to Dr. Fangliang He, and funding from the Canadian Forest Service supporting field and lab work. I would also like to acknowledge the Capital Regional District of Victoria for providing additional financial support and study site access for this project.

I am very grateful for the enthusiastic help of my field assistants, Liane Brooks and Matthew Rempel, for making fieldwork both efficient and entertaining, and Shannah Beattie, for her patience and scrutiny with data quality and compilation. I would especially like to thank my mom, Tracy Schurmann, for volunteering as a field assistant and helping me with last minute data collection. I also would like to recognize all the members of the Biodiversity and Landscape Monitoring research group for their support and advice throughout my study period.

A final and special thank you goes to my parents, Roy and Tracy Schurmann, and the rest of my family and friends for their constant encouragement, understanding, and moral support throughout my studies.

Tables of Contents

List of Tables

List of Figures

Chapter 1: Introduction

1.1 Trends in global forest change

Forests worldwide have undergone substantial changes over the last several decades, bringing attention to the future wellbeing and productivity of forest ecosystems. Growth, recruitment and mortality are the fundamental demographic processes driving forest dynamics and are the key to understanding forest change. Much recent evidence has shown that the three demographic rates are changing rapidly in relation to climate. For example, growth rates in tropical and boreal forests were found to have decreased due to changing regional climates (Feeley et al., 2007; Ma et al., 2012). Mortality has also been rising in forests of the Pacific Northwest and boreal regions, again related to altered climate regimes (van Mantgem and Stephenson, 2009; Peng et al., 2011). Further still, drought was found to increase mortality and decrease growth rates in tree recruits in Malaysian forests (Delissio and Primack, 2003).

These climate-driven changes have been widely appreciated and their consequences are well recognized including the alteration of forest structure and disruption of ecosystem functioning and ecosystem services, such as carbon sequestration, productivity, biodiversity maintenance and regional hydrology (Dale et al., 2001; Schroter et al., 2005; Lindner et al., 2010). As important as the effects of climate are, however, the structure, dynamics and functions of forests could also change over the course of succession as driven by endogenous processes such as competition. In this thesis, I study decadal changes in structure and demographics of a forest in coastal British Columbia in order to understand the roles of climate and competition in driving forest changes. This introductory chapter will review studies on structure and dynamics of British Columbia's coastal forests and outline the chapters of the thesis.

1.2 Structure, dynamics and driving forces in coastal forests of British Columbia

Coastal British Columbia is home to temperate, coniferous rainforests that are highly productive and long-lived, making them the most productive forest ecosystems in Canada (Pojar et al., 1991a). These forests also form spectacular architectures with heights reaching as tall as 100 meters and are dominated by a range of single-species and mixed-coniferous

stands. The structure and dynamics of these forests are primarily governed by the coastal climate and the interactions of the long-lived constituent species. In classifying the biogeoclimatic zones of British Columbia, regional climate and soil characteristics are used to differentiate climax ecosystems. Zones are further characterized based on moisture, temperature and continentality, to infer the associated vegetation sub-communities (Pojar et al., 1991b). This classification of biogeoclimatic zones highlights the importance of climate in determining the dynamics of forest ecosystems in British Columbia, and suggests that changes in climate could greatly affect the dynamics and species compositions. Changes to demographic rates due to climate have already been documented in the western United States where van Mantgem and Stephenson (2009) found large-scale increases in mortality rates over the last half-century were related to rising annual temperatures and climatic water deficits. Long-term declines of long-lived yellow cedar (*Cupressus nootkatensis* D. Don) stands have also been reported in Alaska and British Columbia caused by warmer winter temperatures and reduced snowfall (Hennon et al., 2005; Beier et al., 2008). These documented changes in mortality and growth patterns may result in shifts in forest size and age structures, and new community compositions that could lead to altered successional trajectories (Anderegg et al., 2013). Further, tree species distributions are expected to change in response to climate change. Predictions suggest several conifer species in British Columbia may experience decreases in suitable habitat, while southern species may maintain the range size but experience range shifts to the north (Hamann and Wang, 2006). The change in distribution of suitable habitat will have impacts on tree growth and mortality, as well as cause reductions in successful recruitment at the southern limit and edges of a species' range (Hamann and Wang, 2006). Additional secondary effects on hydrological processes (e.g., water purification and groundwater recharge) and nutrient cycling are expected as a result of altered structure and dynamics due to climate pressures (Anderegg et al., 2013). A major concern related to climate change is the impact on forest productivity and timber production. Forests on British Colombia's coast have among the highest mean annual temperatures and highest annual precipitation of all of Canada's ecosystems (Klinka et al., 1991), making them unique in their high productivity. Reduced growth rates and increased mortality due to altered temperature and precipitation regimes will have impacts on biomass production and carbon sequestration, and cause a reduction of merchantable timber volume (Spittlehouse, 2003).

It is widely known that exogenous processes such as climate are not the only factors driving forest structure and dynamics, and that endogenous processes, specifically

competition, are also important. Competition between individuals for resources such as light, water and nutrients is fundamental in driving succession and assembling species composition. Limited access to resources puts individuals at risk for reduced growth and increased mortality (Begon et al., 1996). Intraspecific competition is thought to play a large role in the dynamics and spatial structure of shade-intolerant pioneer species (Peet and Christensen, 1987; Whitmore, 1989). Following disturbance, pioneer species often establish at high densities and compete for resources among conspecific trees resulting in stand self-thinning and the species becoming more regularly distributed over time (Kenkel, 1988; He and Duncan, 2000). Interspecific competition, on the other hand, is important for the dynamics and establishment of late-successional species. Supressed growth and reduced survival of late-successional, shade-tolerant species in the understory is largely the result of a closed canopy and competition for limited resources with pioneer trees and understory vegetation (Brandeis et al., 2001). As a result of interspecific competition, tree recruitment and growth rates are often highest in canopy gaps formed by the mortality of overstory pioneer trees where resources are more abundant, resulting in spatial aggregation of shade-tolerant species (Moeur, 1997; Stan and Daniels, 2010).

The successional pathway of forests on southern Vancouver Island is well developed. Forests historically regenerated following stand-clearing forest fires, however, recent disturbance is more often dominated by timber harvesting. The progression from post-disturbance landscapes to an old-growth forests occurs over >150 years (Trofymow et al., 2003) and competition plays a large role in driving the succession. Natural recovery from stand-clearing disturbances occurs over several decades beginning with red alder (*Alnus rubra* Bong.) and Douglas fir (*Pseudotsuga menziesii* var. *menziesii* [Mirb.] Franco) recolonizing the landscape. Red alder is a fast-growing but short-lived species, initially competing with Douglas fir seedlings and eventually replaced by a dense stand of Douglas fir trees (Shainsky and Radosevich, 1992). Intraspecific competition between Douglas fir trees leads to stand self-thinning, a reduction in stand density, and promotes the establishment and growth of late-successional species, western hemlock (*Tsuga heterophylla* [Raf.] Sarg.) and western redcedar (*Thuja plicata* Donn ex D. Don), in the understory. As stands transition to mature and older stages, overstory tree mortality caused by competition, biotic agents (e.g., insects and disease) or wind damage results in the further release of late-successional trees into the canopy, and the eventual development of a climax community dominated by large western hemlock trees (Franklin and Hemstrom, 1981). The changes in species composition throughout succession are accompanied by

altered stand structure and dynamics (Fig. 1.1). Immature forests are typically dominated by structurally homogenous, single species stands undergoing a phase of rapid growth. As stands age, tree size increases and density-dependent processes create openings for the establishment of understory species resulting in vertical and horizontal heterogeneity (Spies and Franklin, 1991; DellaSala et al., 2011). Old-growth forests have been found to maintain higher structural heterogeneity and gap formation than second-growth stands (Trofymow et al., 2003), providing habitat for wildlife and contributing to biodiversity and ecosystem services (Franklin et al., 2002).

The unique structure and dynamics of forests at different seral stages highlights the necessity of understanding the mechanisms that bring about the observed forest patterns. However, studying drivers of forest structure and dynamics throughout succession requires data collection from a single stand as it transitions through the stages of succession. In the case of forests on coastal British Columbia, this transition occurs over the period of several centuries. Collection of this type of long-term data is difficult and unrealistic; therefore, a chronosequence approach with three stand ages was used in this thesis. Previous studies have used this approach to approximate stand conditions throughout succession and to infer the drivers of forest structure and dynamics (Milton et al., 1994; Getzin et al., 2006; Gray and He, 2009).

Successional pathways and the role of climate on stand dynamics and structure have been well described for the British Columbia coast region. Despite these studies, there has been a lack of understanding of the role of competition in driving forest change through succession. One difficultly in assessing the importance of competition is a lack of spatial data required for modeling competitive effects on growth and mortality. Fine spatial detail over large spatial scales is required to study changing structure and spatial patterns, and to accurately quantify the effect of competition on demographic rates (Rayburn et al., 2011). The effects of competition on stand structure and dynamics also occur over long periods of time, requiring long-term data with multiple censuses that are often not available. While the overall importance of competition has been widely recognized, the influence of density-dependent processes at older successional stages is less well understood, with some recent studies discounting endogenous processes in old-growth stands under the assumption that competition is important in young stands only (van Mantgem and Stephenson, 2009). However, other studies have shown both endogenous and exogenous processes continue to be important late in succession (Fraver et al., 2014; Lutz et al., 2014), highlighting the need to analyze competition and climate, and their interactions, to understand the full suite of

mechanisms driving forest structure and dynamics through succession. This thesis attempts to fill some of the research gaps by studying forest spatial structure and demographic rates of three dominant species in relation to competition and climate through three successional stages in forests on Vancouver Island, British Columbia.

Figure 1.1. Representative images of forest structure through stages in succession. Complexity and heterogeneity of vertical structure increases from immature (top left), mature (top right), to old-growth (bottom left) forest stands.

1.3 Thesis objectives and outline

The objective of this study was to determine the importance and effect of climate and competition on forest structure and dynamics throughout succession on three dominant conifer species, Douglas fir, western hemlock and western redcedar, in coastal British Columbia. The body of this thesis contains two separate data analyses. In Chapter 2, I used spatial point pattern statistics to analyse the change in tree distribution over time to detect spatial associations of the three tree species and to infer density-dependent processes acting on tree mortality and recruitment, as is evident through the change in stand spatial patterns over time. In Chapter 3, I quantified the effects of potential drivers, particularly competition and climate, on individual tree growth and mortality using nonlinear regression models and logistic regression models, respectively. Combining the two analyses, this thesis will contribute to further understanding the mechanisms underlying the structure and dynamics of forest succession in coastal British Columbia. Knowledge on the drivers of species' spatial distributions and demographics can be incorporated into forestry and conservation management decision-making and used for interpreting and anticipating stand dynamics in the future.

Chapter 2: Spatial Patterns and Density-Dependent Effects on Tree Mortality and Recruitment in a Forest Chronosequence on Vancouver Island

2.1 Introduction

Quantifying changes in forest structure across space and time is important for understanding the endogenous and exogenous processes underlying forest dynamics. Spatial pattern analysis has been widely used to infer such processes. One of the major types of data for spatial pattern analysis is completely mapped forest plots with the x- and y-coordinates for every tree being located (Mateu et al., 1998). Such data are necessary for quantifying spatial distribution of trees (aggregated, random or regular distribution) and for detecting the possible working processes resulting in changes of forest stands.

Tree distribution (forest structure) does not only change over space but also over time. Ecological mechanisms can be detected by comparing the spatial pattern of a stand across multiple censuses and across successional stages to understand how processes are working across stands of different ages. Naturally regenerated young forests show a tendency towards aggregation due to seed dispersal limitations and strong filtering of heterogeneous habitats. As a forest stand develops, pioneer species tends to become more regularly distributed through competition and density-dependent mortality (Stoyan and Penttinen, 2000). For example, Duncan (1991) found tree mortality resulted in a shift from aggregation to regularity in conifer stands in New Zealand. Similar results were found in British Columbia where Douglas fir shifted from aggregated to random with successional age (Getzin et al., 2006).

Much empirical evidence has shown that density-dependent effects are a major force regulating spatial patterns of tree distribution (Duncan, 1991; Lutz et al., 2013; Larson et al., 2015). Density-dependence includes both intraspecific and interspecific interactions. Intraspecific competition is thought to play a larger role in young stands than in older stands (Peet and Christensen, 1987) due to the higher conspecific density and less differentiated stand structure that is characteristic of young stands compared to mature stands. At the immature stage, shade-intolerant pioneer species undergo strong self-thinning resulting in significant growth reduction and mortality (Weiner, 1984; Kenkel et al., 1997). In contrast, interspecific competition and disturbances (e.g., insect and disease infection, wind damage and aging) are often found to dominate the dynamics of mature

stands (Franklin et al., 2002). The operation of these different processes on stands of different ages is certain to leave spatial signatures, with intraspecific competition driving conspecific patterns toward regularity and interspecific competition toward heterospecific segregation. An important method for detecting spatial patterns driven by competition and other ecological mechanisms is to compare observed tree mortality with random mortality. Under random mortality, each tree is assumed to have an equal probability of mortality, regardless of neighbourhood density, and as a result, spatial patterns of trees would remain the same before and after mortality events. Differing from random mortality, if trees experiencing higher intraspecific competition have a higher mortality risk, the species would be expected to become more regularly distributed (Sterner et al., 1986). However, studies have found that not all mortalities in forests are resultant of density-dependent processes. For example, various spatial patterns can occur from density-independent mortality (Larson et al., 2015), density-dependent mortality (He and Duncan, 2000) or aggregated ingrowth (Lutz et al., 2014). These variations highlight the complexity of tree distributions and the driving processes.

In addition to mortality, recruitment can also greatly contribute to spatial patterning. Colonization and establishment patterns vary by species due to species-specific resource requirements and growth strategies. Species-specific characteristics such as seed dispersal, vegetative reproduction and shade-tolerance can directly affect the pattern and success of recruitment (Clark et al., 1998; Hille Ris Lambers and Clark, 2003; Gray et al., 2012). Tree establishment in closed-canopy forests is often aggregated due to these characteristics. It is obvious that mortality and recruitment jointly affect spatial distribution of species and in some circumstances these two demographic processes can offset each other leading to no net change in overall tree distribution (Lutz et al., 2014) and misleading inferences about the mechanisms driving tree recruitment and mortality. Separating spatial patterns attributable to individual demographic processes is necessary for understanding the relative importance of mortality and recruitment in the formation of forest structure.

In addition to conspecific spatial patterns, demographic processes can also significantly mediate spatial associations between species. Interspecific competition can lead to spatial dispersion between species as competing species are often limited by similar requirements for resources such as light and soil nutrients. It has been observed that late-successional, shade-tolerant species have highest survival when dispersed away from large pioneer trees, resulting in a negative spatial distribution between species (Veblen et al., 1980; Taylor and Zisheng, 1988). However, other possible drivers of interspecific dispersion

have been suggested, including habitat heterogeneity (Pielou, 1961) and niche specialization (Getzin et al., 2006). In contrast to interspecific competition that drives spatial dispersion of species, similar resource requirements by interacting species could actually lead to positive associations between them. For example, black spruce (*Picea mariana* [Mill.] B.S.P.) and tamarack (*Larix laricina* [Du Roi] K. Koch) prefer wet, lowland habitats and coexist on moist peatlands in the boreal region of Canada (Nicholson, 1995; Islam and Macdonald, 2004), and species of *Acer* in Japan have shown habitat associations for steep and convex slopes related to preferences for dry conditions (Torimaru et al., 2013). Additionally, other process such as nursing effects, mutualistic symbiosis, and species herd protection could also lead to positive species associations. Lan et al. (2012) found evidence of species herd protection through altering microenvironments which explained the high incidence of positive species association observed in a tropical rainforest in Xishuangbanna, China. It is clear that heterospecific patterns of species distributions are affected by two contrasting processes: competitive exclusion drives species to segregate while environmental filtering attracts species of similar resource requirements. Positive or negative associations between species could occur depending on which mechanisms dominate the interaction, and heterospecific spatial patterns could be useful for interpreting these acting mechanisms.

This chapter aims to study the change in spatial distribution of tree species over a period of 17 years in a BC coastal forest to infer the possible mechanisms underlying the change. The specific objectives of this study were to (i) determine how the spatial pattern of tree distribution changed over time and across stands of different ages, and (ii) analyze the relative importance of intraspecific and interspecific competition in determining tree mortality and recruitment and spatial patterns of conspecific and heterospecific trees. This study is expected to contribute to understanding the change in spatial patterns over succession and the mechanisms that may regulate mortality, growth and recruitment at different stand ages.

2.2 Data and Methods

2.2.1 Study Site Description

The study plots are located within or adjacent to the Greater Victoria Water Supply Area on southeast Vancouver Island (48°38′, 123°43′, Fig. 2.1). Positioned on the leeward side of the south Vancouver Island ranges, the study is within the Coastal Western Hemlock zone, Very Dry Maritime subzone of British Columbia's biogeoclimatic zone classification

(Klinka et al., 1991). This area had a mean annual temperature of 8.7°C and mean annual rainfall of 1624 mm during the study period. The mild climate is characterized by dry, warm summers and wet winters. The forest is dominated by shade-intolerant, pioneer species Douglas fir with shade-tolerant Western Hemlock and Western redcedar as late-successional colonizers. Other species, including western white pine (*Pinus monticola* Dougl. ex D. Don), grand fir (*Abies grandis* [Dougl. ex D. Don] Lindl.), bigleaf maple (*Acer macrophyllum* Pursh), and red alder (*Alnus rubra* Bong.), are present in small numbers. The understory vegetation has variable densities of salal (*Gaultheria shallon* Pursh), dull Oregon grape (*Mahonia nervosa* [Pursh] Nutt.), sword fern (*Polystichum munitum* [Kaulf.] Presl) and other herbaceous species.

Six plots were initially established in 1997 and 1998 to study spatial patterns and tree mortality (He and Duncan, 2000). These plots were part of a larger chronosequence network established by the Canadian Forest Service (Trofymow et al., 1997). The six plots themselves formed a chronosequence of forest stands, with two immature (25-45 years old), two mature (65-85 years old), and two old-growth plots (>200 years old). Stands were classified by age as of the year 1990 (Trofymow et al., 1997). The plots within the chronosequence series were designated as north and south based on location (for example, immature north and immature south plots). The immature stands originated from planted regeneration following clear-cut harvesting. The mature north plot regenerated naturally following harvest, while the old-growth and mature south plots regenerated naturally after stand-clearing fires. All plots are located approximately within a distance of 10 kilometers. Plots range in size from 0.7 to 1.2 hectares, with an average size of 1.1 ha. The maximum elevation difference between plots is 225 m and plots are located on gentle to intermediate slopes with average slope of 18.2%. The old-growth south plot was lost to clear-cut harvesting prior to recensus. Part of the mature north plot was also lost to blowdown caused by adjacent logging (Fig. 2.2) and therefore only the unaffected section was analyzed in this study. As a result, only 5 plots were studied in this thesis and their characteristics, and disturbance and regeneration histories are described in Table 2.1.

Table 2.1. Study plot characteristics and origin history.

Plot name	Age	Size	Elevation	Slope	Origin	Regeneration method
Immature-S	54	0.703	305	20 NE	Harvest	Planting
Immature-N	65	1.187	355	5	Harvest	Planting
Mature-S	122	1.065	240	11 NW	Fire	Natural
Mature-N	116	1.239	260	15 NE	Harvest	Natural
Old-Growth	319	1.139	465	40 NE	Fire	Natural

S or N in plot name refers to the south or north chronosequence series, respectively; age is in years since stand-clearing disturbance as of 2014; size is in hectares; elevation is in meters and slope is in degrees with aspect (slope aspect was not recorded on flat terrain, slope ≤5).

Figure 2.1. Locations of study sites on southern Vancouver Island, British Columbia, Canada.
Red circles show plot locations. Imm, Mat and OG represent the immature, mature, and old-growth plots, respectively. S is the southern and N is the northern chronosequene. OG-N was logged prior to recensus and was not included in analysis. Map adapted from CRD Regional Webmap and used with permission from the Capital Regional District.

2.2.2 Data Collection

Plots were established and first censused in 1997 or 1998. All live and dead trees were tagged and the x, y, z coordinates were recorded relative to a reference point using a total station system (Fig. 2.2). Each tree was identified to species. Diameter at breast height (DBH, 1.3 m above ground level) was measured using a diameter tape or callipers, and tree status was recorded, classified as live, dead standing (snag), log, stump, or as a seedling for trees less than 1.3 m in height.

Re-censuses of the plots were completed in the summer of 2014, making the census interval 16 to 17 years. Diameter and status measurements were repeated on all trees that were live at the first census. Those stems that did not exist in the first census in 1997 and 1998 but were growing in 2014 were new recruits. Recruits were tagged, identified and measured; their locations were calculated by trilateration from distances recorded to three neighbouring trees.

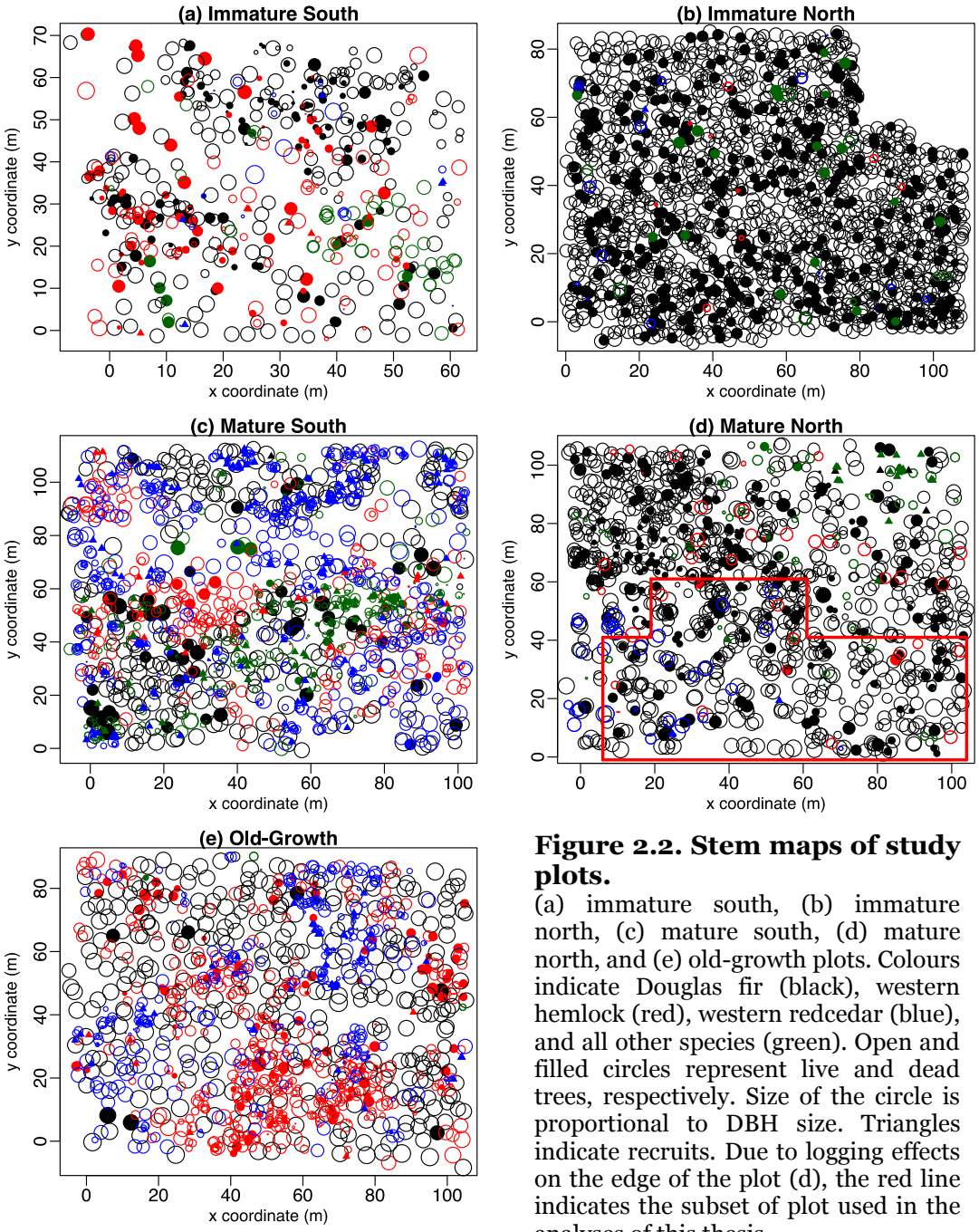

Figure 2.2. Stem maps of study plots.
(a) immature south, (b) immature north, (c) mature south, (d) mature north, and (e) old-growth plots. Colours indicate Douglas fir (black), western hemlock (red), western redcedar (blue), and all other species (green). Open and filled circles represent live and dead trees, respectively. Size of the circle is proportional to DBH size. Triangles indicate recruits. Due to logging effects on the edge of the plot (d), the red line indicates the subset of plot used in the analyses of this thesis.

2.2.3 Spatial Pattern Analysis

The *K*-function, and its derivatives, are widely used for analyzing mapped point patterns in forest ecology (He and Duncan, 2000; Wiegand and Moloney, 2004; Getzin et al., 2008). To quantify spatial patterns of species in stands and to examine changes in pattern, the pair correlation function, derived from Ripley's *K*-function (Ripley, 1977), was used. The *K*-function is defined as

$$K(r) = \lambda^{-1}\mathrm{E}[\#\text{ of trees within distance } r \text{ of a randomly chosen tree excluding the focal tree}]$$

and is estimated as

$$K(r) = \lambda^{-1}N^{-1}\sum_{i=1}^{N}\sum_{\substack{j=1 \\ i\neq j}}^{N} I\left(d_{ij} \leq r\right), \qquad [2.1]$$

where λ is the average point density, *N* is the total number of trees in the data set, d_{ij} is the distance between the i^{th} and j^{th} trees, *r* is the circle radius around the focal tree, and *I* is the indicator function where *I(x)* = 1 if true, and *I(x)* = 0 if false (Dixon, 2002). Values of $K(r) = \pi r^2$ indicate spatial randomness, while $K(r) > \pi r^2$ indicate aggregation and $K(r) < \pi r^2$ suggest spatial regularity.

Edge effects arise when the focal tree is located close to the plot edge and the circles of the *K*-function around a focal tree are partially outside the plot boundary. Because any trees outside the boundary are unknown, estimates of the spatial functions will be biased. Ripley's isotropic edge correction (Ripley, 1977) was applied to all calculations of the pair correlation function to account for edge effects. This correction applies a weight to each focal tree based on the proportion of the circle that is outside the study area. The weight is defined as

$$w(i,j) = \frac{a_{ij}}{2\pi r}, \qquad [2.2]$$

where *w(i,j)* is the weight for focal tree *i* to tree *j*, *r* is the radius of the circle around *i*, a_{ij} is the length of the circumference of the circle inside the boundary. If the circle is entirely within the study area, *w(i,j)* = 1. Using this weighting, the unbiased edge corrected estimate of *K(r)* is

$$K(r) = \lambda^{-1}N^{-1}\sum_{i=1}^{N}\sum_{\substack{j=1 \\ i\neq j}}^{N} \frac{1}{w(i,j)}\, I(d_{ij} \leq r), \qquad [2.3]$$

where λ, d_{ij}, r, N, and I are as above in Equation 2.1 and $w(i,j)$ is from Equation 2.2.

The circles of the K-function are cumulative with distance. Contrastingly, the pair correlation function replaces the circles with rings, making it noncumulative with the ability to separate small-scale and large-scale effects (Stoyan and Penttinen, 2000). The pair correlation function is defined as

$$g(r) = \lambda^{-1}\mathrm{E}[\#\text{ of trees at distance } r \text{ of a randonly chosen tree excluding the focal tree}]$$

and is estimated as

$$g(r) = \frac{K'(r)}{2\pi r}, \qquad [2.4]$$

where $K'(r)$ is the derivative of Ripley's K-function from Equation 2.3 and r is the ring radius. The function $g(r)$ identifies how the tree distribution pattern changes as the distance increases and identifies the distances at which deviations from spatial randomness occur (Wiegand and Moloney, 2004; Pretzsch, 2009). Values of $g(r) = 1$ indicate a random distribution, while $g(r) > 1$ and $g(r) < 1$ indicate spatial aggregation and regularity, respectively.

The univariate, bivariate, and multi-type forms of the pair correlation function were used to analyse the distribution patterns of trees within the forest plots. The univariate form described above, $g(r)$, quantifies the spatial pattern of all trees in the analysis. Marked point patterns are required for bivariate and multi-type analysis with marks indicating tree status (live, dead), species, diameter etc. (Fig. 2.2). The bivariate form, $g_{i,j}(r)$, quantifies the spatial distribution between trees of mark i to mark j. The multi-type form, $g_{i,\cdot}(r)$, quantifies the spatial distribution of trees of mark i to all other mark types.

Analyses were applied at the individual plot level to all species collectively as well as to each of the three dominant species, Douglas fir (DF), western hemlock (HL), and western redcedar (CD), individually. All spatial analyses were implemented using the *spatstat* package (Baddeley and Turner, 2005) within the program R (R Core Team, 2015).

2.2.3.1 Spatial Patterns of Live Trees

The univariate form of the pair correlation function, $g(r)$, was used to compute the spatial pattern of all live trees of the first census and second census to determine if the pattern had changed over time as a result of mortality and recruitment. The statistics $g_{1997}(r)$ and $g_{2014}(r)$ were calculated from the live trees in 1997 and 2014, respectively. These

empirical functions were compared against the null model of complete spatial randomness (CSR) that is expected under a homogenous Poisson process. A dataset of random coordinates was generated 99 times, with the number of coordinates equal to the number of trees in each plot data set. 95% confidence envelopes were estimated from these simulations and points from the empirical *g(r)* lying outside the envelopes express significant departures from complete spatial randomness. Points above and below the envelope indicate aggregation and regularity, respectively.

To test if the change in spatial pattern of live trees was significant, the statistic $g_{2014}(r) - g_{1997}(r)$ was calculated. This quantified the net change in live tree pattern. The null model for this statistic accounted for random labeling of dead trees, where trees from the pre-mortality pattern were randomly labelled as dead and the number of trees labelled dead was equal to the empirical number of dead trees in each plot. The null model also accounted for spatially random recruitment, where random coordinates were generated equal to the number of recruits in each plot. The null model was simulated 99 times and 95% confidence envelopes were calculated. Points lying above the confidence envelope indicate significant increase in aggregation and points lying below the envelope indicate significant increase in regularity between the two censuses (Table 2.2, Hypothesis 1).

Table 2.2. Study hypotheses, null models and pattern analysis functions, and related figures.

	Hypotheses	Analyses and null models	Related figures
1.	Spatial pattern of Douglas fir becomes more regular; western hemlock and western redcedar become more spatially aggregated.	$g(r)$ and $g_{2014}(r) - g_{1997}(r)$ Complete spatial randomness, random labelling of mortality & spatial randomness of recruits	Fig. 2.3
2.	Mortality is spatially non-random, mortality occurred in aggregation.	$g_{d,d}(r)$ Random labelling model	Fig. 2.4
3.	Neighbourhood density is higher for dead trees than for live trees.	$g_{d,all}(r) - g_{l,all}(r)$ Random labelling model	Fig. 2.5, 2.6
4.	Recruitment occurred in neighbourhoods with higher densities of conspecifics.	$g_{sm,all}(r) - g_{l,all}(r)$ Complete spatial randomness model	Fig. 2.7, 2.8
5.	Interspecific competition between Douglas fir and shade-tolerant species leads to spatial dispersion, while hemlock and redcedar show spatial aggregation.	$g_{SP1,SP2}(r)$ Spatial independence, random toroidal shift	Fig. 2.9

2.2.3.2 Random Mortality Testing

The univariate pair correlation function was used to test the hypothesis of random mortality. The statistic $g_{d,d}(r)$ was calculated to determine if the distribution of dead trees differed from what is expected under random mortality (i.e., were dead trees more clustered or regular than expected). The empirical statistic was compared to the null model of random labelling: live trees from the first census were randomly labelled as live or dead, with the number of live and dead labels equal to the observed numbers at the 2014 census. This was simulated 99 times and used to calculate 95% confidence envelopes of random mortality. Aggregation or regularity is expressed if points are above or below the confidence envelope, respectively (Table 2.2, Hypothesis 2).

2.2.3.3 Density-Dependent Mortality and Recruitment

The bivariate function, $g_{i,j}(r)$, and multi-type function, $g_{i,.}(r)$, were used to evaluate density-dependent effects on mortality and recruitment. The function $g_{d,all}(r)$ compared the distribution of dead trees to trees live at the first census and the function $g_{l,all}(r)$ compared the distribution of surviving trees to trees live at the first census. The statistic $g_{d,all}(r) - g_{l,all}(r)$ then compared the initial neighbourhoods of tree that died to those of surviving trees to assess the significance of density-dependent processes. If mortality was random, $g_{d,all}(r) - g_{l,all}(r) = 0$. If density-dependent mortality occurred, $g_{d,all}(r) - g_{l,all}(r) > 0$ and initial neighbourhoods of trees that died were more crowded than those of surviving trees (Lutz et al., 2014). The random labelling null model, as described above in Section 2.2.3.2, was implemented to determine the confidence envelopes and significance (Table 2.2, Hypothesis 3).

In a similar analysis, the neighbourhood of recruits were compared to the neighbourhood of live trees to assess if tree density influenced establishment. The number of recruits (trees that established since the first measurement) was too small in many of the plots to carry out a reliable analysis and therefore all live small trees with DBH less than 5 cm were included as recruits. The statistic used in this analysis was $g_{sm,l}(r) - g_{l,l}(r)$, with *sm* indicating small trees and *l* indicating live trees. An additional analysis was completed for recruits of non-focal species in plots where the establishment of other species was high. Random coordinates of recruits were generated equal to the number of observed recruits in each plot. The distribution of random recruitment was compared to the distribution of live trees and the difference was calculated for each of 99 simulations was used to determine the

95% confidence envelopes. If establishment of small trees was random, $g_{sm,l}(r) - g_{l,l}(r) = 0$. If establishment occurred in gaps and open areas, $g_{sm,l}(r) - g_{l,l}(r) < 0$. If establishment occurred close to possible parent trees (live trees >5 cm in diameter), $g_{sm,l}(r) - g_{l,l}(r) > 0$. Points lying outside the confidence envelope indicate significant departures from random (Table 2.2, Hypothesis 4).

An additional analysis of density-dependent mortality and recruitment was completed by using the statistics outlined above and considering only conspecific neighbours to detect the importance of intraspecific effects.

2.2.3.4 Species Associations

The bivariate form of the pair correlation function, $g_{i,j}(r)$, was used to analyze the spatial association between two species. The statistics $g_{DF,HL}(r)$, $g_{DF,CD}(r)$, and $g_{HL,CD}(r)$ were used to calculate the association between the three dominant tree species. This was tested against the null model of spatial independence, where the structure of both species was retained but species *j* was shifted toroidally around species *i* (Duncan, 1991; Wiegand and Moloney, 2004). This was simulated 99 times and 95% confidence envelopes were generated. Species independence occurred when $g_{i,j}(r) = 1$. If $g_{i,j}(r) > 1$, species were spatially aggregated, and if $g_{i,j}(r) < 1$, species were spatially dispersed (Table 2.2, Hypothesis 5). All species pairs were tested (ex. species 1 to 2 and species 2 to 1) to check for asymmetric associations (Wiegand et al., 2007).

2.3 Results

2.3.1 Net change in spatial patterns

The spatial patterns of live trees pooled over all species experienced significant changes from the first census (1997/1998) to the second census in 2014. Patterns for each census separately are shown in Appendix A. The net change in spatial pattern for both immature plots showed a decrease in aggregation at all scales and mostly strongly at distances <4 m (Fig. 2.3 a, b). The mature south plot experienced a significant increase in aggregation up to 2 m, while showing decreased aggregation at larger distances (Fig. 2.3 c). The mature north and old-growth stands showed little change between the two measurements with only slight evidence of increases and decreases in aggregation (Fig. 2.3 d, e).

Douglas fir in the immature stands showed similar trends as the case when all species were pooled. As the dominant species in the immature stands, the patterns for all species pooled closely reflect the distribution of Douglas fir. Douglas fir showed significant decreases in aggregation in the immature stands at distances of <4 m, as well as at larger distances (Fig. 2.3 f, g), as predicted. However, the pattern for Douglas fir differed in the mature and old-growth plots. In the mature south plot, Douglas fir showed a significant increase in aggregation at 2 m (Fig. 2.3 h). The mature north stand showed a strong increase in aggregation at 4 m but a significant shift to regularity at 10 m (Fig. 2.3 i). The old-growth stand showed a higher degree of aggregation at large scales of 15-18 m (Fig. 2.3 j). The net change of increased aggregation in the older stands is contrary to the expected trend toward regularity.

Western hemlock and western redcedar were only present in large enough numbers for analysis at three of the five plots. Both species showed little significant spatial pattern changes in the immature south plot. Hemlock experienced an increase in spatial aggregation at 12 m and redcedar showed an increase in aggregation at small scales (<2 m) and a decrease in aggregation from 5-7 m and 14 m (Fig. 2.3 k, n). In the mature south stand, hemlock showed only a significant increase in aggregation at 9 m (Fig. 2.3 l), while redcedar showed significant increases in aggregation up to 10 m, decreased aggregation between 11-15 m and increased aggregation again larger distances (Fig. 2.3 o). The old-growth plot experienced strong increases in aggregation across all distances for both species (Fig. 2.3 m, p). Although the trends in the immature plot were weak, the expected increase in aggregation was experienced by hemlock and redcedar trees in the mature and old-growth stands.

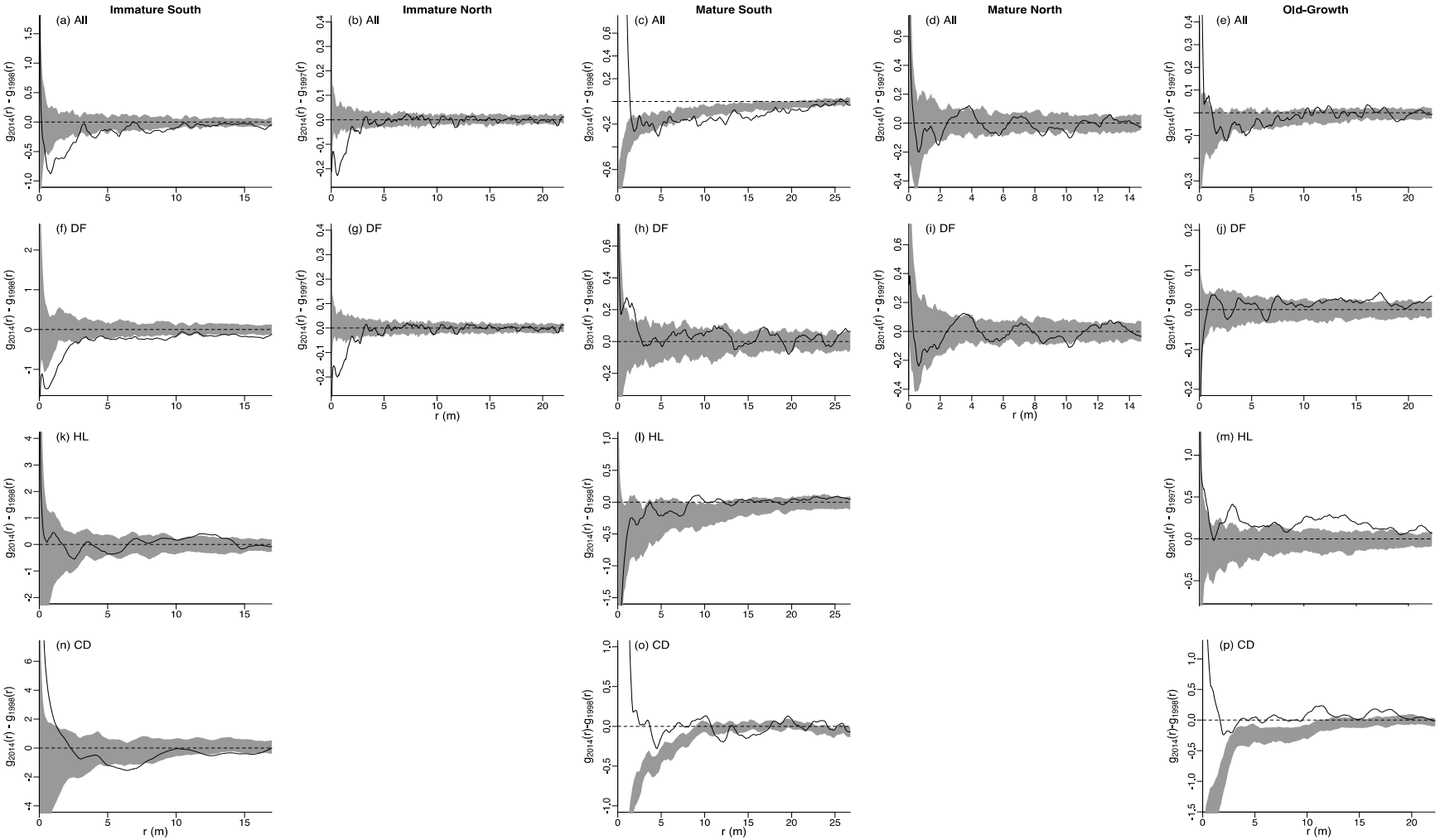

Figure 2.3. Univariate analysis for net change in live tree spatial patterns.
Patterns for all species pooled (a-e), Douglas fir (f-j), western hemlock (k-m), and western redcedar (n-p). Black line shows observed results and grey area represents 95% confidence envelope for complete spatial randomness null model, with results above (below) the envelope indicating aggregation (regularity).

2.3.2 Testing the random mortality hypothesis

As predicted, trees that died were significantly aggregated for all species pooled in all plots. The immature south plot showed highly aggregated mortality at all distances (Fig. 2.4 a) and the immature north stand experienced aggregated mortality up to 1 m (Fig. 2.4 b). Trees in the mature south plot showed significantly aggregated mortality at all distances (Fig. 2.4 c), while the trend in the mature north plot was less clear, showing aggregated tree death only at <0.5 m and 1 m (Fig. 2.4 d). The old-growth stand showed mortality strongly aggregated between 1.5 m to 8.5 m (Fig. 2.4 e).

Douglas fir tree mortality trends were similar to the trends for all species pooled in the immature plots, with the south plot strongly aggregated at all scales with only a few exceptions for random mortality (Fig. 2.4 f). The immature north plot had aggregated mortality at distances less than 1 m (Fig. 2.4 g). Unlike the pattern for all species in the mature south plot, Douglas fir mortality was only aggregated up to 6 m (Fig. 2.4 h) and trees in the mature north plot showed random mortality at all distances (Fig. 2.4 i). In the old-growth plot, Douglas fir tree mortality was aggregated at <2 m and again at large distance of 17-20 m (Fig. 2.4 j). These trends are consistent with the expected aggregated mortality for pioneer species.

Western hemlock and western redcedar mortality analysis was limited to three of the five plots. These shade-tolerant species showed opposite trends for the distribution of mortality with successional stage. Hemlock met the assumption of aggregated mortality in the immature south plot at distances <1.5 m and 3-7 m, and in the mature south plot at scales <1.5 m (Fig. 2.4 k, l). However, mortality for this species was regularly distributed in the old-growth stand at large distances (Fig. 2.4 m). Contrastingly, redcedar mortality was random at all distances in the immature south plot (Fig. 2.4 n), slightly regular in the mature plot at 4 m and 6 m (Fig. 2.4 o), and showed the expected aggregated mortality in the old-growth stand from 0-5 m (Fig. 2.4 p).

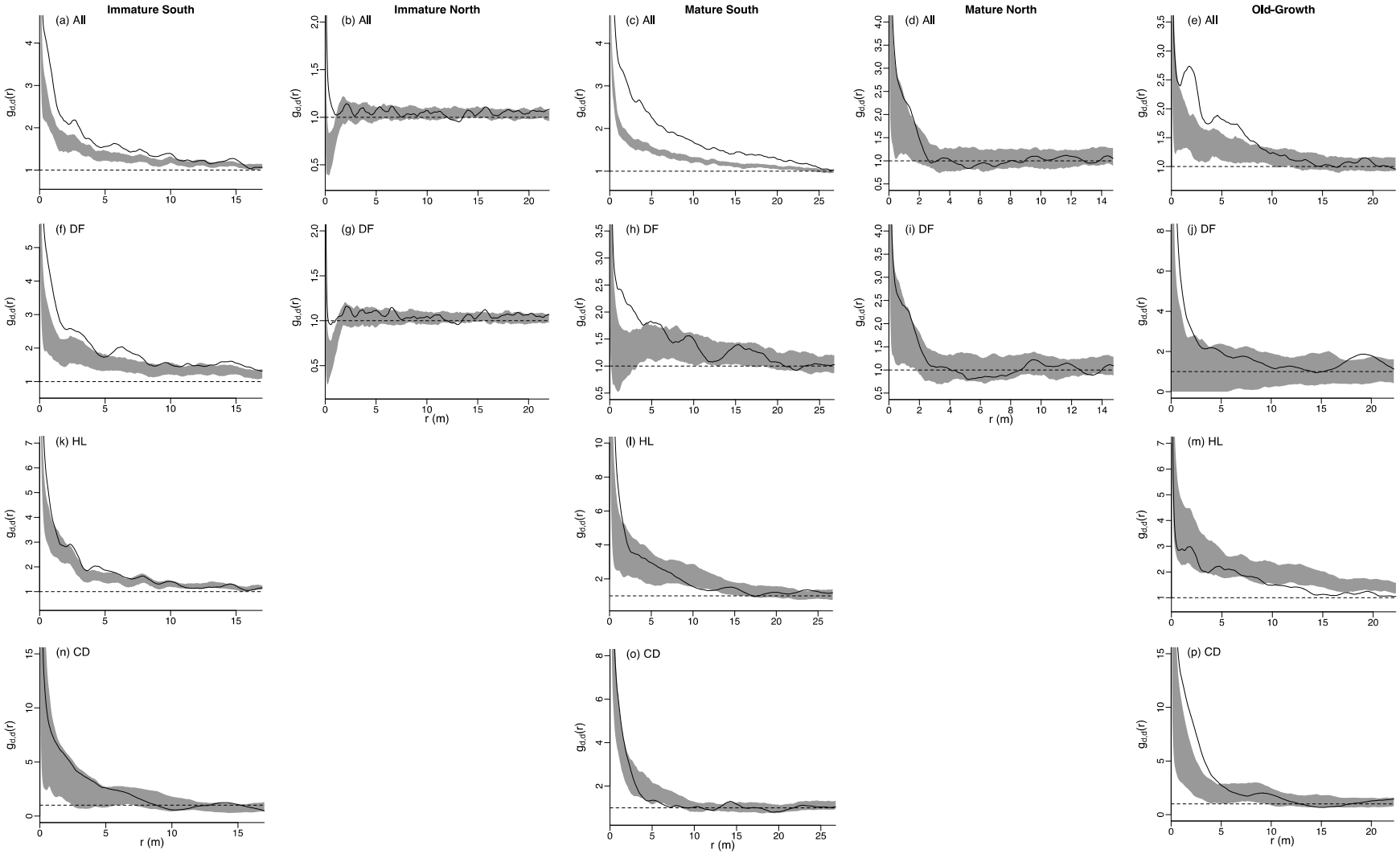

Figure 2.4. Univariate analysis of random mortality.
Mortality patterns for all species pooled (a-e), Douglas fir (f-j), western hemlock (k-m), and western redcedar (n-p). Black line shows observed results and grey area represents 95% confidence envelope for random mortality using random labelling null model, with results above (below) the envelope indicating aggregated (regular) mortality.

2.3.3 Density-dependent processes on tree mortality

If density-dependent processes are at work, tree mortality is predicted to occur in neighbourhoods with higher density than surviving trees. My analysis showed that initial neighbourhoods of trees that died between censuses were significantly more crowded than neighbourhoods of trees that survived for all species pooled in four of the five plots, indicating density-dependent processes led to tree mortality (Fig. 2.5 a-e).

Evidence for density-dependent mortality in Douglas fir trees decreased with successional stage. Mortality neighbourhoods in the immature plots were significantly more crowded at scales of <7 m in the immature south stand and <3 m in the north stand (Fig. 2.5 f, g). In the mature plots, initial neighbourhood densities of Douglas fir trees that died were not significantly different from that of surviving trees at small scales, but showed significant crowding at distances of 5-20 m in the mature south plot (Fig. 2.5 h) and at 11 m in the mature north plot (Fig. 2.5 i). Mortality for this species showed no significant difference in neighbourhood density of trees that died and survived in the old-growth stand (Fig. 2.5 j). Similar trends occurred when looking at conspecific neighbourhoods. Douglas fir showed conspecific density-dependent mortality in the immature plots (Fig. 2.6 a, b), but showed no significant conspecific crowding in the mature and old-growth stands (Fig. 2.6 c-e).

Trends for density-dependent tree mortality differed for western hemlock and redcedar. Both species experienced significantly more crowded neighbourhoods for trees that died than trees that survived at scales <5 m in the immature south plot (Fig. 2.5 k, n). In the mature south stand, hemlock showed evidence of strong density-dependent mortality at distances <1 m (Fig. 2.5 l), while redcedar neighbourhood densities were not significantly different between trees that died and survived (Fig. 2.5 r). In the old-growth plot, hemlock experienced mortality in significantly less crowded neighbourhoods at 1 m and again at larger scales of 12-17 m (Fig. 2.5 m). Contrastingly, redcedar in this plot showed strong crowding effects on mortality at distances of 2-7 m (Fig. 2.5 p). When looking at conspecific neighbourhoods for these species, hemlock showed density-dependent mortality at small scales in the immature stand (Fig. 2.6 f), no effect at the mature level (Fig. 2.6 g), and mortality in less dense neighbourhoods in the old-growth plot (Fig. 2.6 h). Redcedar showed only slightly higher mortality in denser neighbourhoods of conspecifics in the immature (Fig. 2.6 i) and old-growth plots (Fig. 2.6 k), suggesting interspecific density-dependence could play a role in these stands. In the mature stand, redcedar showed mortality in significantly less dense neighbourhoods of conspecifics (Fig. 2.6 j).

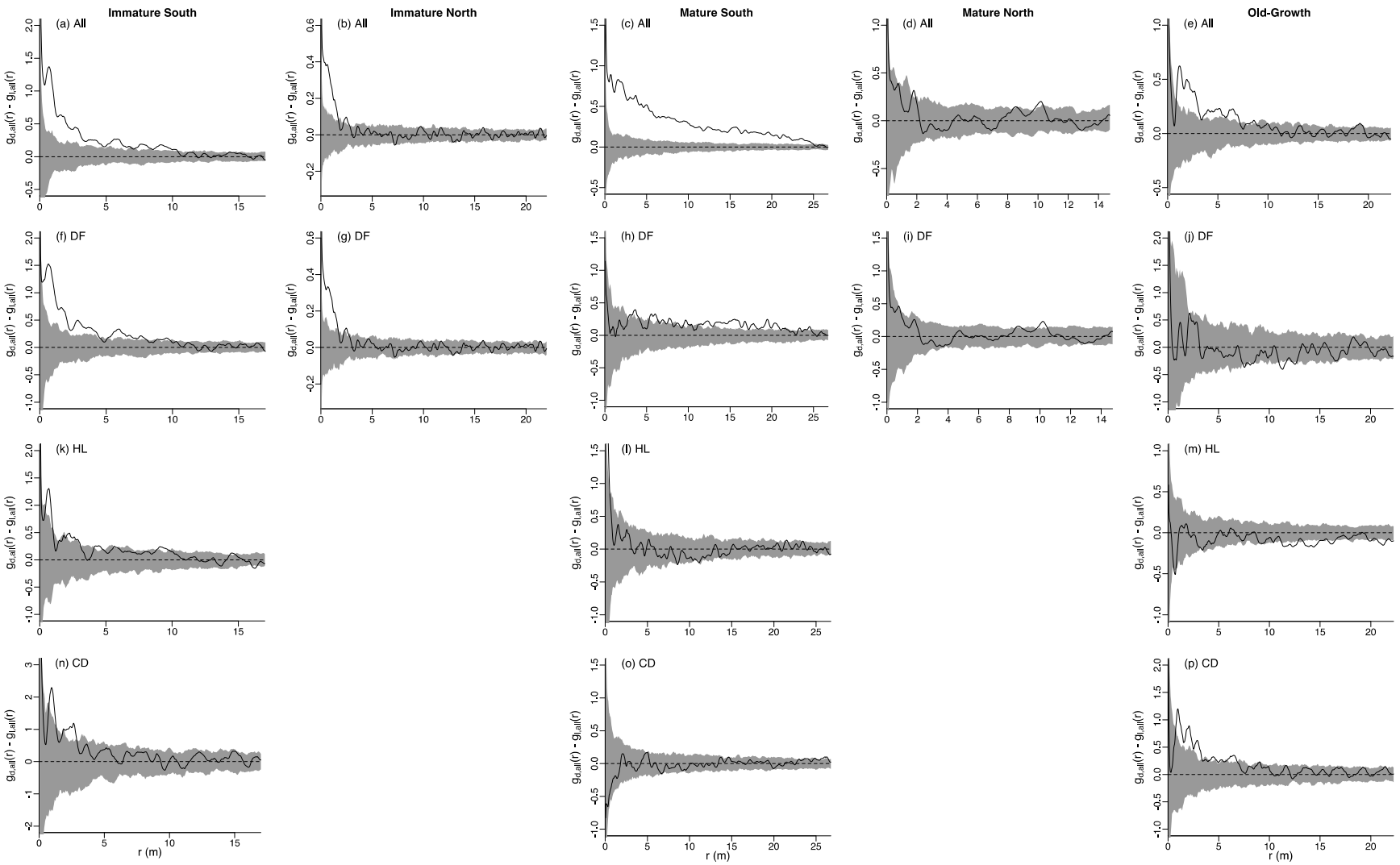

Figure 2.5. Multi-type analysis of density-dependent mortality.
Spatial context of mortality for all species pooled (a-e), Douglas fir (f-j), western hemlock (k-o), and western redcedar (p-t). Black line shows observed results and grey area represents 95% confidence envelope for random labelling null model, with results above (below) the envelope indicating neighbourhoods of trees that died were significantly more (less) crowded than neighbourhoods of surviving trees.

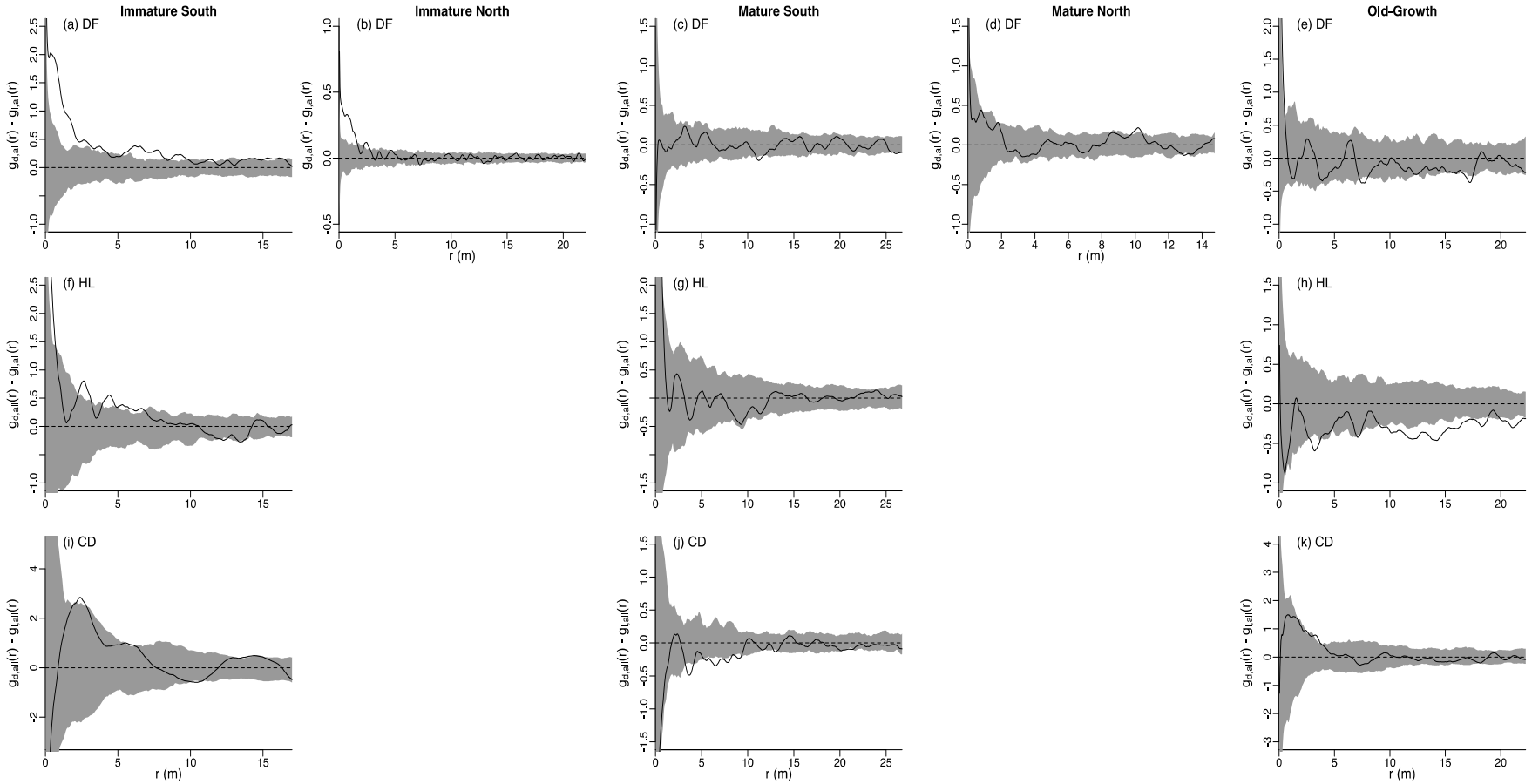

Figure 2.6. Multi-type analysis for density-dependent mortality in conspecific neighbourhoods.
Spatial context of mortality in neighbourhoods of the same species for Douglas fir (a-e), western hemlock (f-h), and western redcedar (i-k). Black line shows observed results and grey area represents 95% confidence envelope for random labelling null model, with results above (below) the envelope indicating neighbourhoods of trees that died were significantly more (less) crowded with conspecifics than neighbourhoods of surviving trees.

2.3.4 Density-dependent processes on tree recruitment

The spatial context of recruitment varied across species and plots. Recruitment analyses included new recruits and small trees because number of recruits was insufficient. All plots showed a degree of significantly aggregated recruitment compared to complete spatial randomness. The immature plots also showed spatial regularity of small trees at large distances (Appendix B).

For density-dependent processes, the neighbourhood of small trees (DBH <5 cm) of all species were significantly more crowded than the neighbourhood of larger trees at varying distances up to 13 m (Fig. 2.7 a) in the immature south stand, while small and large trees in the immature north stand showed no significant difference in neighbourhood crowding (Fig. 2.7 b). The mature south plot showed strongly crowded neighbourhoods for small trees at distances up to 13 m and again at larger scales (Fig. 2.7 c). Small trees in the mature north plot experienced significantly more crowding at <0.5 m and 7 m, but significantly less crowded neighbourhoods than larger trees at 2 m (Fig. 2.7 d). Small trees in the old-growth stand experienced strong crowding up to distances of 15 m compared to larger trees (Fig. 2.7 e).

It was expected that tree recruitment occurred in neighbourhoods with high densities of conspecific trees compared to neighbourhoods of large trees. The strength of the evidence supporting this prediction increased with successional stage for western redcedar. Small redcedar trees showed no significant crowding in the immature plots compared to neighbourhoods of large trees (Fig. 2.7 f, g). For conspecific neighbourhoods, the immature south stand also showed no significant difference in crowding (Fig. 2.8 a). In the mature south plot, redcedar small trees occurred in significantly more crowded neighbourhoods up to 8 m but significantly less crowding at larger distances (Fig. 2.7 h). Trends were similar when looking at conspecific neighbourhoods, with crowding evident up to 7 m and again at >20 m but becoming dispersed between 12-15 m (Fig. 2.8 b). The old-growth plot also had significantly crowded neighbourhoods up to 10 m in neighbourhoods of all species, and up to 25 m in conspecific neighbourhoods (Fig. 2.7 i, 2.8 c). There were not enough small redcedar trees for analysis in the mature north stand.

Western hemlock small trees occurred in sufficient numbers in only three of the five plots and showed the expected trend of recruits occurring in more dense neighbourhoods of conspecifics. This species showed significantly more crowded neighbourhoods at <3 m, 6-9 m and 13 m in the immature plot for neighbourhoods with all species and conspecific

neighbourhoods (Fig. 2.7 j, 2.8 d). In the mature south plot, only slightly significant crowding was detected when looking at neighbourhoods with all species (Fig. 2.7 k); conspecific neighbourhoods of small trees were significantly more crowded than larger trees up to 15 m (Fig. 2.8 e). Trends in the old-growth stand showed strong crowding up to 30 m for neighbourhoods with all species and conspecifics trees only (Fig. 2.7 l, 2.8 f).

Small Douglas fir trees were significantly crowded compared to larger trees in the immature plot at distances of 4 m and 12 m (Fig. 2.7 m) for neighbourhoods with all species. For conspecific neighbourhoods, the trend was similar with strong crowding at 3-6 m and 12-20 m (Fig. 2.8 g). However, in the mature north plot, small trees showed less crowded neighbourhoods than large trees at 1, 3, and 4 m in neighbourhoods with all species and neighbourhoods analyzed with only conspecifics (Fig. 2.7 o, 2.8 i). The numbers of Douglas fir small trees in the other plots were too low for analysis.

Other species made up a larger portion of the small trees in the mature south plot and therefore were analyzed as a separate group. Small trees of these species showed significant crowding for all-species neighbourhoods at varying distances (Fig. 2.7 n). For conspecific neighbourhoods, the strong crowding was evident up to distances of 20 m (Fig. 2.8 h).

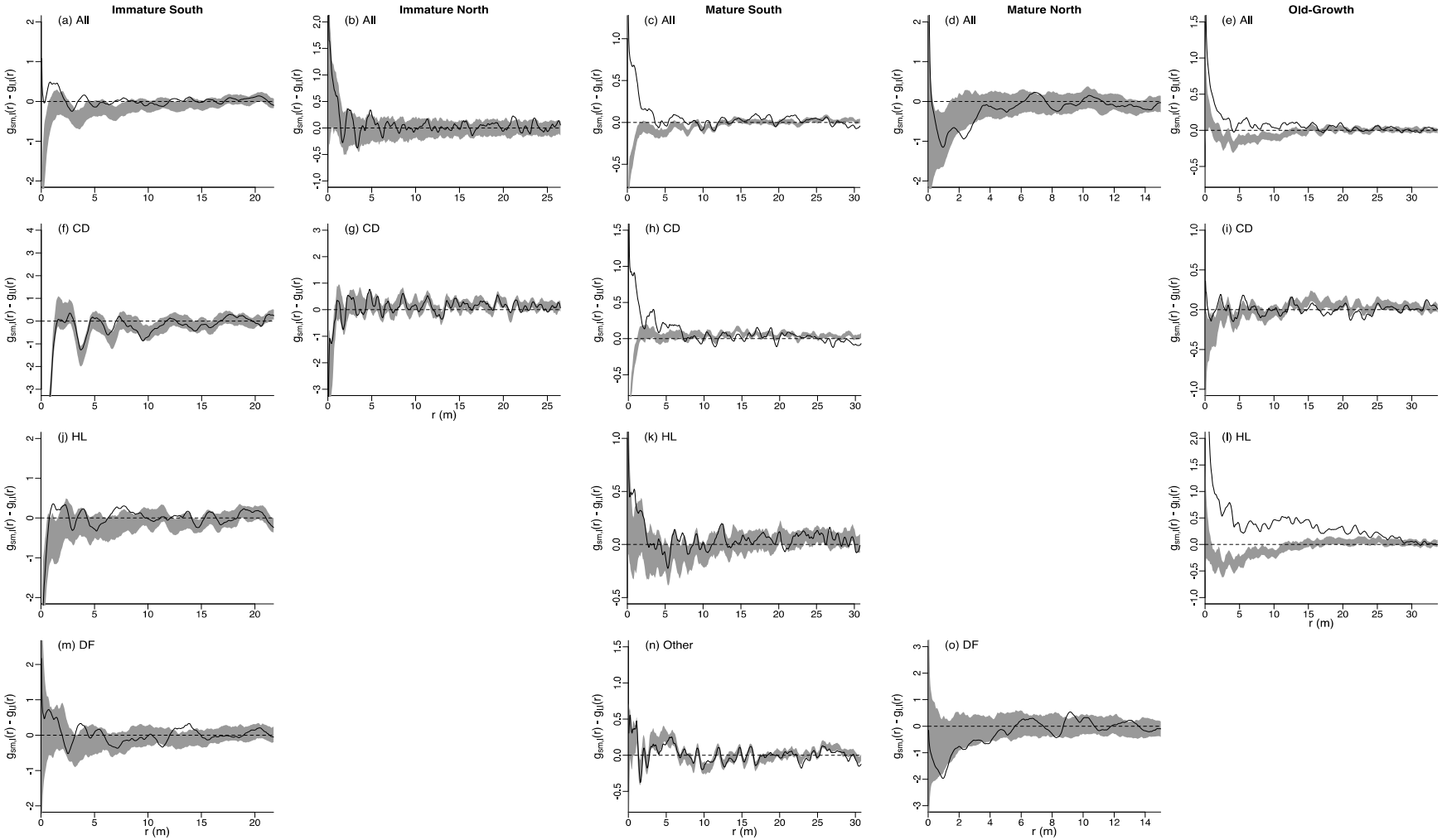

Figure 2.7. Bivariate and multi-type analysis of neighbourhood crowding for small trees and recruits.
Spatial context of small trees and recruits for all species pooled (a-e), western redcedar (f-i), western hemlock(j-l), Douglas fir (m,o), and other species (n). Black line shows observed results and grey area represents 95% confidence envelope for CSR, with results above (below) the envelope indicating neighbourhoods of recruits were significantly more (less) crowded than neighbourhoods of large trees.

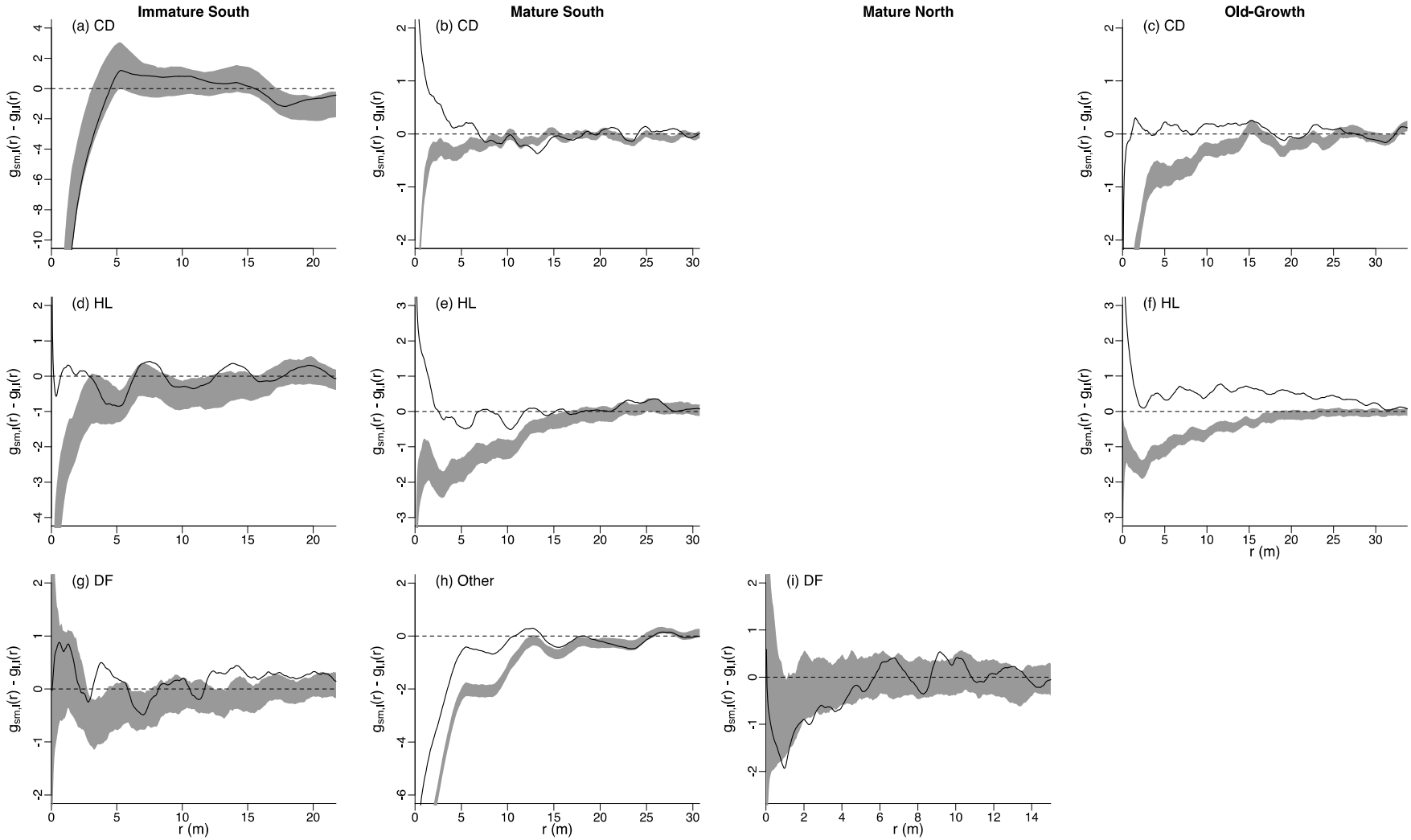

Figure 2.8. Bivariate and multi-type analysis of conspecific neighbourhood crowding of small trees and recruits. Spatial context of small trees and recruits in conspecific neighbourhoods for western redcedar (a-c), western hemlock(d-f), Douglas fir (g, i), and other species (h). Black line shows observed results and grey area represents 95% confidence envelope for CSR, with results above (below) the envelope indicating neighbourhoods of recruits were significantly more (less) crowded than neighbourhoods of large trees.

2.3.5 Evidence of spatial associations between species

Species spatial associations were expected to be positive between western hemlock and western redcedar, and negative between Douglas fir and the shade-tolerant species due to interspecific competition, and habitat and resource requirements.

Bivariate analysis showed Douglas fir and hemlock had no significant interaction in the immature plots (Fig. 2.9 a, b) and in the mature south plot (Fig. 2.9 c). However, evidence for interspecific competition leading to dispersion between the species increased with successional stage. In the mature north stand, hemlock showed dispersion from Douglas fir at 3 m (Fig. 2.9 d) and significant interspecific dispersion in the old-growth plot at small scales up to 3.5 m (Fig. 2.9 e).

For Douglas fir and western redcedar, there was no significant association in the immature plots (Fig. 2.9 f, g). However, these species were significantly aggregated in the mature south plot at distances up to 7 m (Fig. 2.9 h), opposing the prediction of dispersion. The mature north stand showed no interactions between the species (Fig. 2.9 i), and the expectation for interspecific dispersion was met in the old-growth small scales up to 3 m (Fig. 2.9 j).

Only three of the plots had sufficient numbers of both hemlock and redcedar to analyze their interactions. These species were expected to be positively associated with one another. The immature south plot showed significant aggregation of redcedar around hemlock at 5 m (Fig. 2.9 k). However, these species showed interspecific dispersion at scales of <2 m and at 5 m in the mature stand (Fig. 2.9 l), and no significant associations in the old growth plot (Fig. 2.9 m).

Reversed pair combinations for hemlock and redcedar (ex. HL-CD and CD-HL), were tested to analyze asymmetry in associations; interactions between these two species appear symmetric (Appendix C). Reversed combinations for Douglas fir were also tested and appear symmetric. Trends for Douglas fir associations around hemlock and redcedar are less important in these stands where Douglas fir is the pioneer species establishing first, and subsequently influences the establishment patterns of late-successional hemlock and redcedar, rather than hemlock and redcedar influencing the establishment of Douglas fir.

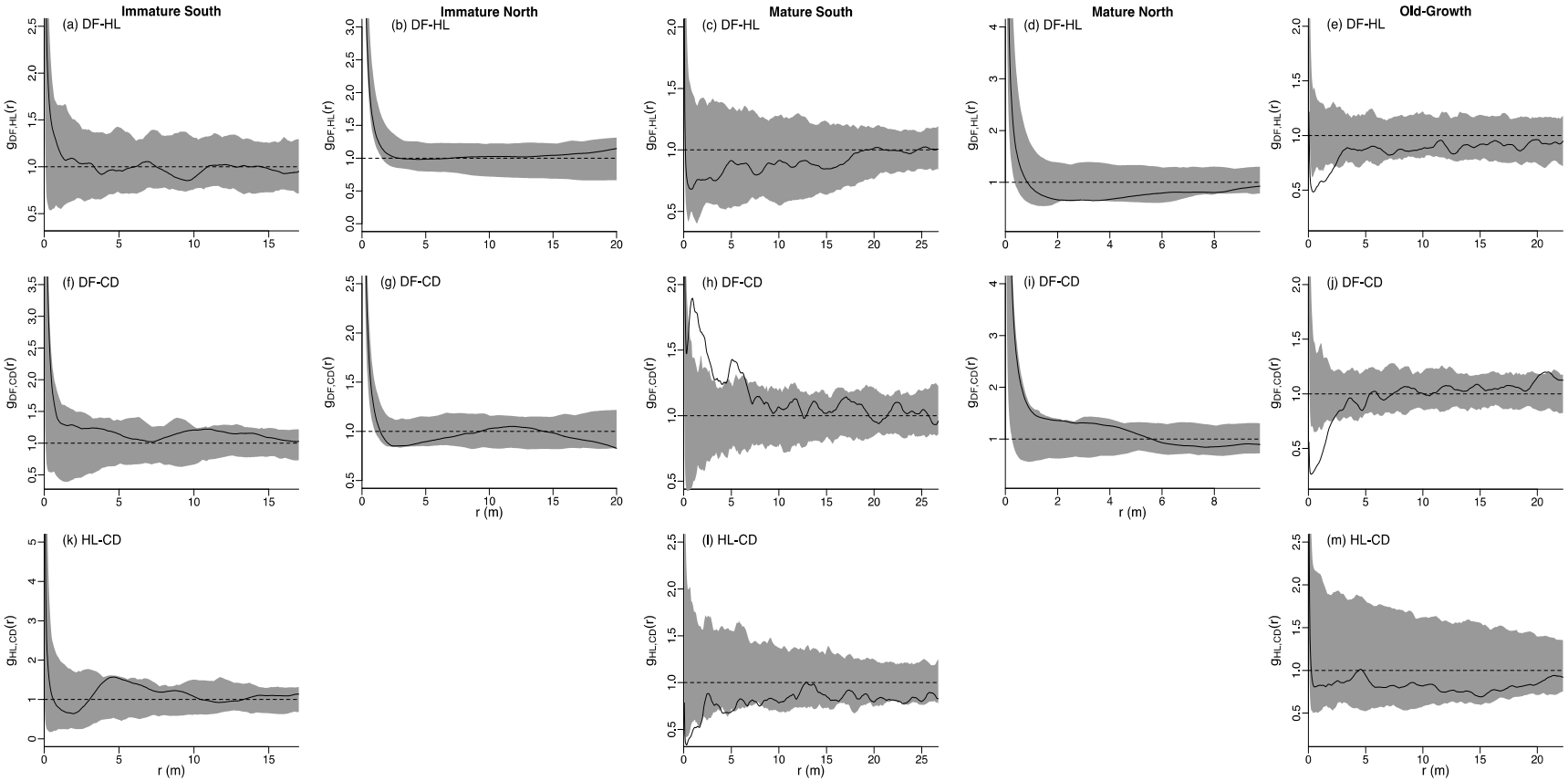

Figure 2.9. Bivariate associations between dominant species pairs.
Interaction between species Douglas fir-hemlock (a-e), Douglas fir-redcedar (f-j), and hemlock-redcedar (k-m) compared to the toroidal shift null model. Black line shows observed results and grey area represents 95% confidence envelope for no spatial association under the null model, with results above (below) the simulation envelope shows positive (negative) spatial associations.

2.4 Discussion

Spatial patterns of the dominant tree species were expected to change over the census interval and between stand ages. It was hypothesized that dominant species in the plots would undergo increasing intraspecific and interspecific competition forces that would lead to changes in their spatial distributions. Forest stands of different ages are thought to be influenced by different processes. Biotic agents, such as insects and disease and physical damage, contribute to mortality and are particularly important for the changes in older stands (Larson and Franklin, 2010; Acker et al., 2015), while competition and self-thinning are more prominent in younger forests (Kenkel, 1988). My results suggest the spatial dynamics of forest stands have changed over time and differed with stand ages, and that density-dependent mortality played a role in these changes at all successional stages.

2.4.1 Changes in spatial patterns and effects of density-dependence

Over the two censuses, Douglas fir distribution became less aggregated and trended towards regularly in all stands as predicted. The regularity of this species increased with stand age, displaying a high degree of aggregation in the immature south plot and spatial regularity in the old-growth stand. These patterns of regularity are expected when there is competition for resources among individuals (Pielou, 1960). The non-random mortality exhibited by Douglas fir is related to density-dependent processes, including both intraspecific and interspecific competition, with tree mortality occurring in significantly more crowded neighbourhoods than those for surviving trees. Conspecific neighbourhood density is particularly important for determining Douglas fir mortality. This was expected in the immature stands, where stand densities are high and self-thinning is overwhelming. Similar results were found in young forests in the western Cascades where suppression mortality occurred in 80% of stands and competition was the dominant process for >50% of tree deaths (Lutz and Halpern, 2006). Contrary to previous studies that found the main drivers of mortality shifted from competition to physical damage and biological agents in mature stands (Franklin and van Pelt, 2004; Larson and Franklin, 2010), my results show density-dependent mortality of Douglas fir occurring in all forest ages, including mature and old-growth stands, suggesting competition continues to play a large role in determining tree mortality in older forests. This trend is confirmed by Das et al. (2011) in California and a previous study at the same old-growth site (He and Duncan, 2000). The significant

evidence of competition-driven mortality of Douglas fir in mature and old-growth forests highlights the importance of processes influencing tree mortality throughout succession.

The trends for late-successional western hemlock and western redcedar were different from that for Douglas fir. These species showed slightly increased aggregation between the first and second censuses and the strength of overall aggregation increased with stand age. Density-dependent mortality was evident in the immature stand for both species but showed no significance in the mature plot. These species may follow the assumption that competition has reduced importance in older stands. However, Lutz and Halpern (2006) found that mortality in young stands was dominated by mechanical damage rather than suppression for hemlock and redcedar which is inconsistent with the density-dependent tree death at the immature stage found in my study. Moeur (1997) found small- and intermediate-sized trees showed aggregated and mixed spatial patterns, respectively, due to their reduced competitive capabilities and smaller crown size. As late-successional species, hemlock and redcedar would be less competitively successful than the dominant and established Douglas fir trees, which could limit success to favourable environments and lead to spatially aggregated distributions. A previous study of plots at this site suggested that hemlock and redcedar mortality in the old-growth stage was not influenced by neighbourhood densities of Douglas fir and that factors such as elevation and moisture may determine the survival distribution of these species (He and Duncan, 2000). There also appeared to be increased mortality for the shade-tolerant species in neighbourhoods with fewer conspecifics in later successional stands indicating survival may be linked to higher conspecific density through intraspecific facilitation.

The aggregated pattern of hemlock and redcedar small trees and the relative neighbourhood crowding, particularly of conspecific adults, suggests that establishment occurs more frequently in proximity to potential parent trees. Seed dispersal is considered one of the most limiting factors in seedling distribution and results in trees establishing in higher numbers around parent trees (Hille Ris Lambers and Clark, 2003). Clustering of small trees around conspecific adults is expected and reflects dispersal limitations and an absence of density-dependent competition. Johnson et al. (2014) found similar results of seedling density being positively correlated with conspecific basal area, indicating short distance of dispersal and suitable habitat associations. However, they also found evidence for density-dependent mortality of seedlings around conspecifics, indicating an important relationship between dispersal limitations and density-dependence in determining seedling dynamics. Western redcedar reproduces through seed development as well as through

vegetative reproduction through layering, fallen branches developing roots, and branches growing up from fallen trees (Burns and Honkala, 1990). Trees established vegetatively will be inherently clumped around adult trees, which would result in the aggregation seen in the mature and old-growth stands.

The pattern of Douglas fir recruitment around parent trees showed a different trend than the shade-tolerant species. This species showed conspecific neighbourhood crowding of recruits in the immature stand suggesting some dispersal limitations and habitat associations, as seen with the other species. However, in the mature stand Douglas fir showed dispersion from larger conspecific trees at small scales. As a shade-intolerant species, Douglas fir survival is limited to open habitats receiving high inputs of light, such as large gap openings. The number of recruits of this species was low overall, suggesting that suitable establishment habitats were limited. The immature and mature stands had a closed canopies and high understory densities of salal over large areas of the plots. Douglas fir seedlings have very low survival in habitats with dense understory vegetation and under closed canopies due to the lack of light, and gaps must be sufficiently large for regeneration to occur (Gray et al., 2012). Successional patterns for Douglas fir recruits were difficult to assess due to insufficient numbers of recruits in three of the five plots.

Establishment conditions is another factor in determining survival and spatial patterns of small trees, with environmental gradients dictating the suitability of micro-sites for survival (Clark et al., 1998). The overall aggregation of small trees at these sites may indicate establishment occurred in favourable microenvironments capable of supporting the germination and survival of high densities of small trees. Facilitation may also play a role in the aggregated distribution of small trees. It has been documented that higher densities of seedlings and adults can increase plant growth and survivorship (Bruno et al., 2003). Intraspecific aggregation at the seedling stage is also suggested to reduce the number of negative interactions between heterospecifics, and therefore support seedling survival (Raventós et al., 2010).

2.4.2 Patterns of interspecific spatial associations

In the forest I studied, shade-tolerant species (hemlock and redcedar) were expected to show dispersion from pioneer shade-tolerant Douglas fir. However, no spatial associations were found in the immature plots for either species around Douglas fir. Numbers of hemlock and redcedar were low in the immature stands and could be

insufficient for detecting associations. Dispersion from Douglas fir became more pronounced in the old-growth stand for western hemlock, and in the mature south and old-growth stands for western redcedar, indicating the degree of spatial dispersion may become more important with stand succession. The negative association could suggest the suppression of Douglas fir on western hemlock and redcedar that results in tree mortality. Getzin et al. (2006) suggest spatial dispersion between species may be the result of niche specialization, rather than interspecific competition, where variation in microenvironments can cause species to establish in different habitats. Habitat heterogeneity has been suggested by others as a mechanism of species dispersion, as well as clumping due to vegetative reproduction (Pielou, 1961). Several processes acting simultaneously may result in the same dispersed spatial patterns exhibited by the species in these stands. However, the positive association of redcedar around Douglas fir in the mature stands cannot be explained by competition but by the nursery effect of Douglas fir on redcedar (Bertness and Callaway, 1994). Western hemlock and redcedar were predicted to show positive spatial associations as a result of their similar shade tolerances and establishment strategies. However, only in the immature stand did the species show a positive heterospecific association and the spatial association became less strong with succession. The lack of strong spatial interactions between these species could indicate that neither negative processes (interspecific competition) nor positive processes (habitat affinity, facilitation) are occurring at sufficient levels to bring about a detectable spatial pattern, or that opposing processes are acting simultaneously causing a neutral association.

2.5 Conclusion

Tree mortality and recruitment are the demographic rates responsible for changes in stand spatial characteristics. This study has confirmed that spatial patterns of tree distribution in forest stands of different ages change over time. As expected, Douglas fir tended towards spatial regularity, and western hemlock and western redcedar toward spatial aggregation with the increase of stand age, indicating life history traits and species characteristics are important indicators in predicting the spatial changes of forest stands at different stages of succession.

Density-dependent mortality was found to be important for all three dominant tree species, and in all ages of stands. Both intraspecific and interspecific competition played important roles in determining the spatial dynamics and distributions of species in forest

stands, and are key mechanisms for understanding tree mortality. Recruitment occurred dominantly in neighbourhoods with high numbers of potential parents trees, suggesting seed dispersal and suitable habitat for establishment are important in determining the spatial distribution of tree recruits.

The potentials for intraspecific and interspecific facilitation and species habitat preferences as drivers of the unexpected species associations and regular mortality experienced by hemlock and redcedar call for further research into understanding the extent to which these processes are driving observed patterns.

Findings from this study show the diversity of mechanisms regulating mortality and recruitment in forest stands of different ages. Understanding the importance of density-dependent effects on demographic rates in stands of all ages, and particularly in old forests, will be critical for determining the implications of climate change and management practices on forest dynamics.

Chapter 3: Growth and Mortality Responses of Three Coastal Conifer Species to Endogenous and Exogenous Factors

3.1 Introduction

The temperate rainforests of the Pacific Northwest are among the most productive ecosystems globally (DellaSala et al., 2011), maintaining a high capacity of carbon sequestration (Emmingham and Waring, 1977). The tree species that dominate these forests are long-lived and capable of surviving several centuries under past and current conditions. Growth and mortality rates of the dominant species are the drivers of forest productivity and stand structure, making them a critical aspect of forest dynamics. These demographic rates have been the focus of many studies with the aim of understanding the main factors influencing growth and mortality, including exogenous (e.g., climate) and endogenous (e.g., competition) processes (McLaughlin et al., 1987; Girardin et al., 2012; Etzold et al., 2014).

Climate is known to have an impact on forest structure and dynamics, and is particularly important in the temperate forests of coastal British Columbia where temperature and moisture are considered to be key factors that classify biogeoclimatic zones and species assemblages (Pojar et al., 1991b). Several recent studies have found evidence suggesting climate as a major factor governing forest dynamics with effects on ecosystem functioning and services including hydrologic processes, productivity, and species composition (Schuur, 2003; Lutz et al., 2010; Suarez and Kitzberger, 2010; Anderegg et al., 2013). This finding has important implications in the context of climate change. IPCC (2007) has predicted temperature increases and precipitation reductions in coastal British Columbia by the end of the 21st century, and these climate changes are expected to cause altered tree growth and mortality regimes. Changes in forest dynamics in relation to regional climate change have been documented in forests around the globe (Allen et al., 2010). Evidence of decreased growth rates as a result of regional warming has been found in tropical forests of Panama and Malaysia (Feeley et al., 2007) and biomass sequestration rates have declined in the boreal forests of Canada related to drought-induced water stress (Ma et al., 2012). Similar findings have related climate change to rising mortality rates in Canada's boreal forest (Peng et al., 2011) and in forests of the Pacific Northwest United States (van Mantgem and Stephenson, 2009). While the long-term effects of climate change on tree demographics are unknown and the responses of individual species and forest types

are likely to differ at regional scales, the observed decreased growth and increased mortality trends highlight the importance of studying the effects of climate on forest dynamics and demographic rates.

In addition to climate, endogenous factors are widely accepted as important drivers of forest dynamics and succession. Competition between individuals, both intraspecific and interspecific, is a key process regulating tree growth and mortality. Limited access to resources, such as light, water and nutrients, puts individuals at risk of reduced growth and increased mortality (Begon et al., 1996). Competition is thought to be a dominant process in young forest stands, where high establishment densities followed by rapid canopy closure results in tree mortality and stand self-thinning (Watkinson et al., 1983; Kenkel, 1988). As forest stands mature, the importance of competition is thought to diminish while the role of insects, disease and wind damage increases as older trees become more susceptible to their attack (Franklin et al., 2002). However, recent evidence has shown competition continues to be an important driver of growth and mortality in all stages of succession (Das et al., 2011; Fraver et al., 2014). Studying the importance of competition and its interactions with other stressors, such as altered temperature and moisture regimes, is necessary for understanding forest demographic changes through succession.

Multiple drivers are likely important for determining the demographic dynamics of forest stands. The factors that ultimately lead to reduced growth or tree mortality are often difficult to disentangle due to their interactive and sequential nature (Franklin et al., 1987). Individual tree modeling is a useful method for analyzing conditions at the tree level and allows for the accurate assessment of mortality risk and growth based on local scale drivers (Pretzsch, 2009). For these models, the determination of neighbourhood scale at which potential drivers (e.g., competition) are evaluated is a challenging problem. Consequently, the various methods for determining possible competitors, using different competition indices, may well result in different outcomes, biasing the inference on competition (Rivas et al., 2005). Assessing various competition indices and neighbourhood sizes is necessary for determining the best representation of local competition. Incorporating local scale drivers into individual tree growth and mortality models allows for quantifying the contribution of driving factors (such as competition, climate, tree size and habitat characteristics) for an in-depth understanding of the dominant processes governing forest dynamics.

Forests are being managed to meet an increasing number of objectives including timber production, carbon sequestration, biodiversity, and soil and water regulation (Curtis

et al., 1998; Pichancourt et al., 2014). Understanding how forests respond to climate and competition pressures is critical for future stand projections and sustainable management of forests. The primary objectives of this study were to (i) analyze the importance of competition and climate on tree growth rates at three stages of forest succession and (ii) determine the degree that competition influences mortality across different stand ages to gain a deeper understanding of forest dynamics under current and future conditions. The results of this study should contribute to better predicting the change of forest ecosystems in response to the change of climate and to sustainably managing forests to meet multiple objectives.

3.2 Data and Methods

3.2.1 Study Site Description

The study plots are located within or adjacent to the Greater Victoria Water Supply Area on southeast Vancouver Island (48°38′, 123°43′, Fig. 2.1). Positioned on the leeward side of the south Vancouver Island ranges, the study is within the Coastal Western Hemlock zone, Very Dry Maritime subzone of British Columbia's biogeoclimatic zone classification (Klinka et al., 1991). This area had a mean annual temperature of 8.7°C and mean annual rainfall of 1624 mm during the study period. The mild climate is characterized by dry, warm summers and wet winters. The forest is dominated by shade-intolerant, pioneer species Douglas fir with shade-tolerant Western Hemlock and Western redcedar as late-successional colonizers. Other species, including western white pine (*Pinus monticola* Dougl. ex D. Don), grand fir (*Abies grandis* [Dougl. ex D. Don] Lindl.), bigleaf maple (*Acer macrophyllum* Pursh), and red alder (*Alnus rubra* Bong.), are present in small numbers. The understory vegetation has variable densities of salal (*Gaultheria shallon* Pursh), dull Oregon grape (*Mahonia nervosa* [Pursh] Nutt.), sword fern (*Polystichum munitum* [Kaulf.] Presl) and other herbaceous species.

Six plots were initially established in 1997 and 1998 to study spatial patterns and tree mortality (He and Duncan, 2000). These plots were part of a larger chronosequence network established by the Canadian Forest Service (Trofymow et al., 1997). The six plots themselves formed a chronosequence of forest stands, with two immature (25-45 years old), two mature (65-85 years old), and two old-growth plots (>200 years old). Stands were classified by age as of the year 1990 (Trofymow et al., 1997). The plots within the chronosequence series were designated as north and south based on location (for example,

immature north and immature south plots). The immature stands originated from planted regeneration following clear-cut harvesting. The mature north plot regenerated naturally following harvest, while the old-growth and mature south plots regenerated naturally after stand-clearing fires. All plots are located approximately within a distance of 10 kilometers. Plots range in size from 0.7 to 1.2 hectares, with an average size of 1.1 ha. The maximum elevation difference between plots is 225 m and plots are located on gentle to intermediate slopes with average slope of 18.2%. The old-growth south plot was lost to clear-cut harvesting prior to recensus. Part of the mature north plot was also lost to blowdown caused by adjacent logging (Fig. 2.2) and therefore only the unaffected section was analyzed in this study. As a result, only 5 plots were studied in this thesis and their characteristics, and disturbance and regeneration histories are described in Table 2.1.

3.2.2 Data Collection

3.2.2.1 Inventory Data

Plots were established and first censused in 1997 or 1998. All live and dead trees were tagged and the x, y, z coordinates were recorded relative to a reference point using a total station system (Fig. 2.2). Each tree was identified to species. Diameter at breast height (DBH, 1.3 m above ground level) was measured using a diameter tape or callipers, and tree status was recorded, classified as live, dead standing (snag), log, stump, or as a seedling for trees less than 1.3 m in height. Tree heights were also measured using a vertex hypsometer for all trees in two of the five plots: immature south and old-growth.

Re-censuses of the plots were completed in the summer of 2014, making the census interval 16 to 17 years. Diameter and status measurements were repeated on all trees that were live at the first census. Tree heights were remeasured for all trees in the immature south and old-growth plots, and measurements were collected for a sample of trees in the other three plots. Stems that did not exist in the first census in 1997 and 1998 but were growing in 2014 were new recruits. Recruits were tagged, identified and measured; their locations were calculated by trilateration from distances recorded to three neighbouring trees.

3.2.2.2 Increment Coring

Within each plot, live trees were selected for coring for annual growth analysis. Trees were divided into diameter classes of 10-20 cm, 20-30 cm, 30-40 cm and >40 cm to ensure all sizes were represented. In each plot, 60 trees were selected, divided evenly among the three focal species (20 Douglas fir, 20 western hemlock and 20 western redcedar) and size classes wherever possible. Western hemlock and western redcedar had insufficient numbers to sample the full range of sizes in some plots. In May of 2015, two increment cores were collected from each stem, 90° apart at 1.3 m in height, using a Haglof 5.1 mm increment borer. A total of 604 cores were collected from 302 trees.

Cores were air dried, secured to mounting boards, and sanded with coarse and fine sand paper until ring boundaries were clearly visible (Fig. 3.1). Rings were measured in the lab using WinDENDRO™ image analysis software (Version 7.6.5, Regent Instruments Inc., Quebec, Canada). All core images were visually inspected after digital analysis to ensure accuracy of ring identification and width measurements. Damaged cores were removed from the analysis. Ring widths from the two cores for each tree were averaged to determine mean annual growth increment and converted to mean annual basal area increment (BAI).

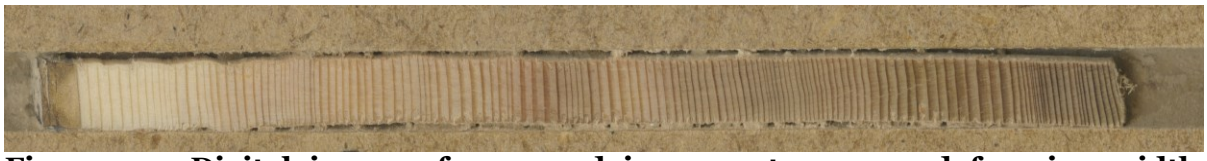

Figure 3.1. Digital image of prepared increment core used for ring width analysis.

3.2.3 Independent Variable Selection and Calculation

Individual tree multiple regression models for growth and mortality were developed and biotic and abiotic variables of focal trees and their environment were included in the models. Variables were chosen *a priori* based on biological meaning and importance.

3.2.3.1 Tree Size

Tree size and age are commonly correlated with tree performance making them important predictors of growth and mortality. Small, young trees generally have larger diameter growth but lower corresponding basal area growth, while the opposite holds for

large, older trees. For very old trees, both diameter and basal area growth are often slow. Therefore, growth rate is expected to differ depending on tree size and age (Stoll et al., 1994). To account for the effect of tree size on growth, initial tree size, recorded at the first census, was included in all models.

Mortality rate is usually highest in small trees and decreases with increasing tree size. However, mortality risk increases again in very large trees, as older trees are more susceptible to biotic and abiotic damage. This trend produces a U-shaped mortality curve with mortality rates lowest in intermediate size classes (Buchman et al., 1983; Lorimer and Frelich, 1984). To account for this trend, DBH and DBH^2 were included as variables in the mortality models (Monserud and Sterba, 1999; Yang et al., 2003).

While age is an important factor affecting growth rate and mortality risk, data on age are intensive to collect and are rarely available for all trees, particularly in large plots. For this reason, tree size is often used as a proxy for age since it captures the effect of size and relative age in one variable (Yao et al., 2001; Yang et al., 2003).

3.2.3.2 Slope and Elevation

Slope and elevation were included in the models to account for potential habitat heterogeneity and topography within the plots. Elevation, in meters, was calculated from a point of known elevation using relative z-coordinates from the stem maps. Slope was calculated using the x, y, and z coordinates for neighbouring trees within 5 m of a focal tree. Slope between focal tree (f) and neighbour tree (i) pairs was calculated as

$$Slope_{f,i} = atan\left(\frac{z_f - z_i}{\sqrt{(x_f - x_i)^2 + (y_f - y_i)^2}}\right) * 57.2958\,, \qquad [3.1]$$

where x, y and z are the tree coordinates, $atan$ is the inverse tangent function and 57.2958 is the constant for converting radians to degrees. The slope between each focal and neighbour tree pair within the 5 m radius was averaged and used as the estimate of degree slope for the focal tree.

3.2.3.3 Competition Indices

Competition intensity was quantified for each tree individually using three primary variables: DBH, basal area, and inter-tree distances. Indices considered include density, basal area of larger trees, Hegyi index, diameter ratio, diameter-distance ratio, and horizontal angle sum. Formulas and sources for the indices are summarized in Table 3.1.

Since many of these indices include focal tree initial size, which is a separate variable in the models, competition indices were modified to exclude focal tree diameter to avoid confounding effects of the predictors. Basal area of the nearest neighbour and the distance to the nearest neighbour of the focal tree were also tested. The final set of competition indices is summarized in Table 3.2 and includes distance-independent (CI1, CI3, CI4, CI5) and distance-dependent (CI2, CI6, CI7) indices.

Table 3.1. Formulas and sources for competition indices.

Competition index	Formula	Sources
Density	n	
Basal area of larger trees	$\sum_{i=1}^{n} BA_{i\ (BA_i > BA_f)}$	(Wykoff et al., 1982)
Hegyi	$\sum_{i=1}^{n} (\frac{DBH_i}{DBH_f}) \ / Dist$	(Hegyi, 1974)
Diameter ratio	$\sum_{i=1}^{n} \frac{DBH_i}{DBH_f}$	(Lorimer and Frelich, 1989)
DBH-distance ratio	$\sum_{i=1}^{n} \frac{DBH_i}{Dist}$	(Cortini and Comeau, 2008a)
Horizontal angle sum	$\sum_{i=1}^{n} \frac{DBH_i}{DBH_j} * \arctan(\frac{DBH_i}{Dist})$	(Rouvinen and Kuuluvainen, 1997; Contreras et al., 2011)

n = number of trees; BA_i = basal area of neighbour *i*; BA_f = basal area of focal tree; DBH_i = diameter at breast height of neighbour *i;* DBH_f = diameter at breast height of focal tree; Dist = distance between focal tree and neighbour *i*.

Table 3.2. Selected competition indices and modified index formulas.

Index no.	Competition index	Formula
CI1	Nearest neighbour basal area	BA_i
CI2	Nearest neighbour distance	$Dist_i$
CI3	Density	n
CI4	Basal area larger	$\sum_{i=1}^{n} BA_{i\ (BA_i > BA_f)}$
CI5	Sum DBH	$\sum_{i=1}^{n} DBH_i$
CI6	DBH-distance ratio	$\sum_{i=1}^{n} \frac{DBH_i}{Dist}$
CI7	Horizontal angle sum	$\sum_{i=1}^{n} \arctan(\frac{DBH_i}{Dist})$

See Tabl3 3.1 for definitions of abbreviations.

When calculating the indices for each tree, correction for edge effects was applied. As discussed in Chapter 2 (Section 2.2.2 Spatial Pattern Analysis), edge effects arise when a focal tree is located near the plot boundary and characteristics of trees outside the plot are unknown. Without edge correction, the competition level for a tree near the edge of the plot would be underestimated because any competitor trees located outside the plot would not be accounted for (Radtke and Burkhart, 1998). Translation edge correction replicates the main plot eight times as border plots and assumes the pattern of trees outside the study area is the same as within. Figure 3.2 shows a diagram example of this edge correction method. Translation edge correction has been showed to reduce bias (Monserud and Ek, 1974) and was the method applied when calculating the competition indices.

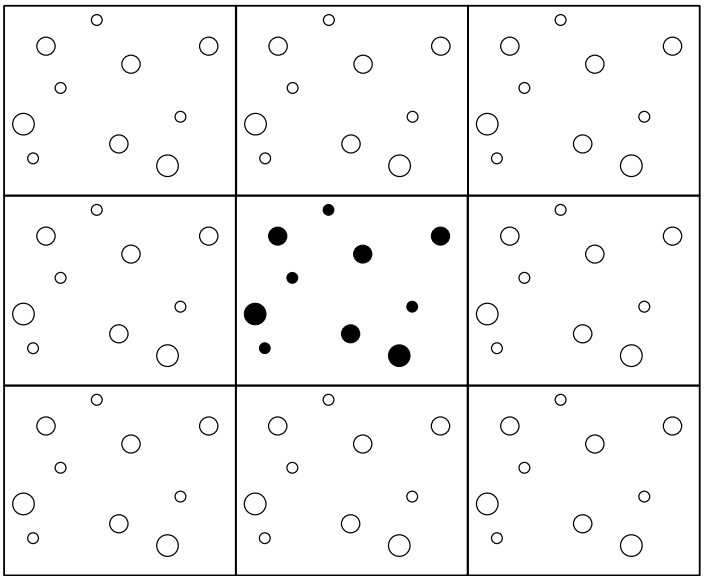

Figure 3.2. Diagram of translation edge correction. Centre rectangle with filled circles (●) represents the main study plot; surrounding replicates with open circles (O) are the translated boundary plots for calculating competition indices of edge trees.

3.2.3.4 Climate Variables

Climate data from three weather stations located within the Greater Victoria Watershed Supply Area were provided by the Victoria Capital Regional District. Hourly data from each station were summarized into daily, monthly and annual variables, and averaged across the three stations. Climate variables were selected based on findings from previous studies and knowledge of species-specific growth preferences. The focal species are adapted to mild, wet winters and dry, warm summers but experience growth limitations under drought conditions (Waring and Franklin, 1979). Altered temperature and precipitation regimes under regional climate change will impact growth and mortality trends for the study species (Laroque and Smith, 2005). Table 3.3 holds a summary of the climate variables over the study period. Mean annual temperature (MAT), mean warmest month temperature (MWMT), mean coldest month temperature (MCMT), and growing degree days over 5°C (DD5) for the calendar year were calculated for temperature variables.

Moisture variables included mean annual precipitation (MAP), mean summer precipitation (MSP) for May to August, and climate moisture index (CMI). Climate moisture index is calculated as precipitation minus potential evapotranspiration and is a measure of water availability and drought. It was calculated monthly, summed for the year (January-December) and reported as annual CMI. Low and negative values of CMI suggest dry or drought conditions. The calculation of CMI follows the methods outlined in Hogg (1997) and Hogg, Barr, and Black (2013). Potential evapotranspiration (PET) is defined by Hogg et

al. (2013) as "the expected rate of water vapour loss to the atmosphere from a well-vegetated landscape assuming adequate soil moisture in the plant rooting zone". This method for estimating CMI assumes that evapotranspiration in conifer forests is driven primarily by vapour pressure rather than net radiation and is calculated with the simplified Penman-Monteith equation as

$$PET = 93\, VPD\, k_t \exp\left(\frac{Elev}{9300}\right), \quad [3.2]$$

where *VDP* is the vapour pressure deficit (Equation 3.3), k_t is a modifier for cold temperatures (Equation 3.5), and *Elev* is the plot elevation. *VDP* is calculated using the mean monthly maximum and minimum temperatures as

$$VPD = 0.5(e^*_{Tmax} + e^*_{Tmin}) - e^*_{Tdew}, \quad [3.3]$$

and where e^*_T is

$$e^*_T = 0.61078 \exp\left(\frac{17.269\, T}{237.3 + T}\right). \quad [3.4]$$

If T is the mean monthly maximum, minimum or dewpoint temperature, the equation corresponds to e^*_{Tmax}, e^*_{Tmin}, or e^*_{Tdew} respectively. Dewpoint temperature is estimated as mean monthly minimum temperature minus 2.5°C.

k_t, the cold temperature modifier, decreases linearly from 1.0, when mean monthly temperature (T_{mean}) is ≥ 10°C, to 0.0 when mean monthly temperature is ≤ -5°C and is calculated by

$$k_t = \max\left(\min\left(\left(\frac{T_{mean} + 5}{15}\right), 1\right), 0\right). \quad [3.5]$$

Table 3.3. Summary of the means, ranges and 5-year averages for the climate variables of interest.

Variable	Mean	Min.	Max.	5 Year Mean	
				1997-2001	2010-2014
MAT	8.75	7.85	10.19	8.29	9.09
MWMT	17.61	15.57	19.89	16.84	17.94
MCMT	1.65	0.15	3.00	1.43	1.84
MAP	1624.68	1149.48	2051.92	1684.20	1584.05
MSP	143.12	70.95	208.68	183.33	134.05
DD5	1728.45	1455.71	2173.17	1582.24	1820.48
CMI	37.34	-17.67	92.99	56.50	32.84

MAT, MWMT and MCMT are in °C; MAP and MSP are in mm; CMI is in cm yr^{-1}.

3.3 Statistical Analysis

3.3.1 Growth-Competition Modeling

Linear and nonlinear regression modeling was used to analyze the absolute basal area increment growth rate of trees as a function of tree size, local habitat, and competition. Trees included in this analysis were >0.5 cm DBH at the first measurement and survived to the second census. Plots were grouped by stand age class (immature, mature and old-growth) and models were developed for each of the three dominant species for each age class separately. A minimum of 20 trees for each age-species group was needed for modeling. Linear and nonlinear mixed effects models were also fit with plot as a random effect to account for variation among study plots. Models with and without the random effect were compared to determine if the increased model complexity resulted in additional explanatory power.

The dependent variable, absolute basal area increment growth, was calculated as

$$Growth\ rate = \ln\left(\frac{BA_{T2} - BA_{T1}}{T_2 - T_1} + 1\right), \qquad [3.6]$$

where T_1 is the year of the first measurement, T_2 is the year of the second measurement, and BA_{T1} and BA_{T2} correspond to basal area tree size at the first and second measurements, respectively. Independent variables of the models included initial size (basal area), slope, elevation and competition. The simplest model tested was a linear function with the form

$$Growth\ rate = \beta_0 + \beta_1 CI + \beta_2 Initial\ Size + \beta_3 Slope + \beta_4 Elevation\,, \qquad [M1]$$

where CI is a competition index, β_0 is the intercept and β_1, β_2, β_3 and β_4 are parameter estimates from the generalized least-squares (GLS) regression analysis. GLS regression allows for variance and correlation structures to be applied to residuals or for repeated measures. However, it is known that the relationship between growth and independent variables is not always linear. Several nonlinear model forms were tested and included different combinations of exponential, power, and linear functions on the independent variables based on exploratory data analysis and models from the literature (Comeau et al., 2003; Cortini and Comeau, 2008b). Exploring different relationships between the response and predictor variables ensures the appropriate relationship is found and the most

parsimonious model is selected (Paine et al., 2012). Table 3.4 shows the full list of models tested in the analysis.

Table 3.4: List of model forms tested for growth-competition analysis.

Model no.	Model form
[M1]	$\beta_o + \beta_1$ CI $+ \beta_2$ Initial Size $+ \beta_3$ Slope $+ \beta_4$ Elevation
[M2]	$\beta_o + \beta_1$ CI $+$ Initial Size$^{\beta_2} + \beta_3$ Slope $+ \beta_4$ Elevation
[M3]	$\beta_o + \exp(\beta_1$ CI$)$ + Initial Size$^{\beta_2} + \beta_3$ Slope $+ \beta_4$ Elevation
[M4]	$\beta_o +$ CI$^{\beta_1}$ + Initial Size$^{\beta_2} + \beta_3$ Slope $+ \beta_4$ Elevation
[M5]	$\beta_o + \beta_1$ CI $+$ Initial Size$^{\beta_2} +$ Slope$^{\beta_3} + \beta_4$ Elevation
[M6]	$\beta_o + \beta_1$ CI $+$ Initial Size$^{\beta_2} + \beta_3$ Slope + Elevation$^{\beta_4}$
[M7]	$\beta_o + \exp(\beta_1$ CI$)$ + Initial Size$^{\beta_2} +$ Slope$^{\beta_3} + \beta_4$ Elevation
[M8]	$\beta_o + \exp(\beta_1$ CI$)$ + Initial Size$^{\beta_2} + \beta_3$ Slope + Elevation$^{\beta_4}$
[M9]	$\beta_o +$ CI$^{\beta_1}$ + Initial Size$^{\beta_2} +$ Slope$^{\beta_3} + \beta_4$ Elevation
[M10]	$\beta_o +$ CI$^{\beta_1}$ + Initial Size$^{\beta_2} + \beta_3$ Slope + Elevation$^{\beta_4}$
[M11]	$\beta_o + \exp(\beta_1$ CI$)$ + Initial Size$^{\beta_2} +$ Slope$^{\beta_3} +$ Elevation$^{\beta_4}$
[M12]	$\beta_o +$ CI$^{\beta_1}$ + Initial Size$^{\beta_2} +$ Slope$^{\beta_3} +$ Elevation$^{\beta_4}$

CI is the competition index, β_o, β_1, β_2, β_3 and β_4 are model specific parameters estimated by the regression analysis.

3.3.1.1 Neighbourhood Radius Selection

The first step in modeling growth rate was to determine the optimum neighbourhood size to evaluate the effect of competition. This was done by sequentially increasing the neighbourhood radius around the focal trees from 1 m to 15 m, in 1 m increments. Five competition indices CI3-CI7 from Table 3.2 were calculated for each neighbourhood size. For example, a neighbourhood radius of 5 m would include all trees within 5 m of a focal tree as neighbours when calculating the competition index. The relationships between growth and dependent variables were explored graphically and with preliminary models. Two nonlinear forms, [M2] and [M3] from Table 3.4, were selected based on exploratory data analysis. Each competition index and radius combination was regressed with the two nonlinear models. Akaike Information Criteria (AIC) was calculated for each model and used to compare models, with a smaller value indicating better model fit (Akaike, 1974).

A total of 150 models with different combinations of competition indices (5), radii (15) and model forms (2) were tested for each age-species pair. Optimum neighbourhood size was defined as the radius that minimized the AIC value across all competition indices,

assuming that top performing models captured the best radius for assessing competition (Silander and Pacala, 1985; Simard and Sachs, 2004; Fraver et al., 2014).

3.3.1.2 Competition Models

After selection of the optimum neighbourhood radius, 12 linear and nonlinear models for growth and competition were tested and evaluated for performance. All model forms used in the analysis are listed in Table 3.4. All models were fit for each age-species group separately using generalized least squares regression analysis. The response and independent variables were the same as described above. Each model was fit with the seven competition indices in Table 3.2. Competition indices were calculated using the optimum neighbourhood radius selected in the previous step.

A total of 84 models were fit to assess the effect of competition, size and habitat variables on absolute basal area increment growth rate (Equation 3.6) for each age-species group. Model AIC values were compared and residual plots were visually analyzed. Top models with ΔAIC <2 were fitted with variance structures to meet the assumption of homogenous residual variance. The model with the lowest AIC value and no residual structure was selected as the final model.

3.3.2 Growth-Climate Modeling

Linear mixed effects models were used to assess the effect of climate on the annual growth rate of individual trees of each species-age group. The response variable, basal area increment (BAI), was log-transformed as ln(BAI + 1) (Martin-Benito et al., 2011). Independent variables in the model included climate for the year of tree ring growth (T) and climate for the year previous to growth (T-1). Seven climate variables were initially considered for inclusion in the model (Table 3.3). However, there was a high degree of multicollinearity between some of the variables when correlation coefficients (Fig. 3.3) and variance inflation factors were calculated. DD5 was strongly correlated with MAT and MWMT (Pearson's correlation coefficient = 0.97 and 0.8, respectively). MAP was highly correlated with CMI (Pearson's correlation coefficient = 0.93). To reduce collinearity among predictor variables, DD5 and MAP were excluded as variables in the final model. MAT and MWMT were also significantly correlated but the correlation was lower (Pearson's correlation coefficient = 0.73) and both were kept as predictors in the model.

MAT	**0.73**	0.39	0.01	-0.38	**0.97**	-0.26
5e-04	MWMT	-0.04	0.2	-0.27	**0.8**	-0.06
0.1128	0.8668	MCMT	0.35	-0.26	0.2	0.24
0.981	0.4153	0.1564	MAP	-0.19	-0.09	**0.93**
0.1252	0.2695	0.294	0.4456	MSP	-0.38	0.01
0	**1e-04**	0.4352	0.7312	0.1196	DD5	-0.36
0.3049	0.8129	0.3392	**0**	0.9716	0.1456	CMI

Figure 3.3. Correlation matrix among climate variables.
Upper panel shows Pearson's correlation coefficients and lower panel shows p-values (α=0.05) for the relationship between climate variables. Bold, red values indicate significant correlations.

Linear mixed effects models were fit for each age-species group separately and the final model form was

$$\ln(BAI+1) = \beta_0 + \beta_1 MAT_T + \beta_2 MWMT_T + \beta_3 MCMT_T + \beta_4 MSP_T + \beta_5 CMI_T + \beta_6 MAT_{T-1} + \beta_7 MWMT_{T-1} + \beta_8 MCMT_{T-1} + \beta_9 MSP_{T-1} + \beta_{10} CMI_{T-1} + Tree, \quad [M13]$$

where β_0, β_1, β_2, ..., β_{10} are parameter estimates from the restricted maximum likelihood regression analysis and *Tree* is the random effect of tree ID. Tree ID was included as a random effect to account for variability in conditions among trees that could influence annual growth. Competition and size were measured only at the beginning and end of the study period and therefore could not be modeled annually, and habitat variables (slope and elevation) did not change throughout the study. The variation in growth attributed to these variables was captured with the random effect of tree ID. Models were also fit with plot as an additional random effect to account for variation among study plots. Models with and without plot as a random effect were compared to determine if the increased model complexity resulted in additional explanatory power.

Tree ring data make up a time-series with observations being temporally correlated. Models were fit with correlation structures to account for autocorrelation between annual

observations. Autoregressive models with time lag 1 and 2 were tested and compared for goodness of fit using AIC values. The lag refers to the number of time units between two observations. For example, lag 1 refers to correlation between observations one time unit (one year) apart (Pinheiro and Bates, 2000). Models were also fit with variance structure to meet residual assumptions and AIC values were compared to test for model improvement. The model with the lowest AIC value was selected as the final model.

Statistical analyses were completed using the R statistics program (R Core Team, 2015). Linear and nonlinear fixed-effects and mixed-effects models were conducted using the *nlme* package (Pinheiro et al., 2015).

3.3.3 Mortality Modeling

Individual tree morality was modeled for each age-species group to analyze the effect of neighbourhood competition and local habitat on survival. All trees with DBH >0.5 cm and "live" status at the first measurement were included in the analysis. The response variable was binomial 0 or 1 indicating whether the tree was dead or alive, respectively, at the second census. Logistic regression has been widely used for modeling tree mortality and was implemented using generalized linear models (Hubbell et al., 2001; Das et al., 2008; Crecente-Campo et al., 2009; Wang et al., 2012). Probability of mortality was modeled as a function of initial tree size (DBH), slope, elevation and competition (CI), and had the form

$$P_m = 1 - \frac{e^{\beta_0 + \beta_1 DBH + \beta_2 DBH^2 + \beta_3 Slope + \beta_4 Elevation + \beta_5 CI}}{1 + e^{\beta_0 + \beta_1 DBH + \beta_2 DBH^2 + \beta_3 Slope + \beta_4 Elevation + \beta_5 CI}}, \qquad \text{[M14]}$$

where P_m is the probability of mortality and β_0, β_1, β_2...β_5 are parameter estimates from the logistic regression analysis. Logistic regression mixed effects models were also fit with plot as a random effect to account for variation among study plots. Models with and without the random effect were compared to determine if the increased model complexity resulted in additional explanatory power and goodness-of-fit.

Optimum radius and competition index selection was completed in a single step in this analysis. The model (M14) was fit with each of the five neighbourhood-dependent competition indices (CI3-CI7, Table 3.2) and 15 radius sizes from 1 m to 15 m. Models with CI1 and CI2 were also fit, resulting in a total of 77 models for each age-species combination. AIC values and Nagelkerke's R^2 (Nagelkerke, 1991) were calculated for each model. For

mixed effects models, R^2 values were calculated using the method suggested by Nakagawa and Schielzeth (2013). The top model for each age-species combination was selected based on AIC and R^2 values. The model with the smallest neighbourhood radius across all competition indices, and within $\Delta AIC < 2$ of the lowest model and R^2 within 0.5% of the highest model was selected. It was assumed that top performing models captured the best radius and index for assessing competition.

The Hosmer and Lemeshow goodness-of-fit test was used to assess model fit. Observations were sorted into 10 equal groups based on their predicted survival probabilities (Hosmer and Lemeshow, 2000; Yao et al., 2001). Pearson's Chi-squared statistic was used to compare the number of observed dead and predicted dead trees, and a p-value > 0.05 indicated no significant difference between observed and predicted survival probabilities or no significant evidence of a poor fit. The area under the receiver-operating curve (AUC) was also calculated to assess model goodness-of-fit. AUC provides a measure of discrimination of the model or the ability of the model to correctly distinguish between live and dead trees. For logistic models, an AUC of ≥ 0.8 is considered excellent discrimination and ≥ 0.7 is considered acceptable discrimination. AUC ≤ 0.5 suggests no discrimination between survival and mortality (Hosmer and Lemeshow, 2000).

Statistical analyses were completed using the R statistics program (R Core Team, 2015). Hosmer and Lemeshow tests were carried out using the *ResourceSelection* package (Lele et al., 2016). AUC was calculated using the *rms* package (Harrell, 2016). R^2 values for logistic models were calculated with the *fmsb* package (Nakazawa, 2015) and R^2 values for mixed models were computed using the *MuMIn* package (Bartoń, 2016).

3.4 Results

3.4.1 Effects of competition on tree growth

3.4.1.1 Optimum radius for assessing competition

Analysis was completed using nonlinear models for all species and ages with the exception of the mature western redcedar model. The addition of plot as a random effect resulted in model improvement ($\Delta AIC>2$) for the mature western redcedar model and therefore it was fit using nonlinear mixed effects models. Profiles of AIC values showed large variation among neighbourhood distances and competition indices. Figures used for optimum radius selection, plotting radius against AIC for all competition indices, are shown

in Appendix D.

Optimum neighbourhood radius for evaluating competition varied among tree species (Table 3.5), but the overall trends were the same: the size of the optimum competition neighbourhood decreased with forest successional age.

The optimum radius for all species was consistently 9 m in the immature stands. The neighbourhood radius decreased for all species in the mature stands, with 7 m for Douglas fir and western redcedar, and 6 m for western hemlock. The competition radius decreased further in the old-growth plot for all species. Western hemlock had the smallest neighbourhood radius at the old-growth stage with 3 m, while the western redcedar radius was 5 m and the Douglas fir radius was 6 m.

Table 3.5. Optimum neighbourhood radius for assessing competition in growth models.

Stand age	Douglas fir		Western hemlock		Western redcedar	
	Radius	RSE	Radius	RSE	Radius	RSE
Immature	9	0.431	9	0.516	9	0.341
Mature	7	0.736	6	0.672	7	0.557
Old-growth	6	0.596	3	0.368	5	0.419

Radius is in meters; RSE is the residual standard error for the top radius model.

3.4.1.2 Competition indices and growth-competition models

Analysis was completed using linear and nonlinear models for all species-age groups separately. The Douglas fir immature model showed model improvement ($\Delta AIC > 2$) when a random effect for plot was included and was therefore modeled using linear and nonlinear mixed effects models. Final models were selected based on lowest AIC value. Appendix E compares the AIC values for the best model for each competition index.

A total of 2287 trees were used to fit the Douglas fir growth-competition models (1396 immature, 575 mature, and 316 old-growth). The basal area growth rate for Douglas fir increased with stand age. Lowest growth rate was observed in the immature stands at 8.8 $cm^2\ yr^{-1}$ and highest growth rate was in the old-growth stand at 33.5 $cm^2\ yr^{-1}$ (Table 3.6). In all Douglas fir models, initial tree size had a power relationship and competition had a linear relationship with growth. However, the relationships of slope and elevation to growth varied with successional stage. Slope had a linear relationship in the mature and old-growth stands, but a power relationship in the immature stand. Elevation had a linear relationship in the immature and old-growth stands, but a power relationship in the mature plot.

Table 3.6. Characteristics of focal trees and predictor variables for growth-competition models.

Species	Stand age	No. trees	Growth	DBH	Height	Elevation	Slope
Douglas fir	Immature	1396	8.8	18.1	23.6	347	5.4
			[0-131.8]	[1.1-55.5]	[3.1-39.6]	[288-356]	[1-80.6]
	Mature	575	21.3	35.8	34.0	247	7.3
			[1.5-200.8]	[1.3-112]	[4.4-55.5]	[229-263]	[0.3-22.1]
	Old-Growth	316	33.5	51.4	34.5	463	15.6
			[0.3-195.6]	[4.3-100.9]	[3.2-55.3]	[449-481]	[2.1-42.6]
Western hemlock	Immature	66	8.8	13.1	14.2	304	14.7
			[0-59.5]	[0.7-61.8]	[1.2-38.8]	[288-354]	[2.7-23.3]
	Mature	180	7.6	10.4	12.4	237	7.1
			[0-75.6]	[0.6-51.4]	[1.7-30.7]	[230-262]	[0.4-23.1]
	Old-Growth	312	2.8	8.9	8.5	463	15.6
			[0.002-70.9]	[0.5-59.9]	[1.3-49.4]	[448-479]	[2.4-33]
Western redcedar	Immature	20	14.7	14.4	11.2	324	11.0
			[0.03-131.1]	[0.6-97.1]	[1.8-35.8]	[295-354]	[1.1-18.7]
	Mature	367	8.7	8.9	7.0	236	6.4
			[0-237.4]	[0.6-111]	[1.6-28.2]	[229-262]	[2.1-18.8]
	Old-Growth	190	4.7	11.1	8.2	468	15.5
			[0.003-61.1]	[0.5-61]	[0.8-35.2]	[450-479]	[2.9-38.1]

Values shown are variable means [minimum - maximum]; growth is in $cm^2\ yr^{-1}$, DBH is initial tree size in cm at the first census; height is in m at the second measurement; elevation is in m; slope is in degrees.

Coefficients and significance values for each Douglas fir model are summarized in Table 3.7. Figures 3.4-3.6 show the relationships between growth and competition, and growth and initial size for each successional stage. Visual assessments of model fit are also included. The mixed models applied to the immature stands allowed for parameter estimates to vary by plot, as shown in Figure 3.4.

Basal area of larger trees (BAL, CI4) showed the best results of all competition indices in the immature and old-growth models. Sum DBH (CI5) was the top index in the mature stand. All top competition indices for this species were distance-independent. Average growth was significantly negatively correlated with competition for all stand ages. The magnitude of the competitive influence was highest in the immature stands and lowest in the mature stands.

Initial size positively influenced growth for all stand ages, as expected, and the magnitude of the effect decreased with successional stage. Habitat variables showed varying significance as predictors of growth for this species. Elevation showed a negative association with Douglas fir growth in the immature stand only, while slope was negatively related in both the immature and mature stands. Neither habitat characteristic showed any effect on growth at the old-growth stage.

Table 3.7. Parameter estimates, standard errors and p-values for the final Douglas fir growth-competition models.

Stand age	Model no.	Independent variable	Parameter estimate	Standard error	p-value
Immature	[M5]	Intercept	1.101	0.598	0.0656
		CI4	**-0.514**	0.158	**0.0012**
		Initial Size$^{\beta}$	**0.235**	0.003	**<0.0001**
		Slope$^{\beta}$	**-0.094**	0.038	**0.0134**
		Elevation	**-0.010**	0.002	**<0.0001**
Mature	[M6]	Intercept	-2.590	2.962	0.3822
		CI5	**-0.001**	0.0002	**0.0004**
		Initial Size$^{\beta}$	**0.207**	0.002	**<0.0001**
		Slope	**-0.014**	0.006	**0.0093**
		Elevation$^{\beta}$	0.055	0.392	0.8876
Old-growth	[M2]	Intercept	1.198	2.325	0.6067
		CI4	**-0.397**	0.102	**0.0001**
		Initial Size$^{\beta}$	**0.191**	0.006	**<0.0001**
		Slope	-0.005	0.006	0.4138
		Elevation	-0.004	0.005	0.3801

Model equations are shown in Table 3.4. CI4 = Basal area of larger trees, and CI5 = Sum DBH. Bold values indicate significant departures from zero.

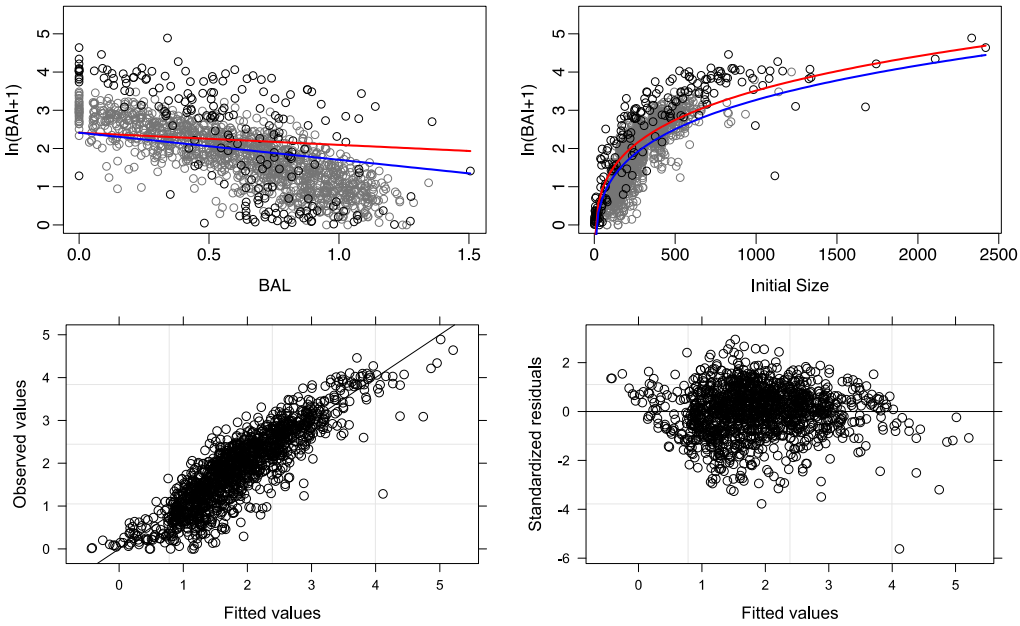

South: Growth = 1.101 - 0.318*CI4 + Initial Size$^{0.235}$ + Slope$^{-0.094}$ - 0.010*Elevation

North: Growth = 1.101 - 0.709*CI4 + Initial Size$^{0.235}$ + Slope$^{-0.094}$ - 0.010*Elevation

Figure 3.4. Scatterplots of immature Douglas fir model fit and relationships between fixed effects and growth rate.

Relationship between growth rate and competition (top left) and initial size (top right) with fitted model line. Immature south stand is shown in black circles and red lines, and north stand in grey circles and blue lines. Scatterplots of observed values (bottom left) and standardized residuals (bottom right) against fitted values show model fit.

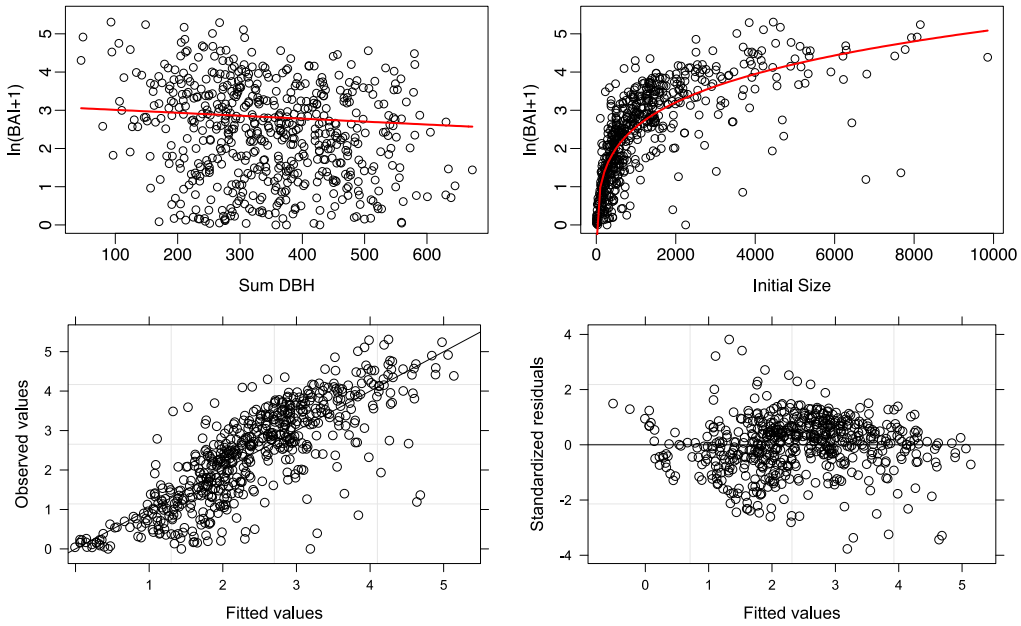

Growth = -2.590 - 0.001*CI5 + Initial Size$^{0.207}$ - 0.014*Slope + Elevation$^{0.055}$

Figure 3.5. Plots of mature Douglas fir model fit and relationships between fixed effects and growth rate.

Relationship between growth rate and competition (top left) and initial size (top right) with fitted model line. Scatterplots of observed values (bottom left) and standardized residuals (bottom right) against fitted values show model fit.

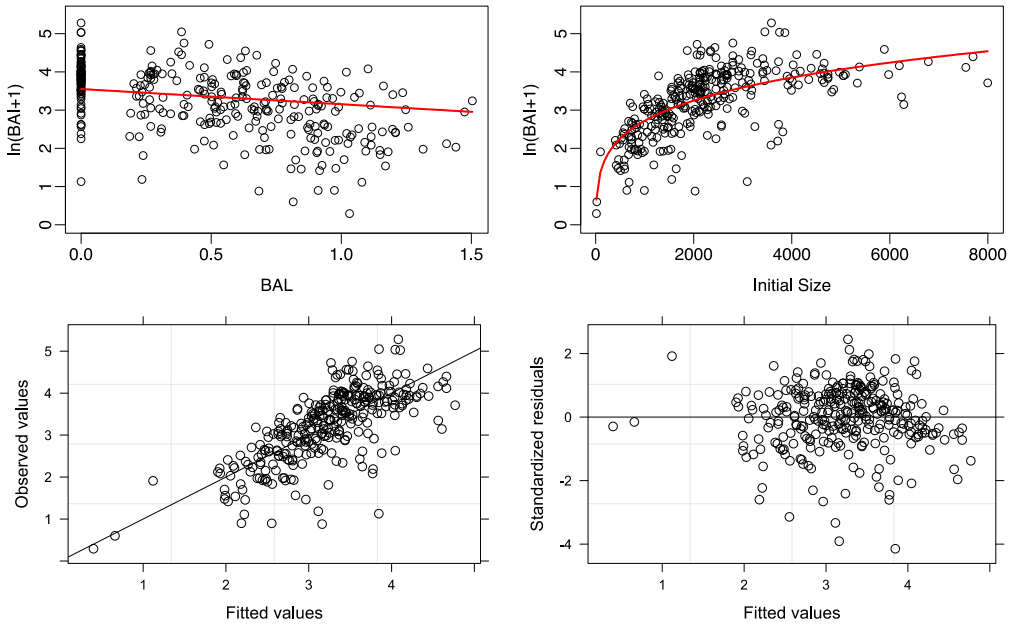

Growth = 1.198 - 0.397*CI4 + Initial Size$^{0.191}$ - 0.005*Slope - 0.004*Elevation

Figure 3.6. Scatterplots of old-growth Douglas fir model fir and relationships between fixed effects and growth rate.

Relationship between growth rate and competition (top left) and initial size (top right) with fitted model line. Scatterplots of observed values (bottom left) and standardized residuals (bottom right) against fitted values show model fit.

558 western hemlock trees from the three stands ages were used in this analysis with the highest sample population in the old-growth stand (66 immature, 180 mature, and 312 old-growth). Average growth rate for western hemlock decreased with successional stage, from 8.8 $cm^2\ yr^{-1}$ in the immature stands to 2.8 $cm^2\ yr^{-1}$ in the old-growth stand (Table 3.6). The top performing models for this species showed a power relationship between initial tree size and growth for all stands. The models for the immature and old-growth stands had the same form with competition, slope and elevation having linear relationships to growth. For the mature model, competition and slope had a power relationship to growth while elevation remained linearly related.

Western hemlock model coefficients and significance values are summarized in Table 3.8. Figures 3.7-3.9 show the relationships between growth and competition, and growth and initial size for each successional stage, as well as visual assessments of model fit.

The top competition index was distance-independent for the immature and mature stands, with sum DBH (CI_5) and nearest neighbour basal area (CI_1) showing the best results, respectively. In the old-growth model, the distance-dependent horizontal angle sum (CI_7) of neighbouring trees was the top index. Increased competition resulted in significantly reduced growth at all successional stages, with the highest intensity of competition occurring in the mature stands.

Initial tree size showed a positive relationship to tree growth rates for all models, with size having the largest influence in the mature stands, followed by immature and old-growth. Habitat variables were important in predicting growth in the old-growth stand only, showing no significance in the immature and mature models. Higher growth rates were shown to occur on steeper slopes and at lower elevations in the old-growth plot.

Table 3.8. Parameter estimates, standard errors and p-values for the final western hemlock growth-competition models.

Stand age	Model no.	Independent variable	Parameter estimate	Standard error	p-value
Immature	[M2]	Intercept	-2.874	1.628	0.0826
		CI5	**-0.002**	0.001	**0.0002**
		Initial Size$^{\beta}$	**0.192**	0.008	**<0.0001**
		Slope	-0.017	0.012	0.1425
		Elevation	0.011	0.006	0.0555
Mature	[M9]	Intercept	1.007	1.962	0.6083
		CI1$^{\beta}$	**-0.132**	0.021	**<0.0001**
		Initial Size$^{\beta}$	**0.203**	0.005	**<0.0001**
		Slope$^{\beta}$	-0.003	0.089	0.9741
		Elevation	-0.014	0.008	0.0818
Old-growth	[M2]	Intercept	**2.348**	1.072	**0.0292**
		CI7	**-0.039**	0.005	**<0.0001**
		Initial Size$^{\beta}$	**0.170**	0.005	**<0.0001**
		Slope	**0.011**	0.004	**0.0070**
		Elevation	**-0.007**	0.002	**0.0023**

Model equations are shown in Table 3.4. CI1 = Nearest neighbour basal area, C5 = Sum DBH, C7 = Horizontal angle sum. Bold values indicate significant departures from zero.

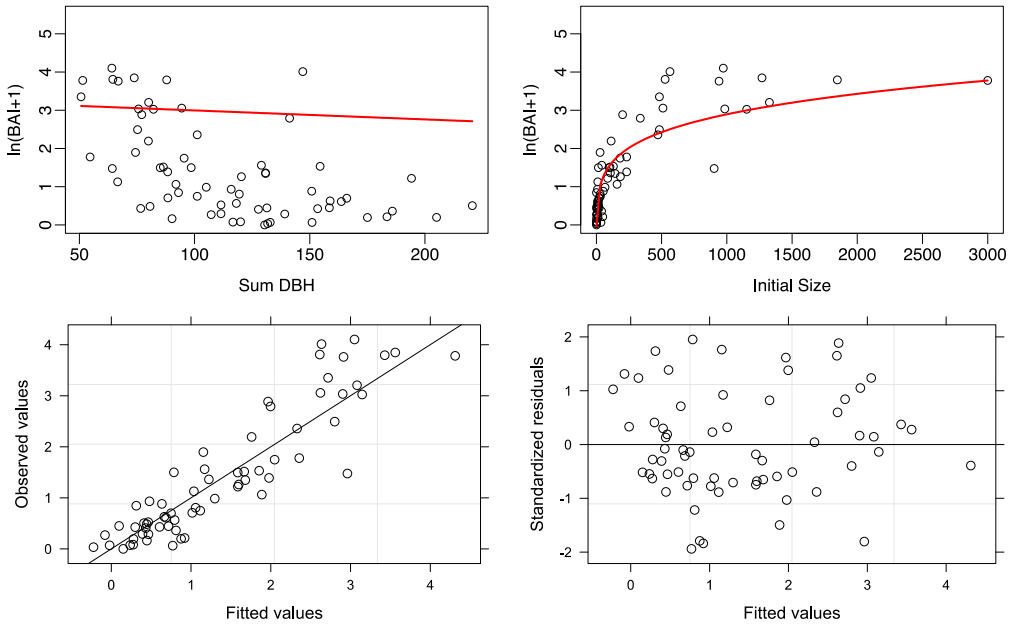

Growth = -2.874 - 0.002*CI + Initial Size$^{0.192}$ – 0.017*Slope + 0.011*Elevation

Figure 3.7. Scatterplots of immature western hemlock fit and relationships between fixed effects and growth rate.
Relationship between growth rate and competition (top left) and initial size (top right) with fitted model line. Scatterplots of observed values (bottom left) and standardized residuals (bottom right) against fitted values show model fit.

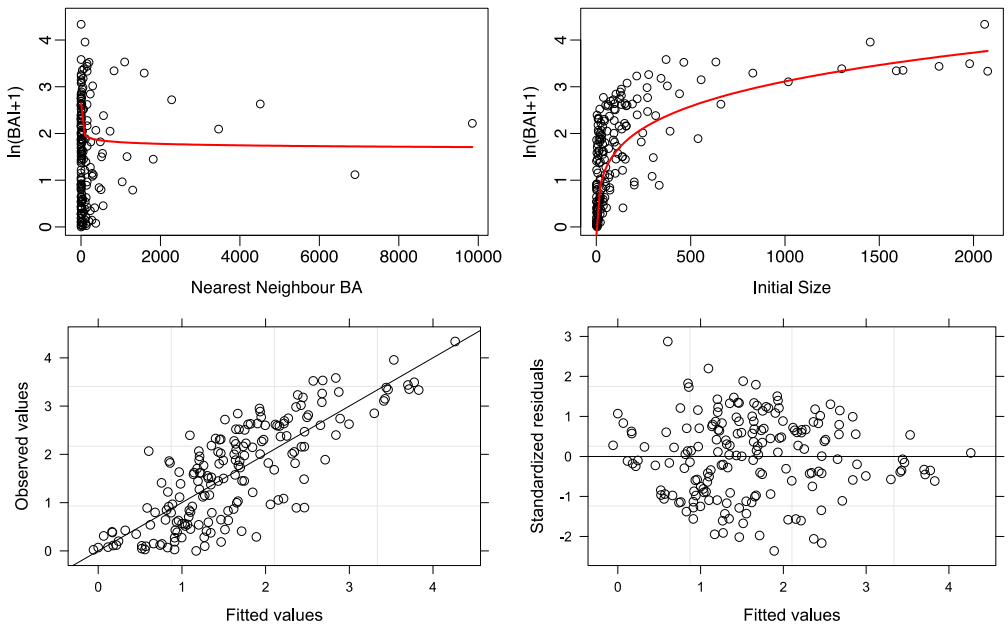

$$\text{Growth} = 1.007 + CI1^{-0.132} + \text{Initial Size}^{0.203} + \text{Slope}^{-0.003} - 0.014*\text{Elevation}$$

Figure 3.8. Scatterplots of mature western hemlock fit and relationships between fixed effects and growth rate.
Relationship between growth rate and competition (top left) and initial size (top right) with fitted model line. Scatterplots of observed values (bottom left) and standardized residuals (bottom right) against fitted values show model fit.

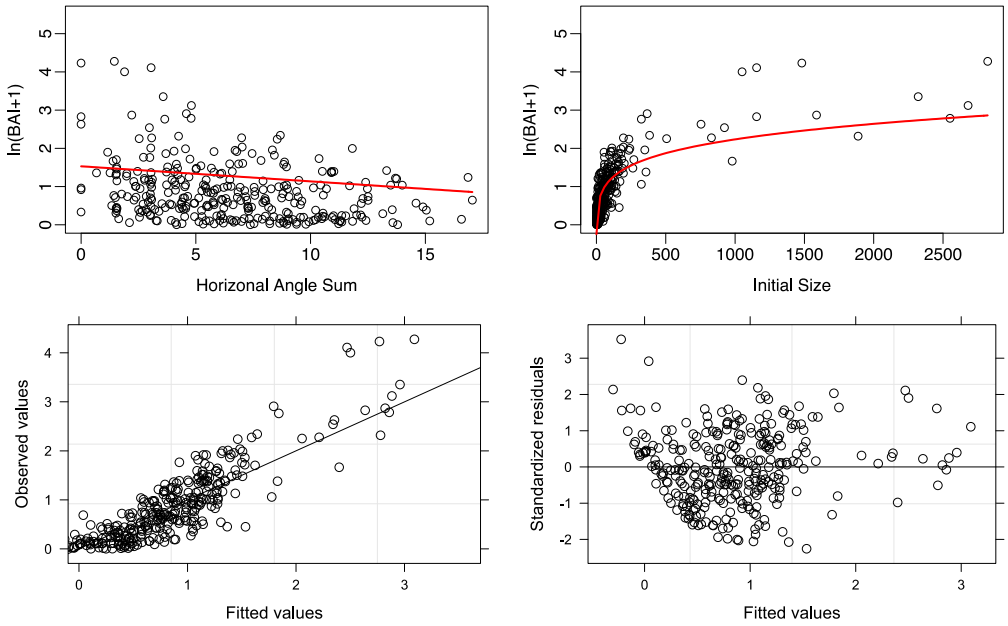

$$\text{Growth} = 2.348 - 0.039*CI7 + \text{Initial Size}^{0.170} + 0.011*\text{Slope} - 0.007*\text{Elevation}$$

Figure 3.9. Scatterplots of old-growth western hemlock fit and relationships between fixed effects and growth rate.
Relationship between growth rate and competition (top left) and initial size (top right) with fitted model line. Scatterplots of observed values (bottom left) and standardized residuals (bottom right) against fitted values show model fit.

A total of 577 western redcedar trees were modeled in the growth-competition analysis with the sample population peaking in the mature stand (20 immature, 367 mature, and 190 old-growth). Growth rate for western redcedar decreased with successional stage. Growth was highest in the immature stands at 14.7 cm^2 yr^{-1} and decreased to 4.7 cm^2 yr^{-1} in the old-growth stand (Table 3.6). The top model form was similar for all stands ages. Growth rates were exponentially related to competition and had a power relationship with initial size in all models. Growth rate was linearly related to elevation in the immature and mature models, but had a power relationship in the old-growth stand. The relationship between slope and growth was linear the immature stand, was a power relationship in the mature and old-growth models.

Coefficients and significance values for each model for western redcedar are summarized in Table 3.9. Figures 3.10-3.12 show the relationships between growth and competition, growth and initial size, and the visual assessments of model fit for each successional stage.

The top competition index for the immature stand was the nearest neighbour basal area (CI1), a distance-independent index. The mature and old-growth stands had more complex, distance-dependent indices with distance-DBH ratio (CI6) and horizontal angle sum (CI7) for the mature and old-growth stands, respectively. Competition in the immature stand showed the only positive relationship with growth in the study. For this stand, a larger nearest neighbour resulted in higher growth rates. However, the trend reversed in the mature and old-growth models where competition negatively impacted growth. The old-growth stand showed the largest influence of competition.

Growth rates were shown to increase with increasing initial size of the trees for all successional stages, and the magnitude of the size effect was largest in the mature stand. Elevation showed a positive relationship to growth in the immature stands but a negative relationship in the mature stands. Slope was not found to be an important variable influencing growth in any of the successional stages.

Table 3.9. Parameter estimates, standard errors and p-values for the final western redcedar growth-competition models.

Stand age	Model no.	Independent variable	Parameter estimate	Standard error	p-value
Immature	[M11]	Intercept	-11.744	3.608	0.0053
		exp(βCI1)	**0.0003**	0.00004	**<0.0001**
		Initial Size$^{\beta}$	**0.195**	0.003	**<0.0001**
		Slope$^{\beta}$	0.061	0.154	0.6972
		Elevation$^{\beta}$	**0.374**	0.065	**<0.0001**
Mature	[M7]	Intercept	0.202	0.623	0.7456
		exp(βCI6)	**-0.024**	0.006	**<0.0001**
		Initial Size$^{\beta}$	**0.208**	0.004	**<0.0001**
		Slope$^{\beta}$	0.001	0.054	0.9859
		Elevation	**-0.009**	0.003	**0.0027**
Old-growth	[M3]	Intercept	0.079	1.434	0.9560
		exp(βCI7)	**-0.128**	0.036	**0.0005**
		Initial Size$^{\beta}$	**0.179**	0.004	**<0.0001**
		Slope	-0.004	0.004	0.2712
		Elevation	-0.002	0.003	0.4169

Model equations are shown in Table 3.4. CI1 = Nearest neighbour basal area, C6 = DBH-distance ratio, C7 = Horizontal angle sum. Bold values indicate significant departures from zero.

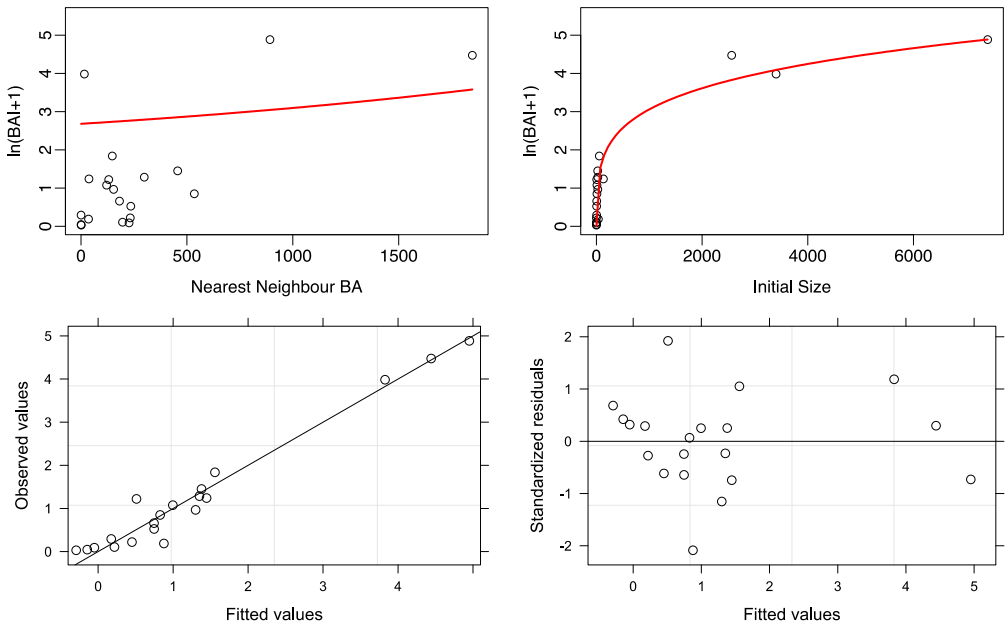

Growth = -11.744 + exp(0.0003*CI1) + Initial Size$^{0.195}$ + Slope$^{0.061}$ + Elevation$^{0.374}$

Figure 3.10. Scatterplots of immature western redcedar fit and relationships between fixed effects and growth rate.

Relationship between growth rate and competition (top left) and initial size (top right) with fitted model line. Scatterplots of observed values (bottom left) and standardized residuals (bottom right) against fitted values show model fit.

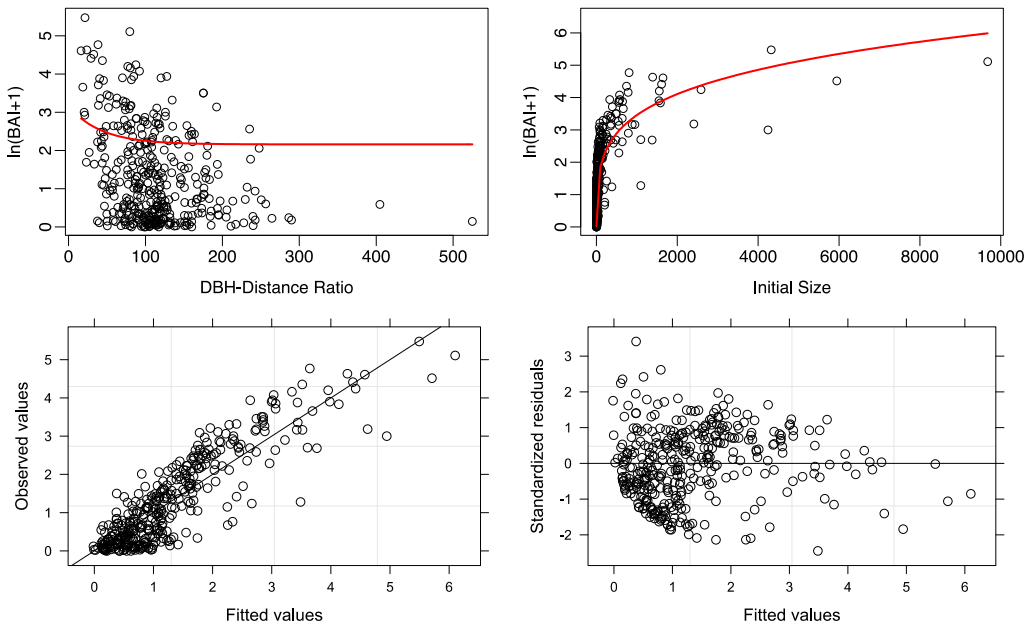

$$\text{Growth} = 0.202 + \exp(-0.024 * \text{CI6}) + \text{Initial Size}^{0.208} + \text{Slope}^{0.001} - 0.009 * \text{Elevation}$$

Figure 3.11. Scatterplots of mature western redcedar fit and relationships between fixed effects and growth rate.
Relationship between growth rate and competition (top left) and initial size (top right) with fitted model line. Scatterplots of observed values (bottom left) and standardized residuals (bottom right) against fitted values show model fit.

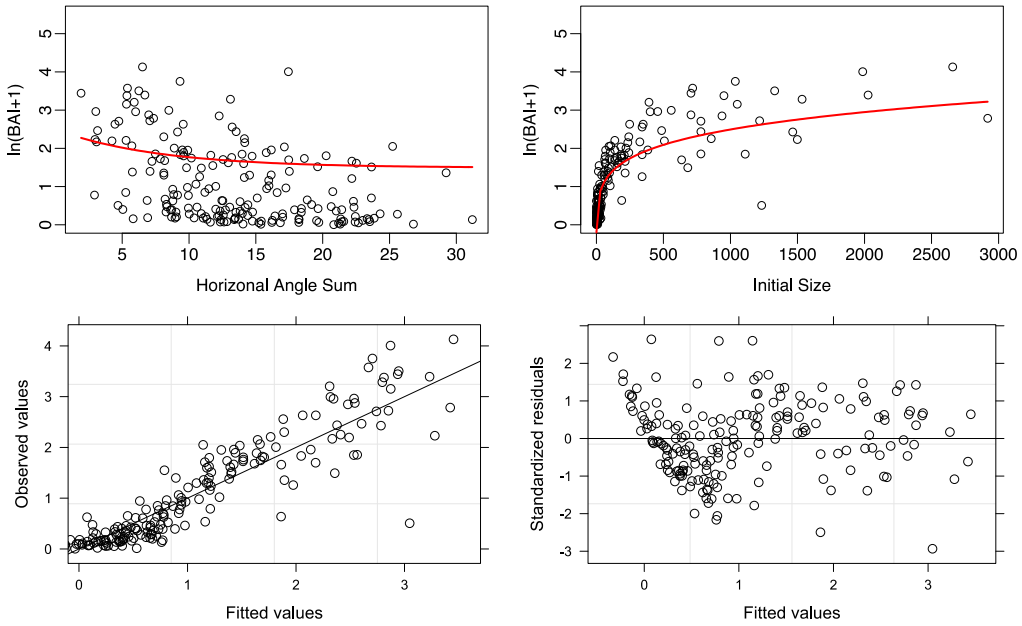

$$\text{Growth} = 0.079 + \exp(-0.128 * \text{CI7}) + \text{Initial Size}^{0.179} - 0.004 * \text{Slope} - 0.002 * \text{Elevation}$$

Figure 3.12. Scatterplots of old-growth western redcedar fit and relationships between fixed effects and growth rate.
Relationship between growth rate and competition (top left) and initial size (top right) with fitted model line. Scatterplots of observed values (bottom left) and standardized residuals (bottom right) against fitted values show model fit.

3.4.2 Effects of climate on annual growth rate

Ten climate variables were used in linear mixed effects models (M13) to account for changes in annual tree ring growth. A random effect of tree number accounted for the variability in conditions among individual trees. Models including plot ID as random effect were also tested, and resulted in model improvement (ΔAIC>2) for the immature Douglas fir model and mature western redcedar model. All other models were fit with only tree number as a random effect. Residual plots for the final models are shown in Appendix F.

Mean annual temperature (MAT), mean warmest month temperature (MWMT), mean coldest month temperature (MCMT), mean summer precipitation (MSP) and climate moisture index (CMI) were modeled as predictors of annual tree growth. Five-year averages were calculated for the beginning and end of the study period to assess if trends in climate variables could be detected. Temperature variables were found to have increased over the study period, with MAT 0.80°C higher in the last 5 years than in the first 5 years. MWMT and MCMT also showed increases of 1.10°C and 0.40°C, respectively. The opposite trend was observed for moisture variables. MSP decreased by 49.3 mm and CMI decreased by 23.66 cm yr^{-1} between the first 5 years and last 5 years of the study (Table 3.3).

Table 3.10. Basal area increment summary for study species in immature, mature and old-growth stands.

Species	Stand age	No. trees	Initial DBH	BAI		
				Mean	Min.	Max.
Douglas fir	Immature	95	21.4	14.7	0.4	97.7
	Mature	63	28.2	9.1	0.2	131.1
	Old-growth	20	37.6	5.2	0.4	25.8
Western hemlock	Immature	18	25.3	18.2	1.0	90.5
	Mature	27	21.8	16.9	0.3	95.9
	Old-growth	19	28.6	8.7	0.5	51.8
Western redcedar	Immature	6	41.2	42.5	1.4	124.3
	Mature	30	20.2	23.1	0.9	216.7
	Old-growth	18	27.7	7.8	0.6	25.9

DBH is mean DBH in cm at the first census; BAI is mean annual basal area increment in cm^2.

A total of 178 Douglas fir trees were sampled and used for annual growth analysis (95 immature, 63 mature and 20 old-growth). Mean annual basal area increment (BAI) decreased with stand age from 14.7 cm^2 in the immature stand to 5.2 cm^2 in the old-growth plot (Table 3.10).

The model for Douglas fir in the immature plots showed many of the climate variables were significantly associated with annual tree growth. MAT and CMI for the current and previous years were both positively related to growth. MWMT and MCMT from the previous year had significant negative associations (Table 3.11). The model captured a large portion of the growth variance with R^2 value of 0.690. The climate model for this species in mature stands showed higher growth was related to higher MAT and CMI in the previous year. Current and previous year MSP and previous year MCMT were negatively associated with growth (Table 3.11). The R^2 value for this model was 0.438, showing the variables explained a moderate portion of the variation. The Douglas fir model for old-growth had significant positive relationships between growth and MAT and CMI of the previous year. MWMT and MSP, current and previous year, as well as MCMT of the previous year were negatively associated with growth (Table 3.11). This model had the highest R^2 value for this species at 0.962, capturing the majority of growth variance.

64 western hemlock trees were selected for coring and climate analysis across all stand ages (18 immature, 27 mature, and 19 old-growth). A decrease in mean annual BAI was seen through the forest chronosequence from 18.2 cm^2 in the immature stands to 8.7 cm^2 in the old-growth plot (Table 3.10).

The immature model showed annual tree growth had a significant negative relationship with MSP of current and previous year (Table 3.12). No other climate variables were significant in this model and the model had R^2 value of 0.332. The mature stand model showed growth increased with MCMT in the current year and increased with MAT in the previous year. However, many other climate variables had significant negative associations with western hemlock growth including MWMT and MSP of current and previous year, as well as MCMT of previous year (Table 3.12). The R^2 value for the model was 0.271. The western hemlock old-growth model showed MCMT of the year of growth was significantly positive, while MCMT for the previous year was significantly negative. MSP for both the current and previous years were also significantly negatively associated with tree growth (Table 3.12). The old-growth model captured the largest amount of growth variance with R^2=0.819.

A total of 54 western redcedar trees were cored and analyzed. The immature plots only had 6 trees large enough for coring; 30 trees were sampled in the mature stands and 18 in the old-growth stand. Mean annual BAI decreased from immature to old-growth stages with mean BAI of 42.5 cm^2 and 7.8 cm^2, respectively.

The western redcedar immature stand model showed growth had a significant positive relationship with MWMT for the current and previous year and with MCMT in the current year. Growth was significantly negatively related to MAT of the current and previous year and MSP of the current year (Table 3.13). The model showed very high explanation of the growth variance with R^2=0.955, however, the sample size was very small (n=6).

The mature model showed growth was significantly positively related to MAT and CMI in the previous year, and negatively related to MWMT and MSP in the current and previous years, CMI in the current year and MCMT in the previous year (Table 3.13). The model had R^2=0.146, the lowest value for all climate models, suggesting other factors may be important in explaining the variation in growth.

The old-growth model for western redcedar showed annual growth had a significant positive relationship with MCMT of the current year and CMI of the previous year but was negatively related to MSP in the current and previous year, CMI of the current year and MCMT of the previous year (Table 3.13). The model R^2 was 0.986 indicating high explanation of variance by the model.

Table 3.11. Douglas fir growth-climate model parameter estimates, standard errors and p-values.

Stand age	Independent variable	Parameter estimate	Standard error	p-value
Immature	Intercept	**2.706**	0.3911	**<0.0001**
	MAT_T	**0.045**	0.0203	**0.0256**
	$MWMT_T$	-0.022	0.0113	0.0512
	$MCMT_T$	0.005	0.0087	0.5969
	MSP_T	-0.0002	0.0001	0.1236
	CMI_T	**0.001**	0.0002	**<0.0001**
	MAT_{T-1}	**0.139**	0.0282	**<0.0001**
	$MWMT_{T-1}$	**-0.083**	0.0137	**<0.0001**
	$MCMT_{T-1}$	**-0.084**	0.0148	**<0.0001**
	MSP_{T-1}	-0.0001	0.0001	0.2937
	CMI_{T-1}	**0.002**	0.0002	**<0.0001**
Mature	Intercept	**1.804**	0.2100	**<0.0001**
	MAT_T	0.040	0.0233	0.0838
	$MWMT_T$	-0.025	0.0128	0.0546
	$MCMT_T$	-0.003	0.0100	0.7665
	MSP_T	**-0.001**	0.0001	**<0.0001**
	CMI_T	0.000	0.0002	0.1884
	MAT_{T-1}	**0.076**	0.0319	**0.0176**
	$MWMT_{T-1}$	-0.028	0.0155	0.0702
	$MCMT_{T-1}$	**-0.059**	0.0165	**0.0004**
	MSP_{T-1}	**-0.0005**	0.0001	**<0.0001**
	CMI_{T-1}	**0.001**	0.0002	**<0.0001**
Old-growth	Intercept	**2.348**	0.2793	**<0.0001**
	MAT_T	0.038	0.0295	0.1973
	$MWMT_T$	**-0.062**	0.0162	**0.0001**
	$MCMT_T$	-0.00002	0.0139	0.9990
	MSP_T	**-0.001**	0.0002	**<0.0001**
	CMI_T	-0.0003	0.0003	0.2940
	MAT_{T-1}	**0.149**	0.0434	**0.0007**
	$MWMT_{T-1}$	**-0.054**	0.0193	**0.0055**
	$MCMT_{T-1}$	**-0.123**	0.0228	**<0.0001**
	MSP_{T-1}	**-0.001**	0.0002	**<0.0001**
	CMI_{T-1}	**0.001**	0.0003	**0.0005**

MAT is mean annual temperature; MWMT is mean warmest month temperature; MCMT is mean coldest month temperature; MSP is mean summer precipitation; CMI is climate moisture index. Subscript T refers to current year, and T-1 refers to previous year.

Table 3.12. Western hemlock growth-climate model parameter estimates, standard errors and p-values.

Stand age	Independent variable	Parameter estimate	Standard error	p-value
Immature	Intercept	**3.383**	0.4743	**<0.0001**
	MAT_T	0.024	0.0629	0.7020
	$MWMT_T$	-0.018	0.0345	0.6106
	$MCMT_T$	0.027	0.0270	0.3258
	MSP_T	**-0.001**	0.0003	**0.0275**
	CMI_T	0.0001	0.0005	0.8279
	MAT_{T-1}	0.014	0.0861	0.8737
	$MWMT_{T-1}$	-0.024	0.0419	0.5667
	$MCMT_{T-1}$	-0.077	0.0446	0.0865
	MSP_{T-1}	**-0.001**	0.0003	**0.0172**
	CMI_{T-1}	0.001	0.0006	0.0887
Mature	Intercept	**3.625**	0.3293	**<0.0001**
	MAT_T	0.060	0.0371	0.1064
	$MWMT_T$	**-0.058**	0.0199	**0.0039**
	$MCMT_T$	**0.048**	0.0158	**0.0025**
	MSP_T	**-0.001**	0.0002	**0.0001**
	CMI_T	-0.0004	0.0003	0.1947
	MAT_{T-1}	**0.137**	0.0487	**0.0052**
	$MWMT_{T-1}$	**-0.083**	0.0241	**0.0006**
	$MCMT_{T-1}$	**-0.110**	0.0247	**<0.0001**
	MSP_{T-1}	**-0.001**	0.0002	**<0.0001**
	CMI_{T-1}	0.0005	0.0003	0.1602
Old-growth	Intercept	**2.354**	0.4204	**<0.0001**
	MAT_T	-0.040	0.0544	0.4659
	$MWMT_T$	-0.013	0.0305	0.6755
	$MCMT_T$	**0.052**	0.0235	**0.0261**
	MSP_T	**-0.002**	0.0003	**<0.0001**
	CMI_T	-0.001	0.0005	0.0676
	MAT_{T-1}	0.110	0.0767	0.1540
	$MWMT_{T-1}$	-0.026	0.0369	0.4863
	$MCMT_{T-1}$	**-0.119**	0.0404	**0.0034**
	MSP_{T-1}	**-0.001**	0.0003	**0.0014**
	CMI_{T-1}	0.001	0.0006	0.0750

MAT is mean annual temperature; MWMT is mean warmest month temperature; MCMT is mean coldest month temperature; MSP is mean summer precipitation; CMI is climate moisture index. Subscript T refers to current year, and T-1 refers to previous year.

Table 3.13. Western redcedar growth-climate model parameter estimates, standard errors and p-values.

Stand age	Independent variable	Parameter estimate	Standard error	p-value
Immature	Intercept	**3.432**	0.7922	**<0.0001**
	MAT_T	**-0.183**	0.0605	**0.0033**
	$MWMT_T$	**0.083**	0.0324	**0.0121**
	$MCMT_T$	**0.106**	0.0258	**0.0001**
	MSP_T	**-0.001**	0.0003	**0.0004**
	CMI_T	-0.0005	0.0005	0.3599
	MAT_{T-1}	**-0.193**	0.0793	**0.0168**
	$MWMT_{T-1}$	**0.081**	0.0393	**0.0417**
	$MCMT_{T-1}$	-0.013	0.0402	0.7482
	MSP_{T-1}	-0.0001	0.0003	0.7657
	CMI_{T-1}	-0.0004	0.0006	0.5009
Mature	Intercept	**3.637**	0.4053	**<0.0001**
	MAT_T	0.023	0.0313	0.4540
	$MWMT_T$	**-0.040**	0.0162	**0.0135**
	$MCMT_T$	0.022	0.0131	0.0990
	MSP_T	**-0.001**	0.0001	**<0.0001**
	CMI_T	**-0.0005**	0.0002	**0.0489**
	MAT_{T-1}	**0.153**	0.0388	**0.0001**
	$MWMT_{T-1}$	**-0.087**	0.0196	**<0.0001**
	$MCMT_{T-1}$	**-0.114**	0.0191	**<0.0001**
	MSP_{T-1}	**-0.001**	0.0001	**0.0002**
	CMI_{T-1}	**0.001**	0.0003	**0.0063**
Old-growth	Intercept	**2.2133**	0.2522	**<0.0001**
	MAT_T	0.0097	0.0275	0.7244
	$MWMT_T$	0.0089	0.0149	0.5528
	$MCMT_T$	**0.0520**	0.0121	**<0.0001**
	MSP_T	**-0.0011**	0.0001	**<0.0001**
	CMI_T	**-0.0005**	0.0002	**0.0313**
	MAT_{T-1}	-0.0008	0.0381	0.9836
	$MWMT_{T-1}$	-0.0156	0.0181	0.3872
	$MCMT_{T-1}$	**-0.0403**	0.0197	**0.0413**
	MSP_{T-1}	**-0.0007**	0.0001	**<0.0001**
	CMI_{T-1}	**0.0007**	0.0003	**0.0114**

MAT is mean annual temperature; MWMT is mean warmest month temperature; MCMT is mean coldest month temperature; MSP is mean summer precipitation; CMI is climate moisture index. Subscript T refers to current year, and T-1 refers to previous year.

Table 3.14. Mortality rates and characteristics of trees used for mortality modeling.

Species	Stand age	No. live trees		Initial DBH		Mortality	
		1997	2014	Survived	Died	Total	Annual
Douglas fir	Immature	2061	1404	18.04 [1.1-55.5]	8.03 [0.6-30.2]	31.88	1.88
	Mature	813	592	35.78 [1.3-112]	20.73 [0.7-109.9]	27.18	1.60
	Old-growth	336	324	51.51 [4.3-100.9]	45.09 [29.5-63.5]	3.57	0.21
Western hemlock	Immature	222	68	12.85 [0.7-61.8]	7.01 [0.6-42.4]	69.37	4.08
	Mature	220	186	10.39 [0.6-51.4]	11.96 [0.9-66.5]	15.45	0.91
	Old-growth	435	325	8.82 [0.5-59.9]	5.22 [0.5-43.2]	25.29	1.49
Western redcedar	Immature	24	21	14.05 [0.6-97.1]	0.9 [0.6-1.1]	12.50	0.74
	Mature	443	381	9.23 [0.6-111]	4.9 [0.6-82.9]	14.00	0.82
	Old-growth	214	202	10.9 [0.5-61]	8.38 [0.8-41.2]	5.61	0.33

DBH is the mean initial DBH [min-max] in cm for trees that survived or died from the first census to the second census; Mortality values are percent total and annual mortality rates.

3.4.3 Effects of competition on probability of tree mortality

Stand mortality rates were calculated and individual tree mortality models were fit using logistic regression for each species and stand age separately. Variables for tree size, competition and habitat were modeled to analyze their effects of tree survival (M14). The top model was selected based on AIC and R^2 values. Appendix G shows the probability curves and Hosmer-Lemeshow goodness-of-fit test tables for all final models. Appendix H compares the AIC values and goodness-of-fit statistics for the best model for each competition index.

A total of 3210 trees were used to fit the Douglas fir mortality models. Annual mortality rates declined from 1.88% in the immature stands to 0.21% in the old-growth stand (Table 3.14). The optimum radius for analyzing competition varied greatly among successional stages with no clear trends (11 m for immature, 15 m for mature, 1 m for old-growth) and the top competition index for each model was different. BAL (CI4) was the best index in the immature model and density (CI3) was selected in the mature model. The old-growth model index was the distance-DBH ratio (CI6) and was the only mortality model with a density-dependent competition index.

Competition was significant in all models. Increased competition resulted in a increased mortality probability and reduced probability of survival. DBH was positively associated and DBH^2 was negatively associated with survival (negatively and positively associated with mortality) in the immature and mature models, but showed no significance in the old-growth model. Elevation was significant in the mature and old-growth models, with higher elevations relating to decreased mortality risk (Table 3.15).

The immature model had the highest Nagelkerke R^2 value of 0.609, and R^2 values decreased to 0.329 and 0.315 in the mature and old-growth models, respectively. The Hosmer-Lemeshow goodness-of-fit test gave no strong evidence of a significant difference between observed and predicted mortality probabilities for the immature and old-growth models (Hosmer-Lemeshow statistic=12.5 (p=0.13) and 4.9 (p=0.77), respectively). However, the mature Douglas fir model showed significant differences in probabilities, suggesting possible issues with model fit (Hosmer-Lemeshow statistic=17.3 (p=0.027)).

Table 3.15. Mortality model parameter estimates, standard errors, p-values, optimum radii, R^2 and AUC values for Douglas fir.

Stand age	Variable	Effect on P_m	Parameter estimate	SE	p-value	Rad.	R^2	AUC
Immature	Intercept		-1.826	2.780	0.511	11	0.61	0.92
	DBH	↓	**0.404**	0.042	**<0.0001**			
	DBH^2	↑	**-0.006**	0.002	**<0.0001**			
	Slope		0.01	0.028	0.705			
	Elevation		0.005	0.008	0.511			
	CI4	↑	**-2.552**	0.317	**<0.0001**			
Mature	Intercept		**-15.690**	3.247	**<0.0001**	15	0.33	0.81
	DBH	↓	**0.169**	0.016	**<0.0001**			
	DBH^2	↑	**-0.001**	0.0002	**<0.0001**			
	Slope		0.012	0.032	0.7124			
	Elevation		**0.058**	0.013	**<0.0001**			
	CI3	↑	**-0.007**	0.002	**0.0002**			
Old-growth	Intercept		**-60.961**	20.196	**<0.0001**	1	0.31	0.85
	DBH		-0.267	0.223	0.2311			
	DBH^2		0.003	0.002	0.1538			
	Slope		0.098	0.062	0.1114			
	Elevation	↓	**0.145**	0.041	**<0.0001**			
	CI6	↑	**-0.004**	0.001	**<0.0001**			

Effect on P_m shows the direction of relationship between independent variables and probability of mortality; Rad. is the optimum neighbourhood radius, m; R^2 values reported are Nagelkerke R^2 for glm models. AUC is the area under the receiver-operating curve. CI3 = Density, CI4 = Basal area of larger trees and CI6 = DBH-distance ratio.

A total of 877 trees were used to fit the western hemlock mortality models (222, 220 and 435 from immature, mature and old-growth stands, respectively). Annual mortality was highest in the youngest stands at 4.08%, decreased to 0.91% in the mature stands, and increased slightly in the old-growth stand to 1.49% (Table 3.14). The critical radius for assessing competition varied little with stand age, with 14 m for immature, 12 m for mature, and 13 m for old-growth. The neighbourhood sum DBH (CI5) was the best competition index in the immature and old-growth models and BAL (CI4) was the best index in the mature model. In all models, competition was significantly negatively related to tree mortality and positively related to tree survival. DBH and DBH^2 were significantly negative and positive, respectively, in determining tree mortality in the old-growth model only. Elevation was significant in the immature and old-growth models, but not the mature model, and increasing elevation was associated with increased mortality (Table 3.16).

The old-growth western hemlock model had the highest explained variance with Nagelkerke R^2 = 0.219, followed by the immature (R^2 = 0.140) and mature models (R^2 = 0.110). No strong evidence was found suggesting a significant difference between the predicted and observed mortality probabilities for any of the models, with the Hosmer-

Lemeshow statistics of 2.9 (p=0.94), 5.3 (p=0.73), and 5.3 (p=0.73) for immature, mature and old-growth models, respectively.

Table 3.16. Mortality model parameter estimates, standard errors, p-values, optimum radii, R^2 and AUC values for western hemlock.

Stand age	Variable	Effect on P_m	Parameter estimate	SE	p-value	Rad.	R^2	AUC
Immature	Intercept		9.401	6.176	0.1280	14	0.14	0.69
	DBH		0.060	0.047	0.2027			
	DBH^2		0.000	0.001	0.7467			
	Slope		-0.001	0.034	0.9807			
	Elevation	↑	**-0.047**	0.022	**0.0345**			
	CI5	↓	**0.003**	0.001	**0.0146**			
Mature	Intercept		2.474	7.720	0.7486	12	0.11	0.70
	DBH		0.041	0.048	0.3883			
	DBH^2		0.000	0.001	0.5913			
	Slope		0.074	0.072	0.3073			
	Elevation		-0.016	0.032	0.6130			
	CI4	↓	**0.911**	0.283	**0.0013**			
Old-growth	Intercept		**34.149**	7.237	**<0.0001**	13	0.22	0.76
	DBH	↓	**0.269**	0.048	**<0.0001**			
	DBH^2	↑	**-0.004**	0.001	**<0.0001**			
	Slope		-0.014	0.026	0.5950			
	Elevation		**-0.080**	0.015	**<0.0001**			
	CI5	↓	**0.002**	0.001	**<0.0001**			

Effect on P_m shows the direction of relationship between independent variables and probability of mortality; Rad. is the optimum neighbourhood radius, m; R^2 values reported are Nagelkerke R^2 for glm models. AUC is the area under the receiver-operating curve. CI4 = Basal area of larger trees and CI5 = Sum DBH.

A total of 681 western redcedar trees were alive at the start of the study period and used in the analysis. The annual mortality rate for this species was highest in the mature stands at 0.82% and lowest in the old-growth plot with 0.33% (Table 3.14). The number of western redcedar was insufficient in the immature stands for mortality modeling, and therefore models were fit for only the mature and old-growth plots. The optimum competition radius varied greatly between the mature and old-growth stands with radii of 2 m and 15 m, respectively. Top competition indices for the models were both distance-independent with neighbourhood density (CI3) for the mature model and sum DBH (CI5) for the old-growth model. In both models, competition was significant. Increased competition resulted in reduced mortality and higher survival probabilities in the mature stands. Conversely, increased competition was associated with increased mortality and reduced survival in the old-growth model. In the mature western redcedar model, DBH was

significantly negatively related and DBH^2 was significantly positively related to mortality, and neither variable was significant in the old-growth model (Table 3.17)

Nagelkerke R^2 values were similar among the models (0.136 and 0.173 for mature and old-growth, respectively) and the Hosmer-Lemeshow goodness-of-fit test gave no strong evidence of a significant difference between observed and predicted mortality probabilities (Hosmer-Lemeshow statistic=9.7 (p=0.29) and 9.0 (p=0.35), for mature and old-growth, respectively).

Table 3.17. Mortality model parameter estimates, standard errors, p-values, optimum radii, R^2 and AUC values for western redcedar.

Stand age	Variable	Effect on P_m	Parameter estimate	SE	p-value	Rad.	R^2	AUC
Mature	Intercept		-3.571	8.179	0.6624	2	0.14	0.73
	DBH	↓	**0.179**	0.042	**<0.0001**			
	DBH^2	↑	**-0.002**	0.0004	**0.0001**			
	Slope		-0.044	0.057	0.4395			
	Elevation		0.017	0.035	0.6329			
	CI3	↓	**0.240**	0.062	**0.0001**			
Old-growth	Intercept		-13.077	18.360	0.4763	15	0.17	0.79
	DBH		0.118	0.078	0.1320			
	DBH^2		-0.002	0.001	0.1926			
	Slope		-0.020	0.061	0.7405			
	Elevation		0.053	0.039	0.1680			
	CI5	↑	**-0.005**	0.002	**<0.0001**			

Effect on P_m shows the direction of relationship between independent variables and probability of mortality; Rad. is the optimum neighbourhood radius, m; R^2 values reported are Nagelkerke R^2 for glm models. AUC is the area under the receiver-operating curve. CI4 = Basal area of larger trees and CI5 = Sum DBH.

3.5 Discussion

Many of the proposed biotic and abiotic drivers had important effects on growth and mortality of the study species. Initial tree size, competition, climate and habitat factors were evaluated for their effect on growth, and size, competition and habitat factors were assessed for their influence on mortality risk. Several factors emerged as important in driving tree demographics. Although the degree of influence of individual variables differs with species and stand successional stages, the models provide insight into species-specific requirements through various life stages and increase our understanding of stand dynamics for management planning and conservation efforts.

3.5.1 Size of optimum competition neighbourhood for assessing growth

Neighbourhood size for evaluating competition has been studied for several decades. Multiple methods have been developed, each having benefits and drawbacks. Using a biologically meaningful, predetermined radius (He and Duncan, 2000; Canham et al., 2006; Contreras et al., 2011) or assigning neighbourhood size as a proportion of focal tree height (von Oheimb et al., 2011) is beneficial for practical application but whether the selected radius is adequate in assessing competition for the target species and stand often remains unknown. Optimum neighbourhood size has been computed using maximum likelihood and global optimization model fitting (Canham et al., 2004; Das, 2012) and by sequentially increasing neighbourhood size until the maximum variance explained is reached (Silander and Pacala, 1985; Simard and Sachs, 2004; Fraver et al., 2014). These methods allow for the study trees to dictate the competition area. However, they require large spatial datasets and large distances to evaluate neighbourhood competition. Trade-offs remain between finding a biologically critical competition zone and the potential bias and costs associated with data collection over larger scales.

The method used for this study sequentially increased the neighbourhood size, assessed the change in AIC value, and selected the radius that minimized the AIC. A previous study using a similar approach found that optimum radius increased with stand age consistently among the study species with little variation in radius size between species in the same stand age (Simard and Sachs, 2004). Similarly in my study, radius size varied little between species of the same successional stage, however, the opposite trend emerged for radius size and stand age, with competition radius decreasing as stands got older. All focal species showed the largest optimum radius at the immature stage and smallest radius at the old-growth stage.

For the immature stands, the competition radius was equal for all focal tree species (radius=9 m). Mean tree diameter was similar for all species in this stand, suggesting neighbourhood size could be related to tree diameter. The area of competition perceived by a tree is known to be related to tree size and height (Opie, 1968; Bella, 1971). For western hemlock and western redcedar, the mean tree sizes were largest in the immature stands. The larger tree size would require a larger growing space and cause trees to perceive neighbours over greater distances. The smaller competition radius for western hemlock in the mature and old-growth stands corresponds with a decrease in mean tree diameter and height. The smaller trees would require fewer resources for growing and perceive competitors over smaller distances. The canopy in the later successional stages also showed increased

stratification, particularly by the dominant Douglas fir trees. It is possible the vertical stratification allowed for more light to reach the understory, further reducing the extent of overstory suppression experienced by western hemlock trees. In the older stands, large hemlock trees also emerged into the upper canopy layer, giving them a competitive advantage. For western redcedar, competition neighbourhood size did not follow the trend of tree size as it did for western hemlock. Western redcedar tree size was smallest in the mature stand but increased in the old-growth stand, while neighbourhood size continued to decrease with stand age. However, the larger neighbourhood radius for western redcedar compared to western hemlock in the older stand could be explained by redcedar's high water requirements (Klinka and Brisco, 2009), which would lead to interactions with competitors at greater distances.

Douglas fir competition radius also decreased with stand age, however, tree size for this species increased. The results of reduced neighbourhood size with successional stage were inconsistent with previous studies (Simard and Sachs, 2004) where competition area increased with stand age and larger trees tended to perceive competitors over greater distances. A possible explanation is that the even canopy layer in the immature stand lead to higher competition and increased the demand for resources over larger scales. Self-thinning and mortality as a result of canopy closure could have increased the tree spacing in older plots, allowing each tree adequate growing space while reducing competitive interactions to only close neighbours (Kenkel, 1988). Neighbourhood size remained larger for Douglas fir than for the shade-tolerant species in the old-growth stand, suggesting the larger size and height requires more space and perceives more competitors than the shade-tolerant neighbours.

A possible limitation to the approach used for identifying the optimum neighbourhood radius is selecting the maximum distance at which to evaluate competition. Analysis is restricted by plot size and by bias associated with the edge correction methods. Stands with high spatial heterogeneity would also likely require larger distances to capture the variability. However in this study, the largest optimum radius selected did not approach the maximum competition radius measured (15 m) suggesting the maximum measured radius was adequate.

3.5.2 Relationship between competition and growth

Several distance-independent and distance-dependent competition indices were

tested to determine the most appropriate index for each species and stand stage. Some studies have found that inter-tree distance is important in explaining competitive relationships (Contreras et al., 2011; Fraver et al., 2014), while other studies have found little evidence to support the use of more complex indices (Lorimer, 1983; Wimberly and Bare, 1996; Wagner and Radosevich, 1998; Comeau et al., 2003). In my study, few trends emerged regarding the best competition index across species and seral stage for predicting growth. For Douglas fir, distance-independent indices were consistently selected as the top indices, suggesting that additional information on neighbour distance is not needed to adequately quantify competition for this species. For immature stands, distance-independent indices were selected for all species, indicating that neighbouring tree size is more important than proximity in young stands. It is also likely that the step of selecting the optimum radius for assessing neighbourhood competition could reduce the necessity of including distance in the competition index (Wagner and Radosevich, 1998). Western redcedar in mature and old-growth stands and western hemlock in the old-growth stand showed model improvement with the addition of distance in the competition indices. This could suggest that neighbour proximity as well as neighbour size is important in determining competition on shade-tolerant species, particularly in older stands. Clusters of western hemlock and redcedar often establish in gaps or close to parent trees. Individuals could experience resource shortages and increased competition in these clusters as trees grow in diameter and emerge into the canopy (Franklin et al., 2002), making distances between trees in a cluster important.

Competition was important in determining growth for all species at all successional stages. This finding extends studies that limit the importance of competition to the dynamics of young forest stands (Franklin and van Pelt, 2004; van Mantgem and Stephenson, 2009). The relationship between competition and growth in the immature stands varied for the focal species. It was expected that negative competitive effects would be highest in younger stands because tree densities are often higher and canopy closure results in increased competition for light and resources (Franklin et al., 2002). This observation was supported for Douglas fir and western hemlock where increasing neighbourhood competition resulted in decreased growth rates. The negative relationship is indicative of the aboveground competition for light and belowground competition for water and nutrients that have been found to become more important after stands have reached canopy closure (Smith et al., 1997). Western redcedar on the other hand showed a positive relationship between growth and competition in this study. One explanation could be that

the sample size for western redcedar was too small for a reliable inference. An alternative explanation could be that facilitation plays a role in redcedar vegetative growth through resource sharing between tree root systems or manipulation of environmental conditions (Burns and Honkala, 1990; Gomez-Aparicio et al., 2011).

In the mature and old-growth stands, competition consistently had a negative effect on tree growth for all focal tree species. For Douglas fir, intraspecific competition was likely dominant due to the larger size of conspecifics and smaller size of heterospecific trees in the older stands. The high growth rate for Douglas fir in the old-growth stand would result in basal area increases that would have a disproportionately large impact on smaller conspecifics. Fraver et al. (2014) also found evidence of reduced growth rates in old-growth stands as a result of competition in Norway spruce (*Picea abies* [L.] H. Karst), with effects on forest dynamics and structure. Western redcedar experienced increasing intensity of competition with stand age while the effect of competition on western hemlock peaked in the mature stands. However, for both shade-tolerant species, higher competition at later successional stages was paralleled by lower species growth rates. The importance of competition in later successional stages for shade-tolerant species was consistent with findings by Lutz et al. (2014).

3.5.3 Relationship between climate and growth

Annual basal area increment was modeled to assess the relationship between growth and climate. A summary of the climate variables showed apparent temperature increases (MAT, MCMT, MWMT) and precipitation decreases (MSP, CMI) from the beginning to the end of the study period, trends that are in line with IPCC projections of increased temperature and decreased summer precipitation by the end of the 21st century (IPCC, 2007).

Climate affected of the three study species differently and the importance of climate variables changed with stand age, suggesting tree species in this region will have varying responses to a changing climate regime. Similar results were found in the boreal forest where jack pine (*Pinus banksiana* Lamb.) and black spruce showed different growth responses to warmer growing seasons (Subedi and Sharma, 2013). Studies also show different responses to climate change for the same species at different elevations and latitudes within the species' natural range (Ettinger et al., 2011). These differences highlight

the complexity of tree-climate interactions, making it difficult to predict with certainty how ecosystems will respond to changing temperature and moisture conditions.

Climate in the year previous to growth appears to be most important for Douglas fir. MAT and CMI of the prior year are positively related to basal area increment (BAI) for all stand ages, suggesting that warm temperatures and sufficient moisture supports the best growing conditions in the following year. Summer water deficit of the previous year is known to cause stress in Douglas fir and affects photosynthetic rates, leaf area index and root development with impacts on stem growth not fully expressed until the following year when the tree must compensate for previous year's losses (Lassoie and Salo, 1981; Case and Peterson, 2005). Summer water deficit in the year of growth is also commonly found to be a major limiting factor to growth for this species (e.g., Beedlow, Lee, Tingey, Waschmann, & Burdick, 2013; Nakawatase & Peterson, 2006; Waring & Franklin, 1979). Contrastingly, my findings show a negative relationship between current year summer precipitation and BAI in the mature and old-growth stands. In this region, Douglas fir is adapted to mild, wet winters and warm, dry summers (Waring and Franklin, 1979). Physiological tolerances have been shown to vary along a moisture gradient with Douglas fir being less tolerant on wet sites (Carter and Klinka, 1992). It is also possible that decreases in net primary productivity are related to increased precipitation as a result of lowered radiation inputs, decreased nutrient levels through leaching and slowed decomposition, and reduced availability of soil oxygen, as have been observed in humid tropical forests (Schuur, 2003). The higher summer precipitation and associated increased cloud cover during the growing season may result in reduced photosynthetic rates and growth (Little et al., 1995).

The negative relationship between previous year MCMT and growth indicate warmer winter temperatures may be detrimental to tree growth. Douglas fir can be photosynthetically active all months of the year, with high rates of carbon assimilation between fall and spring (Emmingham and Waring, 1977; Emmingham, 1982), and contrary to my study, increased winter temperature has been associated with increased growth and productivity (Waring and Franklin, 1979; Little et al., 1995; Zhang and Hebda, 2004). The relationship between MCMT and growth is not well understood but seasonal temperature increases under future climate change may be detrimental to Douglas fir growth.

Western hemlock and western redcedar tend to be less drought-tolerant and generally showed different climate trends than Douglas fir. However, MSP of the previous and growth year continued to be significantly negatively related to growth in 5 out of 6 models for these species. This climate variable was most important for all stands in this

study, and contrasts with previous findings where summer precipitation increases growth by relieving the summer water deficit. Hemlock growth has been found to be highest on mesic sites with this species having low tolerance of drought or excess moisture conditions during the growing season (Kayahara and Pearson, 1996). MSP was the only climate variable significantly related to growth for hemlock in the immature stands. At this stage, western hemlock was largely restricted to the understory, and overtopping Douglas fir trees may have moderated the understory environment and provided protection from weather extremes (Callaway et al., 2002). As the trees grow into the canopy layer, increased exposure to the environmental variables may have a larger impact on growth. At the mature stand age, MWMT for the current and previous year is negatively related to growth in western hemlock. This is confirmed by previous studies which have found growing season temperature to be negatively associated with growth (Ettinger et al., 2011) and have predicted growth rates will decrease under warmer and drier growing season conditions (Laroque and Smith, 2005). A similar trend was found for mountain hemlock (*Tsuga mertensiana* [Bong.] Carr.), with increasing growing season temperature under current moisture levels expected to reduce growth rates (Peterson and Peterson, 2001), supporting the results of reduced growth under warmer summer temperatures.

Climate variables have mixed results for western redcedar, making their importance difficult to disentangle. MWMT of the current and previous year positively influence growth in immature stands but have negative effects in mature stands. This suggests warmer temperatures during the growing season, particularly when water may be most limiting, could be more detrimental in older stands where larger trees increase competition for available moisture. As with western hemlock, western redcedar in young stands may have benefited from protection provided by the canopy layer that lessened as the trees grew into the canopy at later successional stages (Bertness and Callaway, 1994). CMI, an indicator of moisture conditions, was negatively associated with growth in the current year but positively associated in the year previous, for mature and old-growth stands. Sufficient moisture in the previous year ensures resources are available in the following growing season. However, western redcedar is most productive on sites without excess moisture or moisture deficits (Kayahara et al., 1997; Klinka and Brisco, 2009). The inverse relationship between current year CMI and BAI could indicate that excess moisture is a larger limiting factor than drought on these sites. Results from a previous climate study predicted reduced growth for redcedar under warmer, drier summer conditions, and cooler, wetter autumn conditions (Larocque and Smith, 2005). Alternatively, Ettinger et al. (2011) predicted

growth increases with warmer growing season temperature being countered by growth decreases with lower levels of summer precipitation. The variability and contradicting results make it difficult to predict growth trends for this species under changing climate conditions.

MCMT showed mixed results with current and previous year often having positive and negative effects on growth, respectively, for western hemlock and western redcedar. MCMT is particularly difficult to interpret because the coldest month can occur before the growing season (January or February), or after the growing season (November or December). Alternative winter temperature indices may show a more clear relationship with growth in this region, where the mild climate results in small deviations in monthly temperatures between seasons.

3.5.4 Relationship of size and habitat variables with growth

Initial tree size was important in explaining growth for all species and stands, as expected, with larger trees experiencing higher growth rates. However, the magnitude of the effect differed among stands of different ages and the study species. Growth initially increased rapidly with tree size but eventually reached a plateau with tree size having a smaller effect for all species. Size had the largest positive effect on growth for Douglas fir in the immature stands and the effect decreased with stand age. This can be attributed to the population in younger stands being dominated by smaller trees and growth being in the initial phase of rapid increase with increasing tree size. For western hemlock and western redcedar, the effect of tree size on growth peaked in the mature stand. The greater influence of initial size can be related to the small median tree size, where growth increases most rapidly with increasing size. The volume added to a tree is also related to the tree's leaf area (Dale et al., 1985). Leaf area increases as young trees grow resulting in higher photosynthetic rates and diameter increments. However, the diameter increment decreases as the tree gets larger because of the increased growth is spread over a larger perimeter (Stadt et al., 2007). This results in the nonlinear relationship between tree growth and tree size. Rapid tree growth in small trees has typically been related to competition for light and securing a place in the canopy to avoid being shaded out (Franklin et al., 2002). This is especially true for the more shade-intolerant Douglas fir. Growth of shade-tolerant species is less predictable with size or age because they can remain suppressed in the understory for many years and have very slow growth rates before they are released (Canham, 1988; Stan

and Daniels, 2010). Tree size is also a proxy for age. Large trees are typically the oldest and are more susceptible to other stressors (insects and disease) or have reached their maximum potential growth (Franklin et al., 2002; Franklin and van Pelt, 2004) resulting in slowed growth.

The importance of slope and elevation varied with species and stand age. For Douglas fir, habitat variables were most influential in the immature stands where they had a negative impact on growth. Slope was also significant in the mature stands. Steeper slopes and higher elevation indicated less suitable growing conditions in this region. The negative association between growth and elevation in is inconsistent with known habitat preferences for this species (Rehfeldt, 1989; Monserud et al., 1990). However, the elevation range between study plots was small and may not have been adequate in assessing the relationships observed over larger elevation gradients. The significance of slope may represent microhabitat variability and describe preferences in environment selection among a generally uniform topography.

For the other focal species, the effect of elevation showed varying significance. Reduced growth was related to higher elevations in the old-growth stand for western hemlock. A previous study found western hemlock seedling density was greater on lower slopes than upper slopes (Wimberly and Spies, 2001), and this trend may persist through succession resulting in the inverse growth-elevation relationship in the old-growth stand. He and Duncan (2000) also found western hemlock to have reduced survival at higher elevations in old-growth stands. Elevation was negatively associated with growth for western redcedar in the mature stands, while none of the other stand ages showing significant relationships with the habitat variables. Slope was positively related to growth for western hemlock in the old-growth stand, suggesting it may inhabit steeper slopes less suited to other species.

3.5.5 Some limitations and conclusions of this growth study

To gain a more complete understanding of the factors affecting tree growth, many other variables could be tested that were not considered in this study. Several sources of competition were not accounted for, including the influence of tree height, canopy size, light levels, and belowground competition. Understory vegetation was also not quantified. Some of the study sites had very high salal density in the understory. It has been found that tree seedlings have to compete with salal for soil nutrients (Messier, 1993), and that salal

understory density caused reduced growth in Douglas fir and western hemlock seedlings (Brandeis et al., 2001). Salal has also been found to compete with conifer trees for soil water, often having a competitive advantage when soil water is low, resulting in reduced tree growth (Black et al., 1980; Price et al., 1986). The inclusion of herbaceous cover in competition assessments could help explain tree growth, particularly in small trees and saplings. Habitat variables such as soil nutrient status and soil moisture regime are known to be highly correlated with Douglas fir site index, and stand productivity can vary with soil properties on sites regarded as uniform (Curt et al., 2001). Carter and Klinka (1992) found that factors relating to site characteristics can alter species resource demands. For example, Douglas fir showed moderate shade tolerance on mesic sites but was shade-intolerant on moist sites, suggesting that competition for light would have a stronger effect on tree growth on wet sites. It is rarely possible or practical to measure all possible factors influencing tree growth, but understanding the complexity of tree resource requirements under various site and competitive conditions is important for accurately disentangling the drivers that govern tree growth and highlights the need to consider both endogenous and exogenous processes in growth models.

Both competition and climate variables were found to be significant drivers of growth in this study, highlighting the need to understand the complexity and interactions of several dominant factors. Kunstler et al. (2011) found that the intensity of competition remained the same across climate gradients, but the importance of competition as a driving factor may decrease as other stressors increase. This will become increasingly important under future climate changes where the response of trees to temperature and precipitation stress will result in unpredictable dynamics and interactions with existing pressures, including competition.

A distinct trend emerged for Douglas fir growth with the data showing opposing trends when calculated from DBH census measurements and increment core samples. The growth rate of Douglas fir increased with stand age using census data (Table 3.6) but decreased with stand age using increment core ring measurements (Table 3.10). Trees selected for increment coring covered the full range of tree sizes available, making up a different size distribution than the census data. This may have contributed to the different growth trends. It is also possible that measurement errors at the two censuses may have resulted in the reversed trend. This finding highlights the need to understand the possible biases of using census data versus increment core data to increase the reliability of conclusions drawn from the data.

3.5.6 Relationship between competition and mortality

Understanding tree mortality is important for stand dynamics because it is one of the main drivers of forest succession. Overstory mortality creates canopy gaps that support the release and establishment of late-successional and shade-tolerant species. Both biotic and abiotic factors may be responsible for causing mortality within forest stands. Tree size, competition and habitat variables were analyzed as drivers of mortality for the three focal species.

Competition was important for all species and stands, making it the most important driver of mortality assessed in this study. Distance-independent competition indices were selected as the top indices in 7 out of 8 models suggesting simpler competition measures are better than more complex, distance-dependent indices for explaining competition related to mortality. Using the method of optimum competition radius selection could also reduce the necessity of including distance in the competition index, making distance-dependent indices appear to have a poorer fit (Wagner and Radosevich, 1998). Optimum neighbourhood radius for assessing competition varied between species and stand age, indicating species perceive competition from different proximities based on successional stage. Douglas fir showed large competition radii for the immature and mature stands, but the neighbourhood decreased to the smallest radius (1 m) in the old-growth stand. Douglas fir experiences strong self-thinning in developing stands (Franklin et al., 2002) and these results show that trees considerable distances away contribute to mortality through suppression and resource competition. The opposite trend occurred for western redcedar, with competition neighbourhood increasing with stand age. This suggests that the large trees present in old-growth stands are capable of influencing western redcedar mortality over large scales. Western hemlock was the only species that maintained a consistent radius through all stand ages.

As expected, increased neighbourhood competition resulted in increased mortality or lower survival for Douglas fir trees. The intensity of competition was highest in the immature stand and decreased with succession, but competition remained important in all stand ages. Density-dependent mortality and self-thinning are apparent drivers of mortality in young forest stands and have been observed for many species (Kenkel, 1988; Barclay and Layton, 1990; He and Duncan, 2000; Larson et al., 2015). However, mortality in older stands is assumed to shift away from competition as other biotic and abiotic factors (such as windthrow, insects, disease, and climate) become dominant (Franklin and van Pelt, 2004; van Mantgem and Stephenson, 2009; Larson and Franklin, 2010; Larson et al., 2015).

Contrastingly, my study found that competition continues to be important in old-growth stands, although the intensity of competition is lower than in younger stands. Similar evidence has been found in deciduous forests (Ward et al., 1996) and in old-growth stands in California (Das et al., 2011).

Competition was also a significant factor in determining tree mortality and survival for western hemlock and western redcedar. However, the direction of the relationship differs from that for Douglas fir. Increased neighbourhood competition on western hemlock trees showed a negative influence on mortality for all successional stages. This contrasts with previous studies that found competition had a negative effect on survival (He and Duncan, 2000; Lutz et al., 2014). Mechanical damage (Lutz and Halpern, 2006) and snow damage (Barclay and Layton, 1990) have also dominated hemlock mortality in some stands. Western redcedar also showed a negative relationship between mortality and competition in the mature stand, but positive in the old-growth stand. Lutz et al. (2014) found similar results in old-growth forests with redcedar experiencing mortality due to interspecific competition. Conversely, the study by He and Duncan (2000) detected no density-dependent effects for redcedar and mechanical damage has also been found to be important for this species (Lutz and Halpern, 2006).

Positive associations between survival and competition are uncommon, particularly in temperate forests with low biodiversity. However, facilitation has been documented in some mixed stands. For example, a study in mixed-wood stands of Alberta found large trees had lower chances of survival when stand basal area was low and suggested canopy tree mortality increased exposure of other trees to wind and biotic damage (Yao et al., 2001). Paper birch (*Betula papyrifera* Marsh.) has been found to positively influence Douglas fir survival due to increased mycorrhizal fungi diversity and protection against disease (Simard and Vyse, 2006). Paper birch also facilitated shade-tolerant species through higher nutrient turnover rates (Simard and Vyse, 2006). Black spruce was found to grow better under aspen (*Populus tremuloides* Michx.) caused by greater organic matter nutrient concentration compared to other conifer species (Cavard et al., 2011) and canopy trees had ameliorating effects on temperature and moisture in the understory that supported mountain hemlock regeneration and survival (Peterson and Peterson, 2001). These are examples of some the mechanisms that could drive the positive relationships between competition and survival for the shade-tolerant species in this study, highlighting the complexity of neighbourhood interactions operating on different species across forest succession.

The findings of competition as a driver of mortality are supported by the spatial pattern analysis completed in the previous chapter, with only slight deviations. Douglas fir in the old-growth stand was not found to undergo density-dependent mortality in the spatial analysis, but competition was significant driver in the logistic modeling. The small coefficient in the mortality model suggests competition is lowest in the old-growth stand and it is possible that the effects were too low to detect using spatial analysis. Western hemlock showed density-dependent mortality for the immature stand based on point patterns, but positive competitive effects in the model. He and Duncan (2000) found that accounting for elevation in the model changed the relationship between density and survival, making it insignificant. A similar trend could explain the occurrence of negative density-dependence in the spatial analysis.

3.5.7 Relationship of size and habitat variables to mortality

Elevation was positively related to survival and negatively related to mortality of Douglas fir in the mature and old-growth stands across the range of elevation included in this study (229 m to 481 m). Douglas fir develops dominance in stands that are too dry for western hemlock and western redcedar to establish (Franklin and Hemstrom, 1981) and a strong moisture gradient exists with elevation, with soils being drier at higher elevations (He and Duncan, 2000). A negative relationship was found between elevation and western hemlock survival. Hemlock has higher moisture requirements than Douglas fir and along the same moisture gradient, upper slopes would be drier and less suitable for hemlock survival. Slope was not important in models of mortality for any of the focal species.

DBH (diameter at breast height) and DBH^2 were included in the models to assess the impact of tree size on mortality, with the assumption that mortality risk is high for small trees, decreases as trees get larger, and increases again after trees reach a certain size. This hypothesis was confirmed in the immature and mature stands for Douglas fir where DBH was positively related and DBH^2 negatively related to survival. The same trends were confirmed for western hemlock in the old-growth stand, and western redcedar in the mature stands. Larger size equates to a greater chance of acquiring resources and avoiding competitive effects, both of which would reduce the risk of mortality (Monserud and Sterba, 1999). Size is also an indicator of tree age. Once a tree has reached a certain size or age, mortality risk rises. Several mechanisms have been suggested to explain increased mortality in large, old trees. One mechanism points to lower photosynthetic rates caused by reduced

leaf areas and nutrient limitations. Reduced rates of photosynthesis results in higher maintenance costs, slower growth, reduced production of resistance chemicals, and consequently, an increased susceptibility to disease and insect attacks (Yang et al., 2003). Slowing of growth related to tree genetics and hydraulic resistance have also been proposed as the mechanisms driving higher mortality in large, old trees (Ryan and Yoder, 1997).

Tree size was not significant for Douglas fir and western redcedar in the old-growth stand, and western hemlock in the immature and mature stands. While initial size appears unimportant in these models, it is unlikely that size does not influence mortality. Monserud and Sterba (1999) suggest a very large sample size is needed to detect the trend of decreasing mortality in very large trees. Models with less than 400 individuals did not show significant effects of tree size on mortality indicating that a larger sample may be necessary to detect size related mortality effects. Species in these stands are long-lived and capable of living for several centuries under suitable conditions (Franklin and Hemstrom, 1981; Franklin et al., 1981), and the range of tree sizes required to cover the full range of diameter size and tree age for detecting size-related mortality may not be available in these datasets.

3.5.8 Mortality study limitations

The variables used in this study provide knowledge on the conditions influencing mortality risk in forest stands. However, additional variables could be added to improve the mortality models. Tree vigour (i.e., crown ratio, diameter increment) has been shown to be important in determining mortality risk (Monserud and Sterba, 1999; Yang et al., 2003) and would improve the models if included as a variable. Other density-dependent processes not considered in this study may also have played a role in tree mortality at these sites. For example, diseases such as root rot are known to cause growth reductions and mortality, particularly in areas with high densities of the host species (Bloomberg and Reynolds, 1985).

Inclusion of climate variables would also improve model accuracy since recent studies have attributed increases in tree mortality rates to changing climate regimes (van Mantgem and Stephenson, 2009; Allen et al., 2010; Peng et al., 2011). However, the datasets in this study did not allow for evaluating climate effects due to data on tree mortality being restricted to one measurement interval.

3.6 Conclusions

Individual tree growth and mortality was modeled using biotic and abiotic variables to determine the dominant drivers of demographic rates in a chronosequence of forest stands in coastal British Columbia.

This study showed that competition influences growth and mortality in stand of different ages. Optimum competition radius size for growth was found to decrease with successional stage regardless of tree species while no general trends were found for optimum radius for mortality. Having flexibility when analyzing neighbourhood scale helps improve the usefulness of the competition index and provides insight into how trees perceive competition through space and time. In general, distance-independent competition indices were found to adequately assess the effect of competition on growth and mortality, although neighbour distance may become important in quantifying competition for shade-tolerant species in later successional stages. Competition had a negative effect on the growth and mortality of Douglas fir across all successional stages, with the largest influence in young stands. Western hemlock and western redcedar growth was negatively influenced by neighbour competition most heavily in the older stands, but redcedar showed positive competitive interactions in the immature stands. Survival of the shade-tolerant species was positively associated with neighbourhood competition until the old-growth stage, highlighting that possible facilitation and sheltering processes are important for these species.

Initial tree size was positively related to growth for all species and successional stages with the highest importance for Douglas fir in the young stands and in the mature stands the shade-tolerant species, where trees were smallest and in their most rapid growth phases. Tree size was important and the U-shaped diameter trend was detected for mortality for each species in some of the successional stages, however, detection may be restricted to larger sample sizes. The importance of habitat varied among focal species and stand ages, but slope was not important in evaluating mortality risk.

Climate was found to significantly influence annual growth for the focal species in this study. Summer precipitation was the most important variable, with precipitation generally having a negative effect on growth for all species. Overall, climate affected the three focal species differently and the importance of climate variables changed with stand age, suggesting species in this region will have varying responses to a changing climate regime, making it difficult to predict the effect of climate change. Although not included in this study, climate is also expected to play a role in tree survival and inclusion of climate in

future mortality models will provide a more complete understanding of the processes governing mortality risk.

The significance of competition in determining growth and mortality across the chronosequence, and the influence of climate on annual growth rates in this study highlights the necessity of including both sets of variables when studying demographic rates. Failing to adequately account for the complexity of forest dynamics and the diversity of driving processes can lead to inaccurate inferences regarding stand dynamics and undesirable management action, particularly under the uncertainty of a changing climate.

Chapter 4: General Conclusions

Rapid forest changes over recent decades have emphasized the importance of understanding the mechanisms driving changes in forest dynamics and structure. This study analyzed the effects of endogenous and exogenous processes on species' demographic rates and spatial distributions in a chronosequence of forest stands in coastal British Columbia.

Competition was found to negatively affect growth of all study species. Contrary to assumptions of lower competition in later successional forests, density-dependent growth reductions were evident in all stages of the chronosequence. Growth was also driven by tree size and climate. Summer precipitation was the most important climate variable, negatively affecting growth for all study species. Other temperature and precipitation variables were significant for the species, but the direction of the growth response was not consistent. As a result, species in this region will likely have varying responses to altered climate regimes, adding uncertainty to predictions of stand-level changes. The diversity of the mechanisms operating on tree growth rates emphasizes the necessity of understanding the complexity and interactions of the identified dominant factors when analyzing forest stands.

Density-dependent processes were found to alter stand structure through tree mortality and recruitment. Douglas fir mortality was strongly influenced by negative density-dependent processes at all stand ages with the species becoming more regularly distributed in older stands. Facilitative processes may promote the survival of western hemlock and western redcedar in most stands, highlighting the importance of understanding positive interactions for shade-tolerant species. Aggregated recruitment of study species occurred most often in close proximity to adult trees. This study has showed that spatial patterns in stands of different ages change over time, and that competition and species characteristics are important indicators in predicting the spatial changes of forest stands at different stages of succession.

The results of this study underscore the importance of competition and climate as mechanisms driving forest structure and dynamics in all stand ages, necessitating the inclusion of both sets of variables in analyzing demographic rates. Knowledge of competition and climate as drivers of species' demographics and spatial distributions can be incorporated into forestry and conservation management decision-making. Findings from this study provide a better understanding of the processes driving dynamics of forest succession, and can be used for interpreting and anticipating stand structure in the future.

Bibliography

Acker, S.A., Boetsch, J.R., Bivin, M., Whiteaker, L., Cole, C., Philippi, T., 2015. Recent tree mortality and recruitment in mature and old-growth forests in western Washington. For. Ecol. Manage. 336, 109–118.

Akaike, H., 1974. A new look at the statistical model identification. IEEE Trans. Automat. Contr. 19, 716–723.

Allen, C.D., Macalady, A.K., Chenchouni, H., Bachelet, D., McDowell, N., Vennetier, M., Kitzberger, T., Rigling, A., Breshears, D.D., Hogg, E.H., Gonzalez, P., Fensham, R., Zhang, Z., Castro, J., Demidova, N., Lim, J.-H., Allard, G., Running, S.W., Semerci, A., Cobb, N., 2010. A global overview of drought and heat-induced tree mortality reveals emerging climate change risks for forests. For. Ecol. Manage. 259, 660–684.

Anderegg, W.R.L., Kane, J.M., Anderegg, L.D.L., 2013. Consequences of widespread tree mortality triggered by drought and temperature stress. Nat. Clim. Chang. 3, 30–36.

Baddeley, A.J., Turner, R., 2005. spatstat: An R package for analyzing spatial point patterns. J. Stat. Softw. 12, 1–42.

Barclay, H.J., Layton, C.R., 1990. Growth and mortality in managed Douglas fir: Relation to a competition index. For. Ecol. Manage. 36, 187–204.

Bartoń, K., 2016. MuMIn: Multi-model inference. R Packag. version 1.15.6. https://cran.r-project.org/web/packages/MuMIn

Beedlow, P.A., Lee, E.H., Tingey, D.T., Waschmann, R.S., Burdick, C.A., 2013. The importance of seasonal temperature and moisture patterns on growth of Douglas-fir in western Oregon, USA. Agric. For. Meteorol. 169, 174–185.

Begon, M., Harper, J.L., Townsend, C.R., 1996. Ecology: Individuals, populations and communities, 3rd ed. Blackwell, Oxford.

Beier, C.M., Sink, S.E., Hennon, P.E., D'Amore, D. V., Juday, G.P., 2008. Twentieth-century warming and the dendroclimatology of declining yellow-cedar forests in southeastern Alaska. Can. J. For. Res. 38, 1319–1334.

Bella, I.E., 1971. A new competition model for individual trees. For. Sci. 364–372.

Bertness, M.D., Callaway, R.M., 1994. Positive interactions in communities. Trends Ecol. Evol. 9, 187–191.

Black, T.A., Tan, C.S., Nnyamah, J.U., 1980. Transpiration rate of Douglas fir trees in thinned and unthinned stands. Can. J. Soil Sci. 60, 625–631.

Bloomberg, W.J., Reynolds, G., 1985. Growth loss and mortality in laminated root rot infection centers in on Vancouver Island. For. Sci. 31, 497–508.

Brandeis, T.J., Newton, M., Cole, E.C., 2001. Underplanted conifer seedling survival and growth in thinned Douglas-fir stands. Can. J. For. Res. 31, 302–312.

Bruno, J.F., Stachowicz, J.J., Bertness, M.D., 2003. Inclusion of facilitation into ecological theory. Trends Ecol. Evol. 18, 119–125.

Buchman, R.G., Pederson, S.P., Walters, N.R., 1983. A tree survival model with application to the Great Lakes region. Can. J. For. Res. 13, 601–608.

Burns, R.M., Honkala, B.H., 1990. Silvics of North America: Conifers, in: Agriculture Handbook 654. U.S. Department of Agriculture, Forest Service, Washington, D.C.

Callaway, R.M., Brooker, R.W., Choler, P., Kikvidze, Z., Lortie, C.J., Michalet, R., Paolini, L., Pugnaire, F.I., Newingham, B., Aschehoug, E.T., Armas, C., Kikodze, D., Cook, B.J., 2002. Positive interactions among alpine plants increase with stress. Nature 417, 844–848.

Canham, C.D., 1988. Growth and canopy architecture of shade-tolerant trees: Response to canopy gaps. Ecology 69, 786–795.

Canham, C.D., LePage, P.T., Coates, K.D., 2004. A neighborhood analysis of canopy tree competition: Effects of shading versus crowding. Can. J. For. Res. 34, 778–787.

Canham, C.D., Papaik, M.J., Uriarte, M., McWilliams, W.H., Jenkins, J.C., Twery, M.J., 2006. Neighborhood analyses of canopy tree competition along environmental gradients in New England forests. Ecol. Appl. 16, 540–554.

Carter, R.E., Klinka, K., 1992. Variation in shade tolerance of Douglas fir, western hemlock, and western red cedar in coastal British Columbia. For. Ecol. Manage. 55, 87–105.

Case, M.J., Peterson, D.L., 2005. Fine-scale variability in growth-climate relationships of Douglas-fir, North Cascade Range, Washington. Can. J. For. Res. 35, 2743–2755.

Cavard, X., Bergeron, Y., Chen, H.Y.H., Paré, D., Laganière, J., Brassard, B., 2011. Competition and facilitation between tree species change with stand development. Oikos 120, 1683–1695.

Clark, J.S., Macklin, E., Wood, L., 1998. Stages and spatial scales of recruitment limitation in southern Appalachian forests. Ecol. Monogr. 68, 213–235.

Comeau, P.G., Wang, J.R., Letchford, T., 2003. Influences of paper birch competition on growth of understory white spruce and subalpine fir following spacing. Can. J. For. Res. 33, 1962–1973.

Contreras, M.A., Affleck, D., Chung, W., 2011. Evaluating tree competition indices as predictors of basal area increment in western Montana forests. For. Ecol. Manage. 262, 1939–1949.

Cortini, F., Comeau, P.G., 2008a. Effects of red alder and paper birch competition on juvenile growth of three conifer species in southwestern British Columbia. For. Ecol. Manage. 256, 1795–1803.

Cortini, F., Comeau, P.G., 2008b. Evaluation of competitive effects of green alder, willow and other tall shrubs on white spruce and lodgepole pine in northern Alberta. For. Ecol. Manage. 255, 82–91.

Crecente-Campo, F., Marshall, P.L., Rodríguez-Soalleiro, R., 2009. Modeling non-catastrophic individual-tree mortality for Pinus radiata plantations in northwestern Spain. For. Ecol. Manage. 257, 1542–1550.

Curt, T., Bouchaud, M., Agrech, G., 2001. Predicting site index of Douglas-fir plantations from ecological variables in the Massif Central area of France. For. Ecol. Manage. 149, 61–74.

Curtis, R.O., DeBell, D.S., Harrington, C., Lavender, D.P., St. Clair, J.B., Tappeiner, J.C., Walstad, J.D., 1998. Silviculture for multiple objectives in the Douglas-fir region, General Technical Report PNW-GTR-435. U.S. Department of Agriculture, Forest Service, Pacific Northwest Research Station.

Dale, V.H., Doyle, T.W., Shugart, H.H., 1985. A comparison of tree growth models. Ecol. Modell. 29, 145–169.

Dale, V.H., Joyce, L.A., McNulty, S., Neilson, R.P., Ayres, M.P., Flannigan, M.D., Hanson, P.J., Irland, L.C., Lugo, A.E., Peterson, C.J., Simberloff, D., Swanson, F.J., Stocks, B.J., Michael Wotton, B., 2001. Climate change and forest disturbances. Bioscience 51, 723–734.

Das, A., 2012. The effect of size and competition on tree growth rate in old-growth coniferous forests. Can. J. For. Res. 42, 1983–1995.

Das, A., Battles, J., Stephenson, N.L., van Mantgem, P.J., 2011. The contribution of competition to tree mortality in old-growth coniferous forests. For. Ecol. Manage. 261, 1203–1213.

Das, A., Battles, J., van Mantgem, P.J., Stephenson, N.L., 2008. Spatial elements of mortality risk in old-growth forests. Ecology 89, 1744–1756.

Delissio, L.J., Primack, R.B., 2003. The impact of drought on the population dynamics of canopy-tree seedlings in an aseasonal Malaysian rain forest. J. Trop. Ecol. 19, 489–500.

DellaSala, D.A., Moola, F., Alaback, P., Paquet, P.C., Schoen, J.W., Noss, R.F., 2011. Temperate and boreal rainforests of the pacific coast of North America, in: DellaSala, D.A. (Ed.), Temperate and Boreal Rainforests of the World: Ecology and Conservation. Island Press, Washington, pp. 42–81.

Dixon, P.M., 2002. Ripley's K function. Encycl. Environmetrics 3, 1796–1803.

Duncan, R.P., 1991. Competition and the coexistence of species in a mixed podocarp stand. J. Ecol. 79, 1073–1084.

Emmingham, W.H., 1982. Ecological indexes as a means of evaluating climate, species distribution, and primary production, in: Edmonds, R.L. (Ed.), Analysis of Coniferous Forest Ecosystems in the Western United States. Hutchinson Ross Publishing Company, Stroudsburg, PA, pp. 45–67.

Emmingham, W.H., Waring, R.H., 1977. An index of photosynthesis for comparing forest sites in western Oregon. Can. J. For. Res. 7, 165–174.

Ettinger, A.K., Ford, K.R., Hille Ris Lambers, J., 2011. Climate determines upper, but not lower, altitudinal range limits of Pacific Northwest conifers. Ecology 92, 1323–1331.

Etzold, S., Waldner, P., Thimonier, A., Schmitt, M., Dobbertin, M., 2014. Tree growth in Swiss forests between 1995 and 2010 in relation to climate and stand conditions: Recent disturbances matter. For. Ecol. Manage. 311, 41–55.

Feeley, K.J., Wright, S.J., Supardi, M.N.N., Kassim, A.R., Davies, S.J., 2007. Decelerating growth in tropical forest trees. Ecol. Lett. 10, 461–469.

Franklin, J.F., Cromack, K., Denison, W., McKee, A., Maser, C., Sedell, J., Swanson, F.J., Juday, G.P., 1981. Ecological characteristics of old growth Douglas-fir forests, General Technical Report PNW-GTR-118. U.S. Department of Agriculture, Forest Service, Pacific Northwest Research Station.

Franklin, J.F., Hemstrom, M.A., 1981. Aspects of succession in the coniferous forests of the Pacific Northwest, in: West, D.C., Shugart, H.H., Botkin, D.F. (Eds.), Forest Succession: Concepts and Applications. Springer-Verlag New York, New York, pp. 212–229.

Franklin, J.F., Shugart, H.H., Harmon, M.E., 1987. Tree death as an ecological process. Bioscience 37, 550–556.

Franklin, J.F., Spies, T.A., van Pelt, R., Carey, A.B., Thornburgh, D.A., Berg, D.R., Lindenmayer, D.B., Harmon, M.E., Keeton, W.S., Shaw, D.C., Bible, K.J., Chen, J., 2002. Disturbances and structural development of natural forest ecosystems with silvicultural implications, using Douglas-fir forests as an example. For. Ecol. Manage. 155, 399–423.

Franklin, J.F., van Pelt, R., 2004. Spatial aspects of structural complexity in old-growth forests. J. For. 102, 22–28.

Fraver, S., D'Amato, A.W., Bradford, J.B., Jonsson, B.G., Jönsson, M., Esseen, P.A., 2014. Tree growth and competition in an old-growth Picea abies forest of boreal Sweden: Influence of tree spatial patterning. J. Veg. Sci. 25, 374–385.

Getzin, S., Dean, C., He, F., Trofymow, J.A., Wiegand, K., Wiegand, T., 2006. Spatial patterns and competition of tree species in a Douglas-fir chronosequence on Vancouver Island. Ecography 29, 671–682.

Getzin, S., Wiegand, T., Wiegand, K., He, F., 2008. Heterogeneity influences spatial patterns and demographics in forest stands. J. Ecol. 96, 807–820.

Girardin, M.P., Guo, X.J., Bernier, P.Y., Raulier, F., Gauthier, S., 2012. Changes in growth of pristine boreal North American forests from 1950 to 2005 driven by landscape demographics and species traits. Biogeosciences 9, 2523–2536.

Gomez-Aparicio, L., Garcia-Valdes, R., Ruiz-Benito, P., Zavala, M.A., 2011. Disentangling the relative importance of climate, size and competition on tree growth in Iberian forests: Implications for forest management under global change. Glob. Chang. Biol. 17, 2400–2414.

Gray, A.N., Spies, T.A., Pabst, R.J., 2012. Canopy gaps affect long-term patterns of tree growth and mortality in mature and old-growth forests in the Pacific Northwest. For. Ecol. Manage. 281, 111–120.

Gray, L., He, F., 2009. Spatial point-pattern analysis for detecting density-dependent competition in a boreal chronosequence of Alberta. For. Ecol. Manage. 259, 98–106.

Hamann, A., Wang, T., 2006. Potential effects of climate change on ecosystem and tree species distribution in British Columbia. Ecology 87, 2773–2786.

Harrell, F.H.J., 2016. rms: Regression modeling strategies. R Packag. version 5.0-0. https://cran.r-project.org/package=rms

He, F., Duncan, R.P., 2000. Density-dependent effects on tree survival in an old-growth Douglas fir forest. J. Ecol. 88, 676–688.

Hegyi, F., 1974. A simulation model for managing Jack pine stands, in: Royal College of Forestry (Ed.), Growth Models for Tree and Stand Simulation. Stockholm, Sweden, pp. 74–90.

Hennon, P.E., D'Amore, D. V., Zeglen, S., Grainger, M., 2005. Yellow-cedar decline in the north coast forest district of British Columbia, Research Note PNW-RN-549. U.S. Department of Agriculture, Forest Service, Pacific Northwest Research Station.

Hille Ris Lambers, J., Clark, J.S., 2003. Effects of dispersal, shrubs, and density-dependent mortality on seed and seedling distributions in temperate forests. Can. J. For. Res. 33, 783–795.

Hogg, E.H., 1997. Temporal scaling of moisture and the forest-grassland boundary in western Canada. Agric. For. Meteorol. 84, 115–122.

Hogg, E.H., Barr, A.G., Black, T.A., 2013. A simple soil moisture index for representing multi-year drought impacts on aspen productivity in the western Canadian interior. Agric. For. Meteorol. 178–179, 173–182.

Hosmer, D.W., Lemeshow, S., 2000. Chapter 5: Assessing the fit of the model, in: Applied Logistic Regression. John WIley & Son, New York, pp. 143–202.

Hubbell, S.P., Ahumada, J.A., Condit, R., Foster, R.B., 2001. Local neighborhood effects on long-term survival of individual trees in a neotropical forest. Ecol. Res. 16, 859–875.

IPCC, 2007. Climate change 2007: Syntehsis report, in: Core Writing Team, Pachauri, R.K., Reisinger, A. (Eds.), A Contribution of Working Groups I, II, III to the Forth Assessment Report of the Intergovernmental Panel on Climate Change. IPCC, Genenva, Switzerland, p. 104.

Islam, M.A., Macdonald, S.E., 2004. Ecophysiological adaptations of black spruce (Picea mariana) and tamarack (Larix laricina) seedlings to flooding. Trees 18, 35–42.

Johnson, D.J., Bourg, N.A., Howe, R., McShea, W.J., Wolf, A., Clay, K., 2014. Conspecific negative density-dependent mortality and the structure of temperate forests. Ecology 95, 2493–2503.

Kayahara, G.J., Klinka, K., Schroff, A.C., 1997. The relationship of site index to synoptic estimates of soil moisture and nutrients for western redcedar (Thuja plicata) in southern coastal British Columbia. Northwest Sci. 71, 167–173.

Kayahara, G.J., Pearson, A.F., 1996. Relationships between site index, and soil moisture and nutrient regimes for western hemlock and Sitka spruce. B.C. Work. Pap. 1–15.

Kenkel, N.C., 1988. Pattern of self-thinning in jack pine: Testing the random mortality hypothesis. Ecology 69, 1017–1024.

Kenkel, N.C., Hendrie, M.L., Bella, I.E., 1997. A long-term study of Pinus banksiana population dynamics. J. Veg. Sci. 8, 241–254.

Klinka, K., Brisco, D., 2009. Silvics and silviculture of coastal western redcedar: A literature review. BC Spec. Rep. Ser. 11.

Klinka, K., Pojar, J., Meidinger, D.V., 1991. Revision of biogeoclimatic units of coastal British Columbia. Northwest Sci. 65, 32–47.

Kunstler, G., Albert, C.H., Courbaud, B., Lavergne, S., Thuiller, W., Vieilledent, G., Zimmermann, N.E., Coomes, D.A., 2011. Effects of competition on tree radial-growth vary in importance but not in intensity along climatic gradients. J. Ecol. 99, 300–312.

Lan, G., Getzin, S., Wiegand, T., Hu, Y., Xie, G., Zhu, H., Cao, M., 2012. Spatial distribution and interspecific associations of tree species in a tropical seasonal rain forest of China. PLoS One 7, 1–9.

Larocque, S.J., Smith, D.J., 2005. A dendroclimatological reconstruction of climate since AD 1700 in the Mt. Waddington area, British Columbia Coast Mountains, Canada. Dendrochronologia 22, 93–106.

Laroque, C.P., Smith, D.J., 2005. Predicted short-term radial-growth changes of trees based on past climate on Vancouver Island, British Columbia. Dendrochronologia 22, 163–168.

Larson, A.J., Franklin, J.F., 2010. The tree mortality regime in temperate old-growth coniferous forests: The role of physical damage. Can. J. For. Res. 40, 2091–2103.

Larson, A.J., Lutz, J.A., Donato, D.C., Freund, J.A., Swanson, M.E., Hille Ris Lambers, J., Sprugel, D.G., Franklin, J.F., 2015. Spatial aspects of tree mortality strongly differ between young and old-growth. Ecology 96, 2855–2861.

Lassoie, J.P., Salo, D.J., 1981. Physiological response of large Douglas-fir to natural and induced soil water deficits. Can. J. For. Res. 11, 139–144.

Lele, S.R., Keim, J.L., Solymos, P., 2016. ResourceSelection: Resource selection (probability) functions for use-availability data. R Packag. version 0.2-6. https://cran.r-project.org/web/packages/ResourceSelection

Lindner, M., Maroschek, M., Netherer, S., Kremer, A., Barbati, A., Garcia-Gonzalo, J., Seidl, R., Delzon, S., Corona, P., Kolström, M., Lexer, M.J., Marchetti, M., 2010. Climate change impacts, adaptive capacity, and vulnerability of European forest ecosystems. For. Ecol. Manage. 259, 698–709.

Little, R.L., Peterson, D.L., Silsbee, D.G., Shainsky, L.J., Bednar, L.F., 1995. Radial growth patterns and the effects of climate on second-growth Douglas-fir (Pseudotsuga menziesii) in the Siskiyou Mountains, Oregon. Can. J. For. Res. 25, 724–735.

Lorimer, C.G., 1983. Tests of age-independent competition indices for individual trees in natural hardwood stands. For. Ecol. Manage. 6, 343–360.

Lorimer, C.G., Frelich, L.E., 1989. A methodology for estimating canopy disturbance frequency and intensity in dense temperate forests. Can. J. For. Res. 19, 651–663.

Lorimer, C.G., Frelich, L.E., 1984. A simulation of equilibrium diameter distributions of sugar maple (Acer saccharum). Bull. Torrey Bot. Club 111, 193–199.

Lutz, J.A., Halpern, C.B., 2006. Tree mortality during early forest development: A long-term study of rates, causes, and consequences. Ecol. Monogr. 76, 257–275.

Lutz, J.A., Larson, A.J., Freund, J.A., Swanson, M.E., Bible, K.J., 2013. The importance of large-diameter trees to forest structural heterogeneity. PLoS One 8, 1–13.

Lutz, J.A., Larson, A.J., Furniss, T.J., Donato, D.C., Freund, J.A., Swanson, M.E., Bible, K.J., Chen, J., Franklin, J.F., 2014. Spatially nonrandom tree mortality and ingrowth maintain equilibrium pattern in an old-growth Pseudotsuga-Tsuga forest. Ecology 95, 2047–2054.

Lutz, J.A., van Wagtendonk, J.W., Franklin, J.F., 2010. Climatic water deficit, tree species ranges, and climate change in Yosemite National Park. J. Biogeogr. 37, 936–950.

Ma, Z., Peng, C., Zhu, Q., Chen, H., Yu, G., Li, W., Zhou, X., Wang, W., Zhang, W., 2012. Regional drought-induced reduction in the biomass carbon sink of Canada's boreal forests. Proc. Natl. Acad. Sci. U.S.A. 109, 2423–24277.

Martin-Benito, D., Kint, V., del Río, M., Muys, B., Cañellas, I., 2011. Growth responses of West-Mediterranean Pinus nigra to climate change are modulated by competition and productivity: Past trends and future perspectives. For. Ecol. Manage. 262, 1030–1040.

Mateu, J., Uso, J.L., Montes, F., 1998. The spatial pattern of a forest ecosystem. Ecol. Modell. 108, 163–174.

McLaughlin, S.B., Downing, D.J., Blasing, T.J., Cook, E.R., Adams, H.S., 1987. An analysis of climate and competition as contributors to decline of red spruce in high elevation Appalachian forests of the Eastern United states. Oecologia 72, 487–501.

Messier, C., 1993. Factors limiting early growth of western redcedar, western hemlock and Sitka spruce seedlings on ericaceous-dominated clearcut sites in coastal British Columbia. For. Ecol. Manage. 60, 181–206.

Milton, K., Laca, E.A., Demment, M.W., 1994. Successional patterns of mortality and growth of large trees in a Panamanian lowland forest. J. Ecol. 82, 79–87.

Moeur, M., 1997. Spatial models of competition and gap dynamics in old-growth Tsuga heterophylla/Thuja plicata forests. For. Ecol. Manage. 94, 175–186.

Monserud, R.A., Ek, A.R., 1974. Plot edge bias in forest stand growth simulation models. Can. J. For. Res. 4, 419–423.

Monserud, R.A., Moody, U., Breuer, D.W., 1990. A soil-site study for inland Douglas-fir. Can. J. For. Res. 20, 686–695.

Monserud, R.A., Sterba, H., 1999. Modeling individual tree mortality for Austrian forest species. For. Ecol. Manage. 113, 109–123.

Nagelkerke, N.J.D., 1991. A note on a general definition of the coefficient of determination. Biometrika 78, 691–692.

Nakagawa, S., Schielzeth, H., 2013. A general and simple method for obtaining R^2 from generalized linear mixed-effects models. Methods Ecol. Evol. 4, 133–142.

Nakawatase, J.M., Peterson, D.L., 2006. Spatial variability in forest growth-climate relationships in the Olympic Mountains, Washington. Can. J. For. Res. 36, 77–91.

Nakazawa, M., 2015. fmsb: Functions for medical statistics book with some demographic data. R Packag. version 0.5.2. https://cran.r-project.org/web/packages/fmsb

Nicholson, B.J., 1995. The wetlands of Elk Island National Park: Vegetation classification, water chemistry, and hydrotopographic relationships. Wetlands 15, 119–133.

Opie, J.E., 1968. Predictability of individual tree growth using various definitions of competing basal area. For. Sci. 14, 314–323.

Paine, C.E.T., Marthews, T.R., Vogt, D.R., Purves, D., Rees, M., Hector, A., Turnbull, L.A., 2012. How to fit nonlinear plant growth models and calculate growth rates: An update for ecologists. Methods Ecol. Evol. 3, 245–256.

Peet, R.K., Christensen, N.L., 1987. Competition and tree death. Bioscience 37, 586–595.

Peng, C., Ma, Z., Lei, X., Zhu, Q., Chen, H., Wang, W., Liu, S., Li, W., Fang, X., Zhou, X., 2011. A drought-induced pervasive increase in tree mortality across Canada's boreal forests. Nat. Clim. Chang. 1, 467–471.

Peterson, D.W., Peterson, D.L., 2001. Mountain hemlock growth responds to climatic variability at annual and decadal time scales. Ecology 82, 3330–3345.

Pichancourt, J.B., Firn, J., Chadès, I., Martin, T.G., 2014. Growing biodiverse carbon-rich forests. Glob. Chang. Biol. 20, 382–393.

Pielou, E.C., 1961. Segregation and symmetry in two-species populations as studied by nearest-neighbour relationships. J. Ecol. 49, 255–269.

Pielou, E.C., 1960. A single mechanism to account for regular, random and aggregated populations. J. Ecol. 48, 575–584.

Pinheiro, J., Bates, D., 2000. Mixed-Effects Models in S and S-PLUS. Springer-Verlag New York, New York.

Pinheiro, J., Bates, D., DebRoy, S., Sarkar, D., R Core Team, 2015. nlme: Linear and nonlinear mixed effects models. R Packag. version 3.1-122. https://cran.r-project.org/web/packages/nlme

Pojar, J., Klinka, K., Demarchi, D.A., 1991a. Coastal western hemlock zone, in: Meidinger, D.V., Pojar, J. (Eds.), Ecosystems of British Columbia. B.C. Ministry of Forests, Victoria, B.C., pp. 95–111.

Pojar, J., Meidinger, D.V., Klinka, K., 1991b. Biogeoclimatic ecosystem classification, in: Meidinger, D.V., Pojar, J. (Eds.), Ecosystems of British Columbia. B.C. Ministry of Forests, Victoria, B.C., pp. 9–37.

Pretzsch, H., 2009. Forest Dynamics, Growth and Yield. Springer-Verlag Berlin Heidelberg.

Price, D.T., Black, T.A., Kelliher, F.M., 1986. Effects of salal understory removal on photosynthetic rate and stomatal conductance of young Douglas-fir trees. Can. J. For. Res. 16, 90–97.

R Core Team, 2015. R: A language and environment for statistical computing. R Foundation for Statistical Computing, Vienna, Austria.

Radtke, P.J., Burkhart, H.E., 1998. A comparison of methods for edge-bias compensation. Can. J. For. Res. 28, 942–945.

Raventós, J., Wiegand, T., de Luis, M., 2010. Evidence for the spatial segregation hypothesis: A test with nine-year survivorship data in a Mediterranean shrubland. Ecology 91, 2110–2120.

Rayburn, A.P., Schiffers, K., Schupp, E.W., 2011. Use of precise spatial data for describing spatial patterns and plant interactions in a diverse Great Basin shrub community. Plant Ecol. 212, 585–594.

Rehfeldt, G.E., 1989. Ecological adaptations in Douglas-fir (Pseudotsuga menziesii var. glauca) populations: A synthesis. For. Ecol. Manage. 28, 203–315.

Ripley, B.D., 1977. Modelling spatial patterns. J. R. Stat. Soc. 39, 172–212.

Rivas, J.J.C., González, J.G.Á., Aguirre, O., Hernández, F.J., 2005. The effect of competition on individual tree basal area growth in mature stands of Pinus cooperi Blanco in Durango (Mexico). Eur. J. For. Res. 124, 133–142.

Rouvinen, S., Kuuluvainen, T., 1997. Structure and asymmetry of tree crowns in relation to local competition in a natural mature Scots pine forest. Can. J. For. Res. 890–902.

Ryan, M.G., Yoder, B.J., 1997. Hydraulic limits to tree height and tree growth. Bioscience 47, 235–242.

Schroter, D., Cramer, W., Leemans, R., Prentice, I.C., Araujo, M.B., Arnell, N.W., Bondeau, A., Bugmann, H., Carter, T.R., Gracia, C.A., de la Vega-Leinert, A.C., Erhard, M., Ewert, F., Glendining, M., House, J.I., Kankaanpaa, S., Klein, R.J.T., Lavorel, S., Lindner, M., Metzger, M.J., Meyer, J., Mitchell, T.D., Reginster, I., Rounsevell, M., Sabate, S., Sitch, S., Smith, B., Smith, J., Smith, P., Sykes, M.T., Thonicke, K., Thuiller, W., Tuck, G., Zaehle, S., Zierl, B., 2005. Ecosystem service supply and vulnerability to global change in Europe. Science 310, 1333–1337.

Schuur, E.A.G., 2003. Productivity and global climate revisited: The sensitivity of tropical forest growth to precipitation. Ecology 84, 1165–1170.

Shainsky, L.J., Radosevich, S.R., 1992. Mechanisms of Competition between Douglas-fir and red alder seedlings. Ecology 73, 30–45.

Silander, J.A., Pacala, S.W., 1985. Neighborhood predictors of plant performance. Oecologia 66, 256–263.

Simard, S.W., Sachs, D.L., 2004. Assessment of interspecific competition using relative height and distance indices in an age sequence of seral interior cedar-hemlock forests in British Columbia. Can. J. For. Res. 34, 1228–1240.

Simard, S.W., Vyse, A., 2006. Trade-offs between competition and facilitation: A case study of vegetation management in the interior cedar-hemlock forests of southern British Columbia. Can. J. For. Res. 36, 2486–2496.

Smith, D.M., Larson, B.C., Kelty, M.J., Ashton, P.M.S., 1997. The practice of silviculture: Applied forest ecology, 9th ed. John WIley & Sons., New York.

Spies, T.A., Franklin, J.F., 1991. The structure of natural young, mature, and old-growth Douglas-fir forests in Oregon and Washington. USDA For. Serv. Gen. Tech. Rep. PNW-GTR-285 91–109.

Spittlehouse, D.L., 2003. Water availability, climate change and the growth of Douglas-fir in the Georgia Basin. Can. Water Resour. J. 28, 673–688.

Stadt, K.J., Huston, C., Coates, K.D., Feng, Z., Dale, M.R.T., Lieffers, V.J., 2007. Evaluation of competition and light estimation indices for predicting diameter growth in mature boreal mixed forests. Annu. For. Sci. 64, 477–490.

Stan, A.B., Daniels, L.D., 2010. Growth releases of three shade-tolerant species following canopy gap formation in old-growth forests. J. Veg. Sci. 21, 74–87.

Sterner, R.W., Ribic, C.A., Schatz, G.E., 1986. Testing for life historical changes in spatial patterns of four tropical tree species. J. Ecol. 74, 621–633.

Stoll, P., Weiner, J., Schmid, B., 1994. Growth variation in a naturally established population of Pinus sylvestris. Ecology 75, 660–670.

Stoyan, D., Penttinen, A., 2000. Recent applications of point process methods in forestry statistics. Stat. Sci. 15, 61–78.

Suarez, L., Kitzberger, T., 2010. Differential effects of climate variability on forest dynamics along a precipitation gradient in northern Patagonia. J. Ecol. 98, 1023–1034.

Subedi, N., Sharma, M., 2013. Climate-diameter growth relationships of black spruce and jack pine trees in boreal Ontario, Canada. Glob. Chang. Biol. 19, 505–516.

Taylor, A.H., Zisheng, Q., 1988. Regeneration patterns in old-growth Abies-Betula forests in the Wolong Natural Reserve, Sichuan, China. J. Ecol. 76, 1204–1218.

Torimaru, T., Akada, S., Ishida, K., Matsuda, S., Narita, M., 2013. Spatial associations among major tree species in a cool-temperate forest community under heterogeneous topography and canopy conditions. Popul. Ecol. 55, 261–275.

Trofymow, J.A., Addison, J., Blackwell, B.A., He, F., Preston, C.A., Marshall, V.G., 2003. Attributes and indicators of old-growth and successional Douglas-fir forests on Vancouver Island. Environ. Rev. 11, S187–S204.

Trofymow, J.A., Porter, G.L., Blackwell, B.A., Arksey, R., Marshall, V.G., Pollard, D., 1997. Chronosequences for research into the effects of converting coastal British Columbia old-growth forests to managed forests: An establishment report.

van Mantgem, P.J., Stephenson, N.L., 2009. Widespread increase of tree mortality rates in the western United States. Science 323, 521–524.

Veblen, T.T., Schlegel, F.M., Escobar, B., 1980. Structure and dynamics of old-growth Nothofagus forests in the Valdivian Andes, Chile. J. Ecol. 68, 1–31.

von Oheimb, G., Lang, A.C., Bruelheide, H., Forrester, D.I., Wäsche, I., Yu, M., Härdtle, W., 2011. Individual-tree radial growth in a subtropical broad-leaved forest: The role of local neighbourhood competition. For. Ecol. Manage. 261, 499–507.

Wagner, R.G., Radosevich, S.R., 1998. Neighborhood approach for quantifying interspecific competition in coastal Oregon forests. Ecol. Appl. 8, 779–794.

Wang, X., Comita, L.S., Hao, Z., Davies, S.J., Ye, J., Lin, F., Yuan, Z., 2012. Local-scale drivers of tree survival in a temperate forest. PLoS One 7, 22–28.

Ward, J.S., Parker, G.R., Ferrandino, F.J., 1996. Long-term spatial dynamics in an old-growth deciduous forest. For. Ecol. Manage. 83, 189–202.

Waring, R.H., Franklin, J.F., 1979. Evergreen coniferous forests of the Pacific Northwest. Science 204, 1380–1386.

Watkinson, A.R., Lonsdale, W.M., Firbank, L.G., 1983. A neighbourhood approach to self-thinning. Oecologia 56, 381–384.

Weiner, J., 1984. Neighbourhood interference amongst Pinus rigida individuals. J. Ecol. 72, 183–195.

Whitmore, T.C., 1989. Canopy gaps and the two major groups of forest trees. Ecology 70, 536–538.

Wiegand, T., Gunatilleke, S., Gunatilleke, N., 2007. Species associations in a heterogeneous Sri Lankan dipterocarp forest. Am. Nat. 170, 77–95.

Wiegand, T., Moloney, K.A., 2004. Rings, circles, and null models for point pattern analysis in ecology. Oikos 104, 209–229.

Wimberly, M.C., Bare, B.B., 1996. Distance-dependent and distance-independent models of Douglas-fir and western hemlock basal area growth following silvicultural treatment. For. Ecol. Manage. 89, 1–11.

Wimberly, M.C., Spies, T.A., 2001. Modeling landscape patterns of understory tree regeneration in the Pacific Northwest, USA. Appl. Veg. Sci. 4, 277–286.

Wykoff, W.R., Crookston, N.L., Stage, A.R., 1982. User's guide to the stand prognosis model. Gen. Tech. Report, Intermt. For. Range Exp. Station. USDA For. Serv. 112.

Yang, Y., Titus, S.J., Huang, S., 2003. Modeling individual tree mortality for white spruce in Alberta. Ecol. Modell. 163, 209–222.

Yao, X., Titus, S.J., MacDonald, S.E., 2001. A generalized logistic model of individual tree mortality for aspen, white spruce, and lodgepole pine in Alberta mixedwood forests. Can. J. For. Res. 31, 283–291.

Zhang, Q. Bin, Hebda, R.J., 2004. Variation in radial growth patterns of Pseudotsuga menziesii on the central coast of British Columbia, Canada. Can. J. For. Res. 34, 1946–1954.

Appendices

Appendix A. Univariate analysis of the spatial patterns for all live trees.

Patterns for all species pooled (a-e), Douglas fir (f-j), western hemlock (k-m), and redcedar (n-p). Black line shows observed result for 2014 and dashed line for 1998. Light grey area shows 95% confidence envelope for CSR in 2014 and dark grey for 1998, with results above (below) the envelope indicating aggregation (regularity).

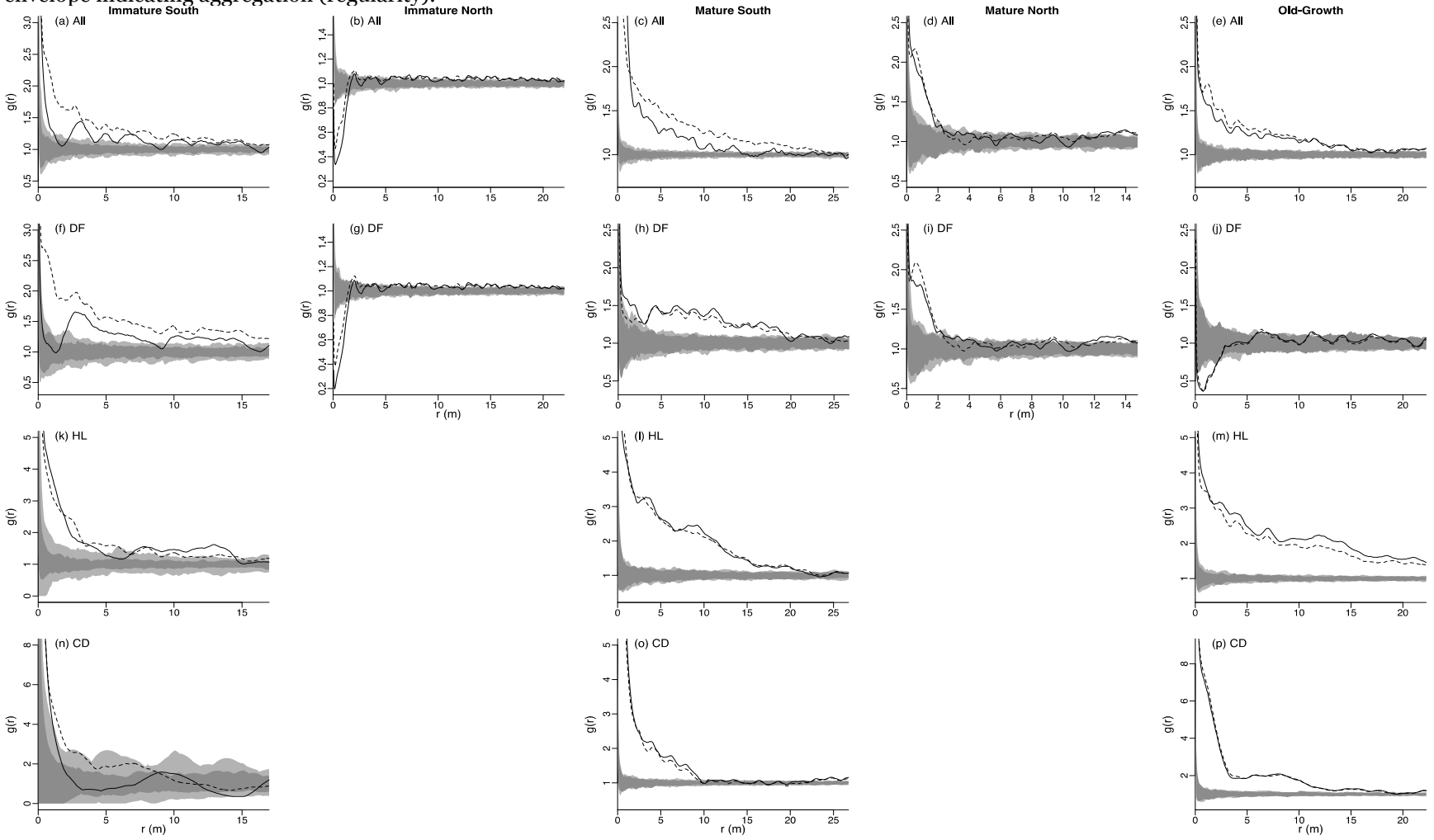

Appendix B. Univariate analysis of random recruitment.

Recruitment pattern for all species pooled (a-e), western redcedar (f-i), western hemlock (j-l), Douglas fir (m,o), and all other species (n) compared to random recruitment under complete spatial randomness. Black line shows observed results and grey area shows 95% confidence envelope for CSR, with results above (below) the envelope indicating aggregation (regularity).

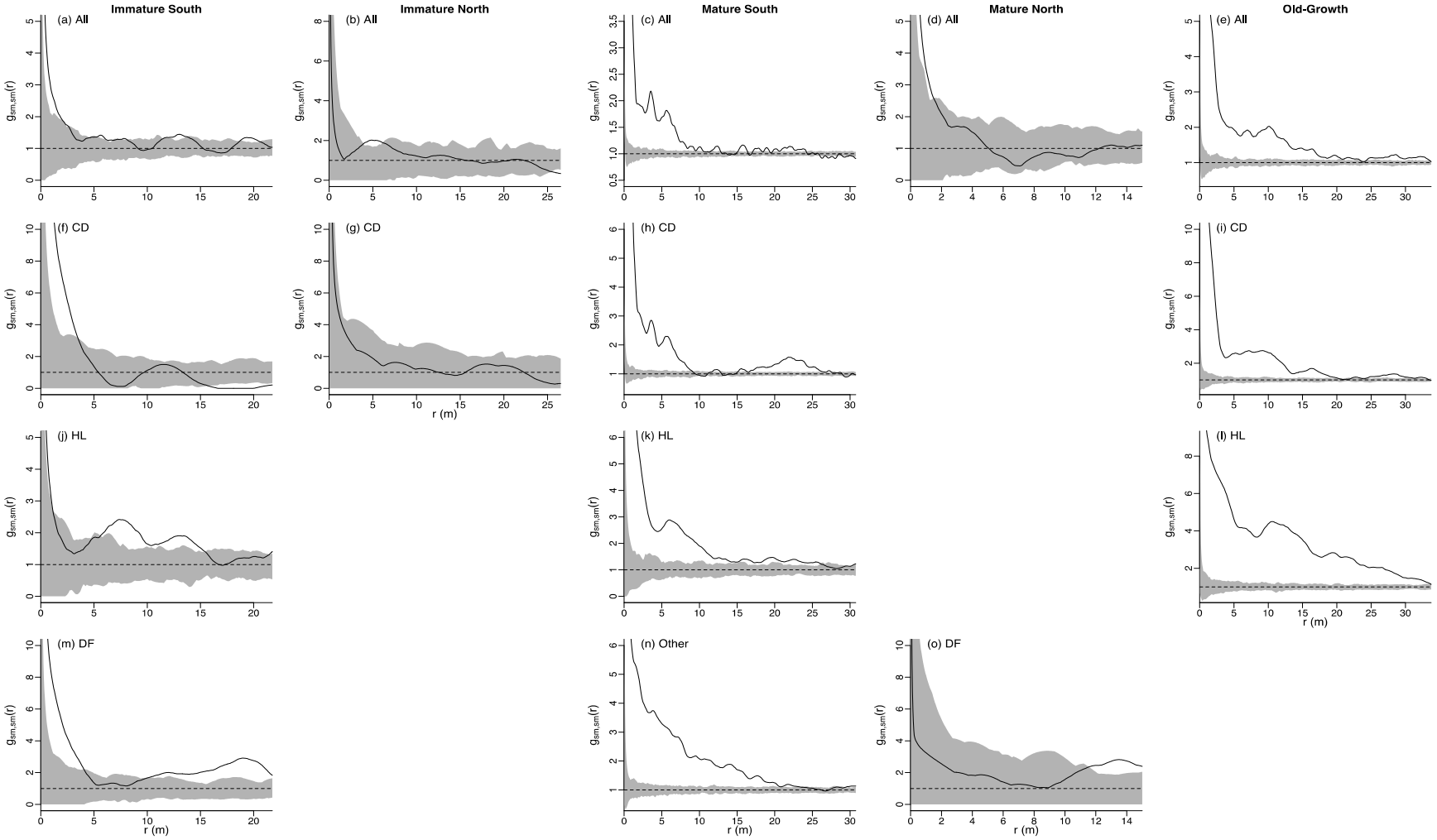

Appendix C. Reversed bivariate associations between dominant species pairs.

Interaction between species hemlock-Douglas fir (a-e), redcedar-Douglas fir (f-j), and redcedar-hemlock (k-m) to test for asymmetric interactions between species pairs. Black line shows observed result and the grey area shows 95% confidence envelope under the toroidal shift null model. Observed results above (below) simulation envelope shows positive (negative) spatial associations.

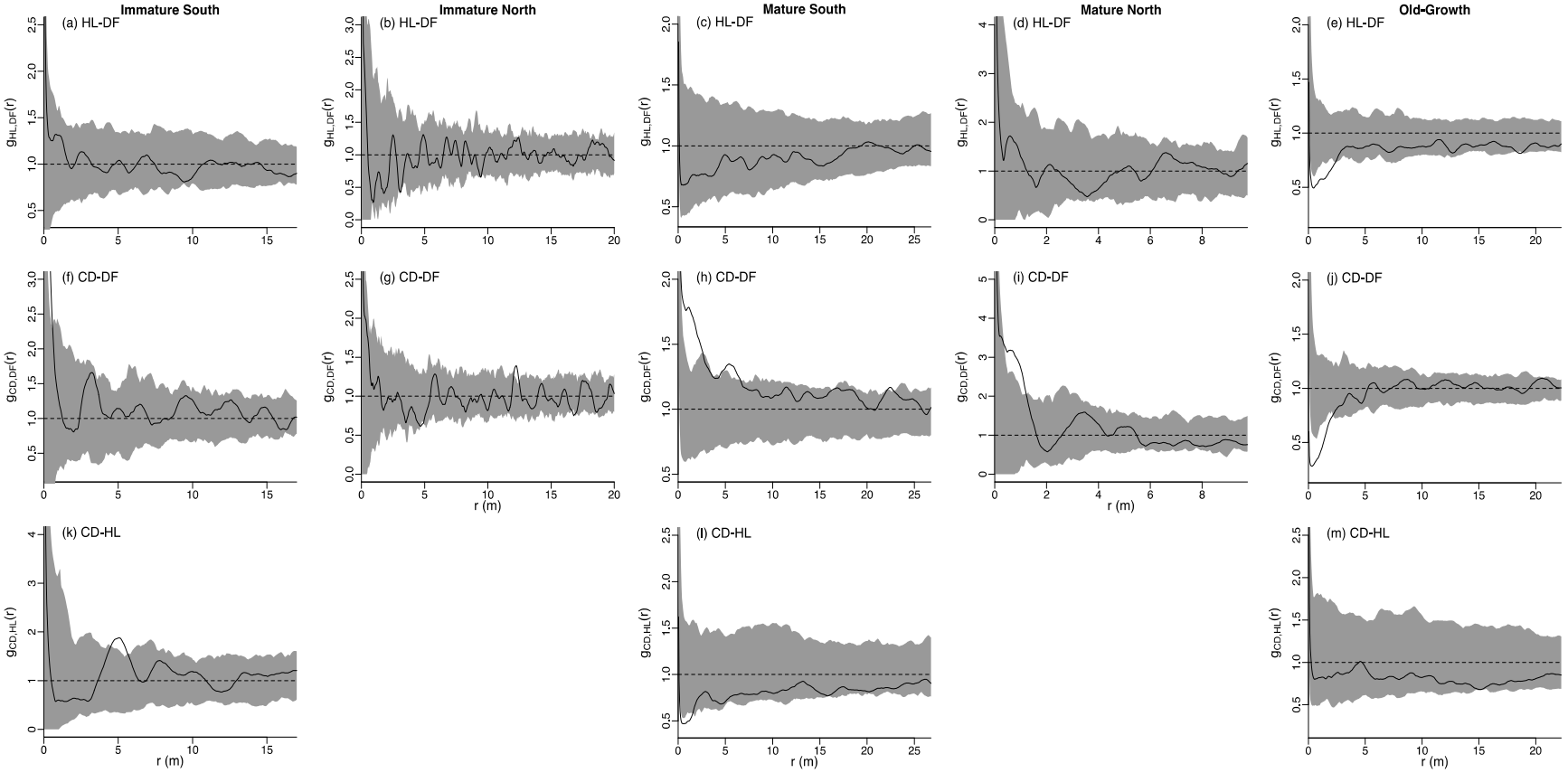

Appendix D. Optimum neighbourhood radius selection for competition indices.

AIC value for each competition index against neighbourhood radius for immature (a), mature (b), and old-growth (c). Vertical dotted line indicates selected optimum radius.

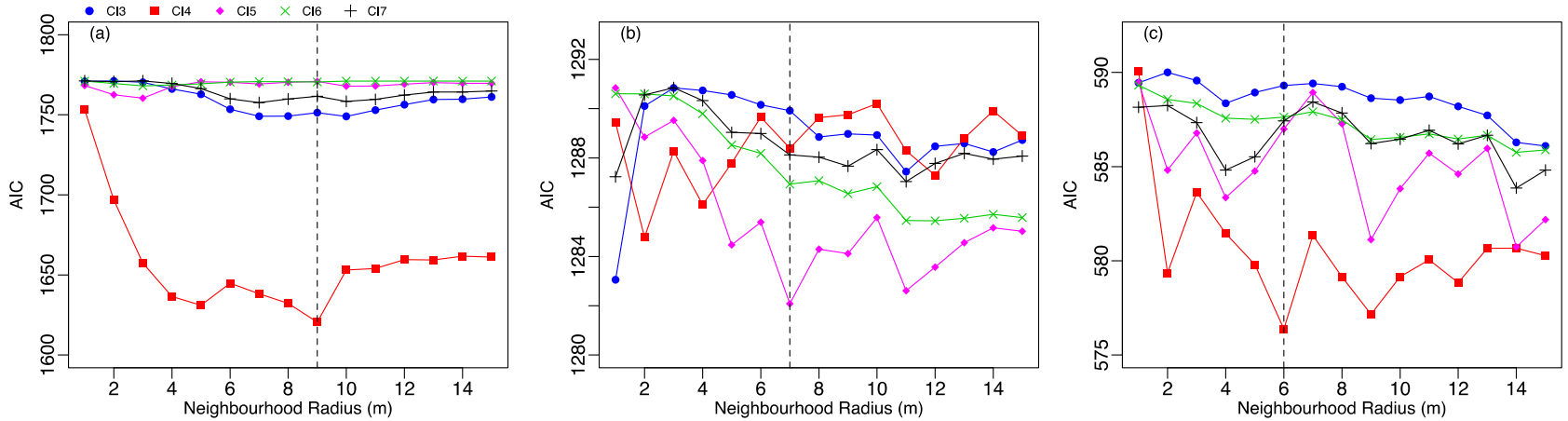

Figure D1. Douglas fir competition radius selection based on AIC values across increasing neighbourhood radii.

Appendix D continued.

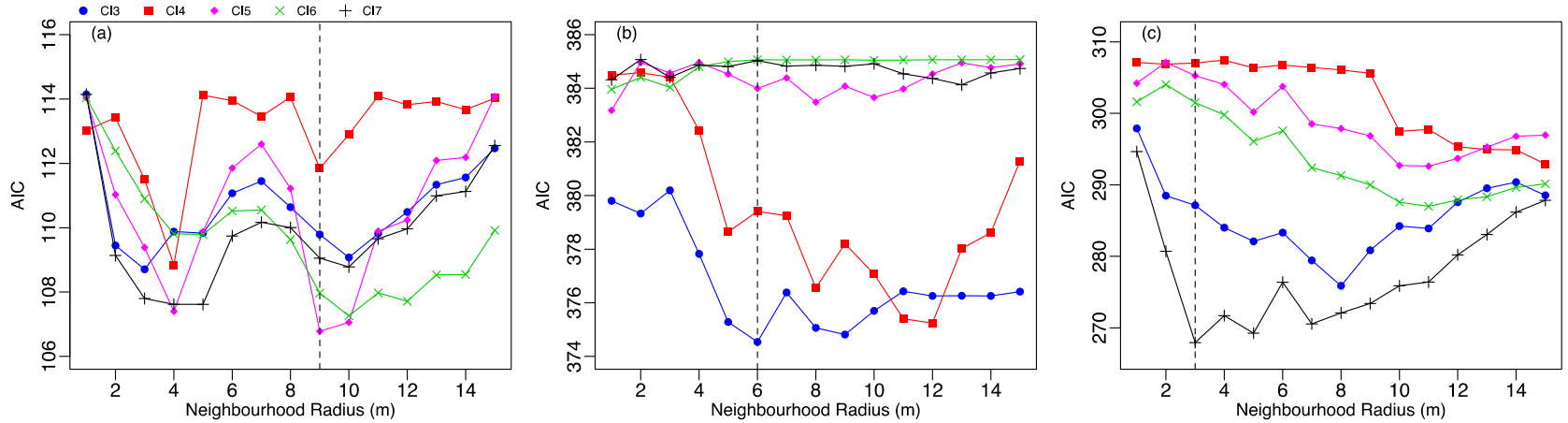

Figure D2. Western hemlock competition radius selection based on AIC values across increasing neighbourhood radii.

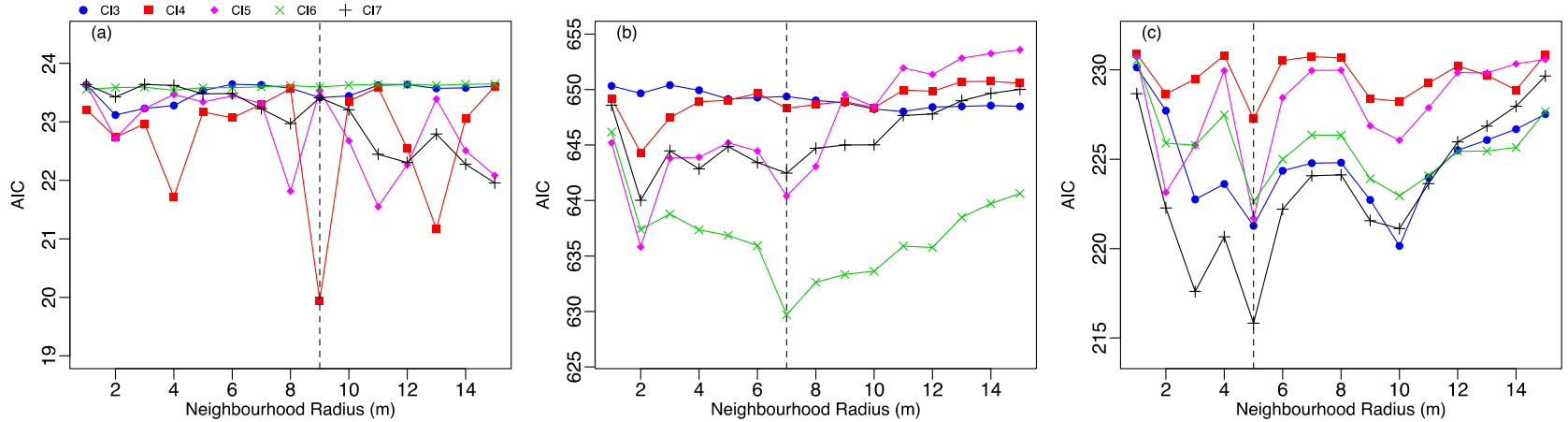

Figure D3. Western redcedar competition radius selection based on AIC values across increasing neighbourhood radii.

Appendix E. Top competition-growth models for each competition index.

Models were selected based on lowest AIC value. Model equations are shown in Table 3.4. Competition index (CI) formulas are shown in Table 3.2.

Table E1. Comparison of top Douglas fir competition-growth models for each competition index.

Stand age	Model no.	CI no.	CI	AIC	ΔAIC
Immature	[M5]	CI4	Basal area of larger trees	1617.21	0
	[M7]	CI2	Nearest Neighbour BA	1745.43	128.22
	[M9]	CI3	Density	1747.44	130.23
	[M5]	CI6	DBH-Dist. Ratio	1759.48	142.27
	[M5]	CI5	Sum DBH	1767.01	149.80
	[M7]	CI7	Horizontal Angle Sum	1767.35	150.14
	[M5]	CI1	Nearest Neighbour Dist.	1767.37	150.16
Stand age	**Model no.**	**CI no.**	**CI**	**AIC**	**ΔAIC**
Mature	[M6]	CI5	Sum DBH	1282.70	0
	[M8]	CI6	DBH-Dist. Ratio	1286.57	3.87
	[M4]	CI3	Density	1287.27	4.57
	[M4]	CI7	Horizontal Angle Sum	1287.31	4.61
	[M3]	CI4	Basal area of larger trees	1288.39	5.69
	[M4]	CI1	Nearest Neighbour Dist.	1288.89	6.19
	[M3]	CI2	Nearest Neighbour BA	1290.69	7.99
Stand age	**Model no.**	**CI no.**	**CI**	**AIC**	**ΔAIC**
Old-growth	[M2]	CI4	Basal area of larger trees	576.38	0
	[M11]	CI6	DBH-Dist. Ratio	584.30	7.92
	[M9]	CI1	Nearest Neighbour Dist.	586.71	10.33
	[M5]	CI5	Sum DBH	586.91	10.52
	[M5]	CI7	Horizontal Angle Sum	587.32	10.94
	[M9]	CI2	Nearest Neighbour BA	587.45	11.07
	[M5]	CI3	Density	589.24	12.86

Appendix E continued.

Table E2. Comparison of top western hemlock competition-growth models for each competition index.

Stand age	Model no.	CI no.	CI	AIC	ΔAIC
Immature	[M2]	CI5	Sum DBH	106.78	0
	[M5]	CI6	DBH-Dist. Ratio	106.78	0.01
	[M5]	CI7	Horizontal Angle Sum	107.90	1.12
	[M5]	CI3	Density	108.70	1.92
	[M7]	CI4	Basal area of larger trees	110.02	3.24
	[M7]	CI1	Nearest Neighbour Dist.	110.92	4.14
	[M7]	CI2	Nearest Neighbour BA	111.67	4.90
Stand age	**Model no.**	**CI no.**	**CI**	**AIC**	**ΔAIC**
Mature	[M9]	CI2	Nearest Neighbour BA	352.68	0
	[M5]	CI3	Density	374.24	21.56
	[M2]	CI4	Basal area of larger trees	379.41	26.73
	[M9]	CI1	Nearest Neighbour Dist.	383.15	30.47
	[M4]	CI5	Sum DBH	383.93	31.25
	[M2]	CI7	Horizontal Angle Sum	385.04	32.36
	[M4]	CI6	DBH-Dist. Ratio	385.06	32.38
Stand age	**Model no.**	**CI no.**	**CI**	**AIC**	**ΔAIC**
Old-growth	[M2]	CI7	Horizontal Angle Sum	269.04	0
	[M3]	CI3	Density	287.14	18.11
	[M3]	CI1	Nearest Neighbour Dist.	287.26	18.23
	[M3]	CI6	DBH-Dist. Ratio	301.50	32.46
	[M5]	CI2	Nearest Neighbour BA	301.84	32.80
	[M7]	CI5	Sum DBH	305.20	36.17
	[M7]	CI4	Basal area of larger trees	306.91	37.88

Appendix E continued.

Table E3. Comparison of top western redcedar competition-growth models for each competition index.

Stand age	Model no.	CI no.	CI	AIC	ΔAIC
Immature	[M11]	CI2	Nearest Neighbour BA	17.39	0
	[M12]	CI4	Basal area of larger trees	19.55	2.16
	[M12]	CI3	Density	22.81	5.42
	[M12]	CI1	Nearest Neighbour Dist.	23.11	5.73
	[M6]	CI7	Horizontal Angle Sum	23.22	5.84
	[M11]	CI5	Sum DBH	23.30	5.91
	[M11]	CI6	DBH-Dist. Ratio	23.32	5.94
Stand age	**Model no.**	**CI no.**	**CI**	**AIC**	**ΔAIC**
Mature	[M7]	CI6	DBH-Dist. Ratio	634.79	0
	[M7]	CI2	Nearest Neighbour BA	642.51	7.72
	[M2]	CI7	Horizontal Angle Sum	645.95	11.16
	[M7]	CI5	Sum DBH	646.54	11.75
	[M7]	CI1	Nearest Neighbour Dist.	649.52	14.73
	[M3]	CI3	Density	650.32	15.53
	[M3]	CI4	Basal area of larger trees	650.85	16.06
Stand age	**Model no.**	**CI no.**	**CI**	**AIC**	**ΔAIC**
Old-growth	[M3]	CI7	Horizontal Angle Sum	215.83	0
	[M9]	CI3	Density	218.54	2.71
	[M7]	CI5	Sum DBH	221.23	5.41
	[M7]	CI6	DBH-Dist. Ratio	221.75	5.93
	[M7]	CI1	Nearest Neighbour Dist.	225.94	10.11
	[M7]	CI4	Basal area of larger trees	226.49	10.66
	[M5]	CI2	Nearest Neighbour BA	229.31	13.49

Appendix F. Residual plots for final growth-climate models for each stand age.

Normalized residuals plotted against fitted values showing goodness of fit of growth-climate models for immature (left), mature (centre), and old-growth (right) stands. Plots are shown for Douglas fir (a-c), western hemlock (d-f), and western redcedar (g-i).

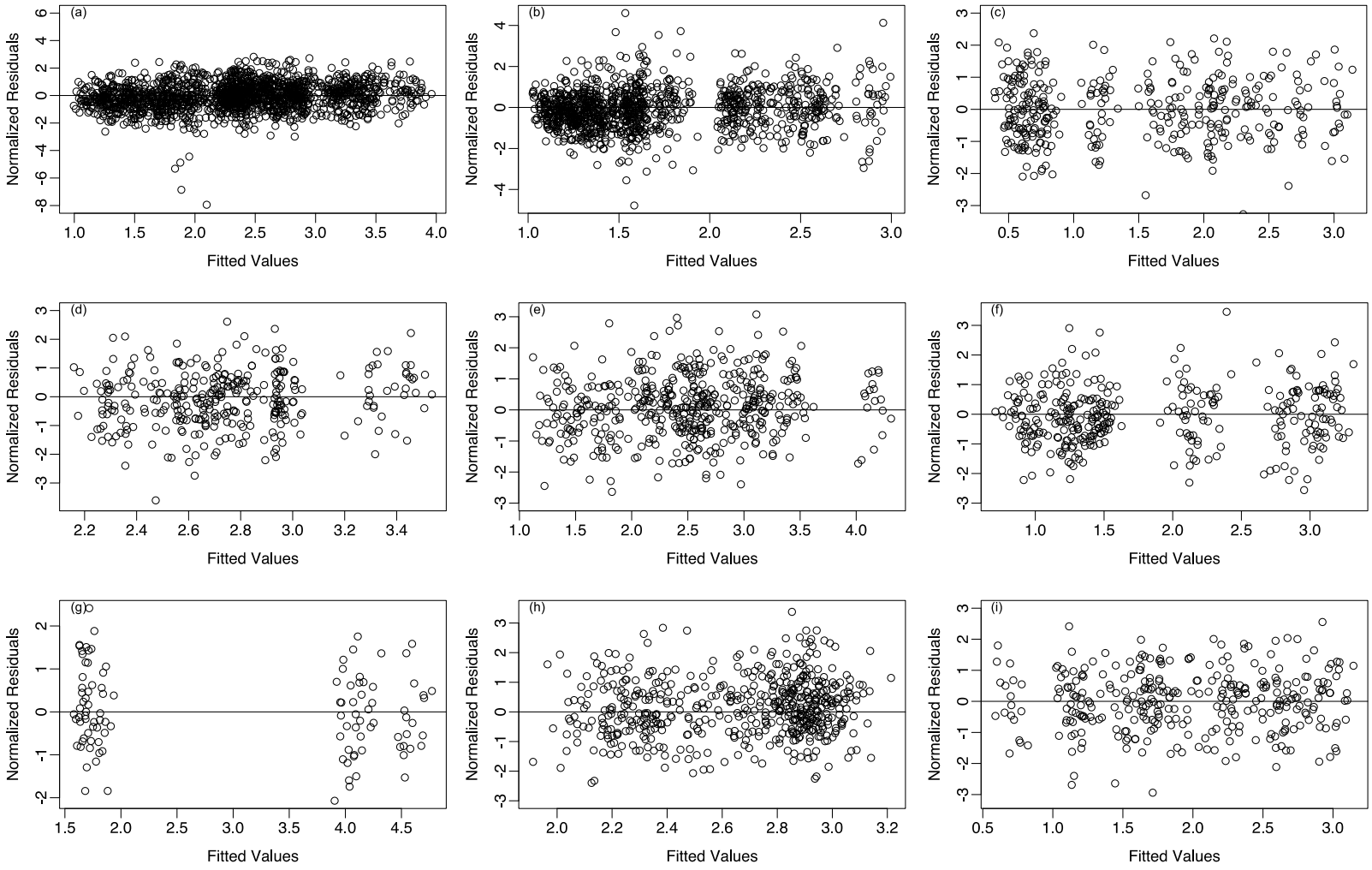

Appendix G. Probability curves and Hosmer-Lemeshow tables for morality models.

Competition (left) and tree size (right) probability curves for immature (a, b), mature (c, d), and old-growth (e, f) models and corresponding table results from Hosmer-Lemeshow goodness-of-fit test.

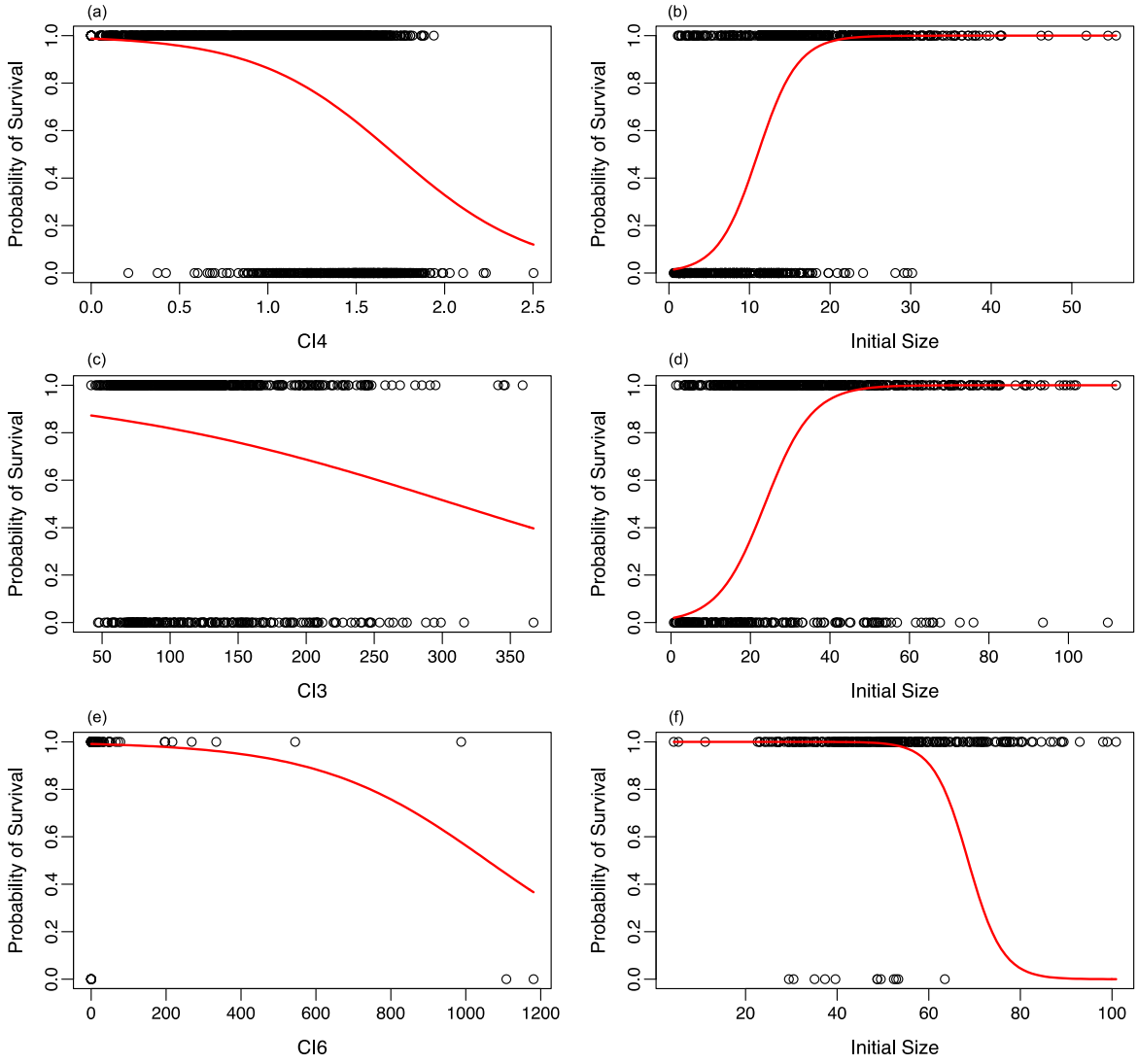

Figure G1. Douglas fir probability curves for mortality models.

Competition (left) and tree size (right) probability curves for immature (a, b), mature (c, d), and old-growth (e, f) models.

Appendix G continued.

Table G1. Hosmer-Lemeshow goodness-of-fit test for Douglas fir mortality models.

			No. dead trees		
Age	**Group**	**No. trees**	**Observed**	**Expected**	**Difference**
Immature	1	207	194	196	-2
	2	206	168	164	4
	3	206	127	120	7
	4	206	78	79	-1
	5	206	43	50	-7
	6	206	23	27	-4
	7	206	9	13	-4
	8	206	8	6	2
	9	206	5	2	3
	10	206	2	1	1
	Total	2061	657	657	
Age	**Group**	**No. trees**	**Observed**	**Expected**	**Difference**
Mature	1	82	56	57	-1
	2	81	57	46	11
	3	81	28	35	-7
	4	81	26	26	0
	5	82	12	20	-8
	6	81	17	13	4
	7	81	11	9	2
	8	81	7	7	0
	9	81	7	4	3
	10	82	0	2	-2
	Total	813	221	221	
Age	**Group**	**No. trees**	**Observed**	**Expected**	**Difference**
Old-growth	1	34	8	8	0
	2	34	1	2	-1
	3	33	0	1	-1
	4	34	1	1	0
	5	33	1	0	1
	6	34	0	0	0
	7	33	1	0	1
	8	34	0	0	0
	9	33	0	0	0
	10	34	0	0	0
	Total	336	12	12	

Hosmer-Lemeshow statistic = 12.5 (p=0.13) for immature, 17.3 (p=0.027) for mature, and 4.9 (p=0.77) for old-growth models with 8 df.

Appendix G continued.

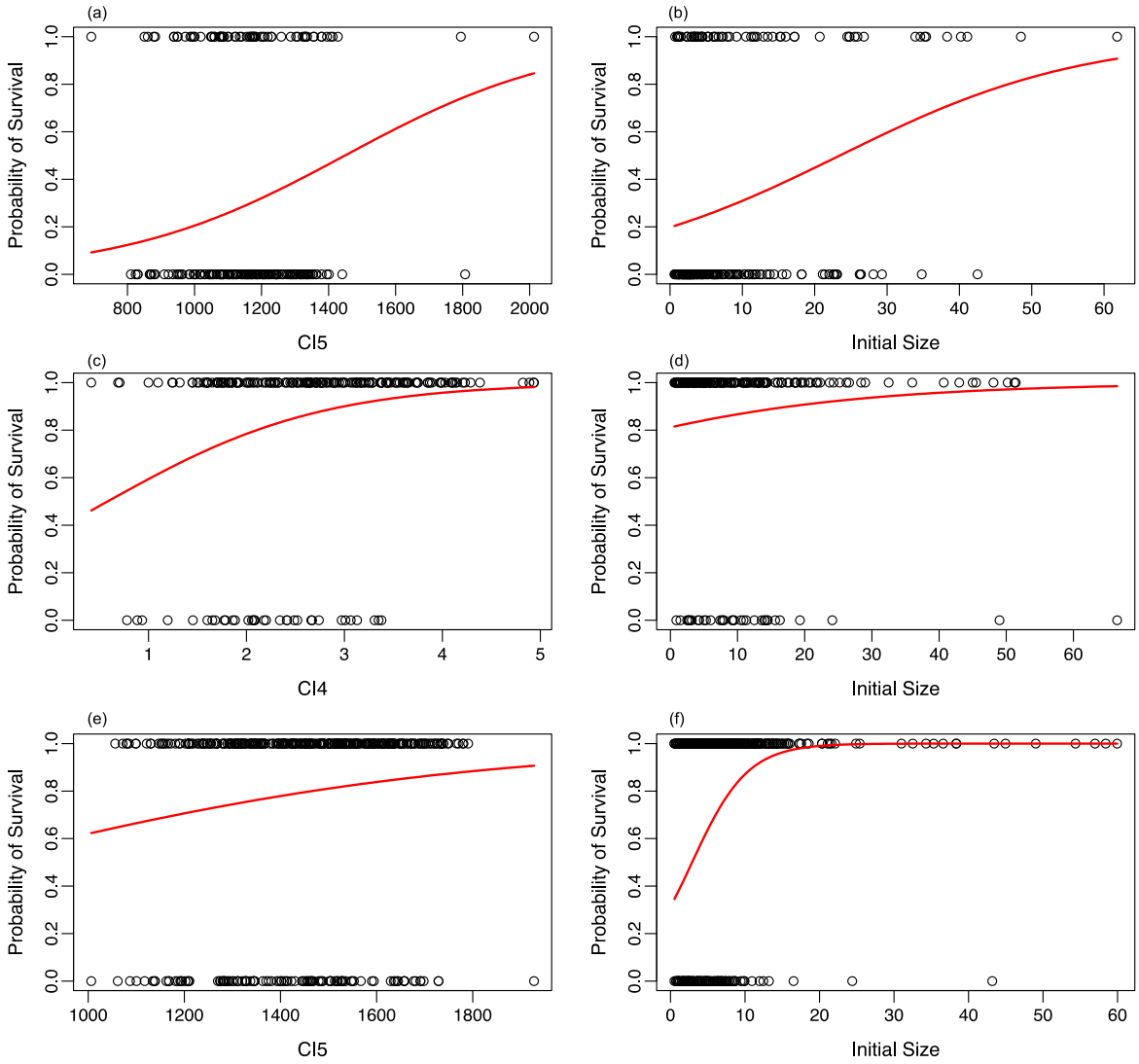

Figure G2. Western hemlock probability curves for mortality models.
Competition (left) and tree size (right) probability curves for immature (a, b), mature (c, d), and old-growth (e, f) models.

Appendix G continued.

Table G2. Hosmer-Lemeshow goodness-of-fit test for Western hemlock mortality models.

			No. dead trees		
Age	**Group**	**No. trees**	**Observed**	**Expected**	**Difference**
Immature	1	23	20	20	0
	2	22	18	18	0
	3	22	17	17	0
	4	22	19	17	2
	5	22	16	16	0
	6	22	14	16	-2
	7	22	15	15	0
	8	22	16	14	2
	9	22	12	13	-1
	10	23	7	8	-1
	Total	222	154	154	
Age	**Group**	**No. trees**	**Observed**	**Expected**	**Difference**
Mature	1	22	6	8	-2
	2	22	7	6	1
	3	22	4	5	-1
	4	22	5	4	1
	5	22	3	3	0
	6	22	3	3	0
	7	22	4	2	2
	8	22	2	2	0
	9	22	0	1	-1
	10	22	0	1	-1
	Total	220	34	34	
Age	**Group**	**No. trees**	**Observed**	**Expected**	**Difference**
Old-growth	1	44	30	27	3
	2	43	19	19	0
	3	44	14	15	-1
	4	43	14	12	2
	5	44	10	11	-1
	6	43	5	8	-3
	7	43	7	7	0
	8	44	4	5	-1
	9	43	4	3	1
	10	44	3	1	2
	Total	435	110	110	

Hosmer-Lemeshow statistics = 2.9 (p=0.94) for immature, 5.3 (p=0.73) for mature, and 5.3 (p=0.73) for old-growth models with 8 df.

Appendix G continued.

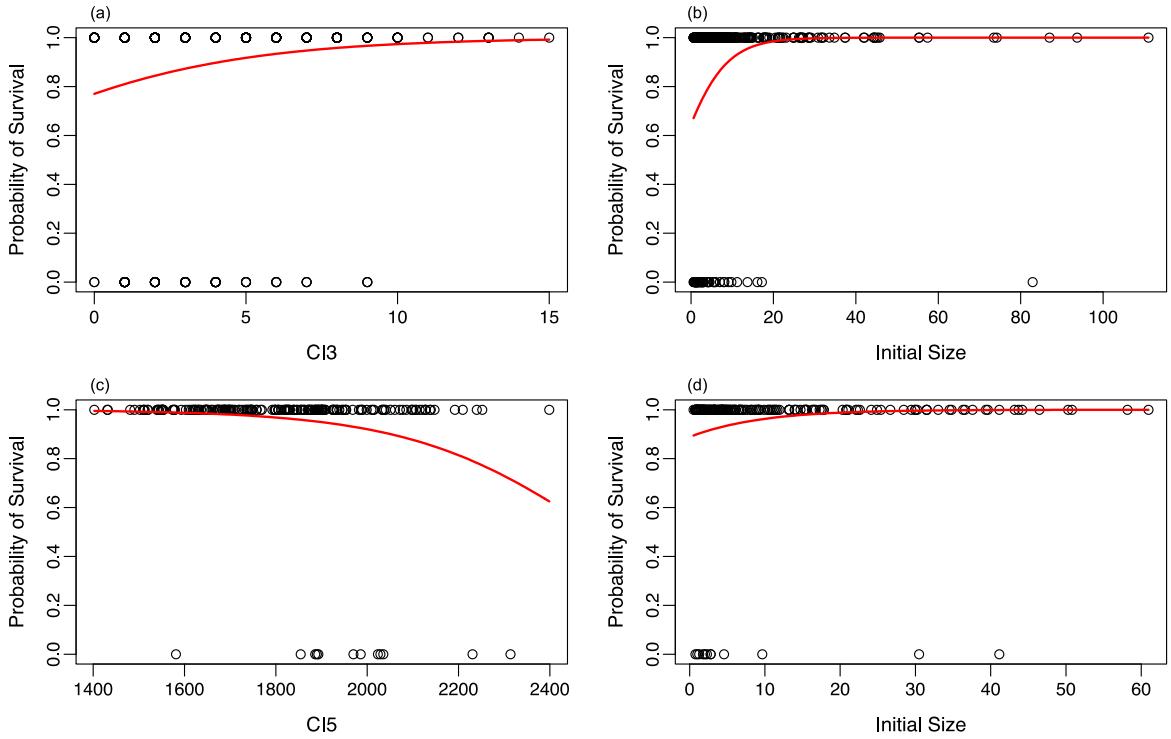

Figure G3. Western redcedar probability curves for mortality models. Competition (left) and tree size (right) probability curves for immature (a, b), mature (c, d), and old-growth (e, f) models.

Appendix G continued.

Table G3. Hosmer-Lemeshow goodness-of-fit test for Western redcedar mortality models.

			No. dead trees		
Age	**Group**	**No. trees**	**Observed**	**Expected**	**Difference**
Mature	1	45	12	14	-2
	2	44	18	11	7
	3	44	6	9	-3
	4	44	8	7	1
	5	45	7	6	1
	6	44	2	5	-3
	7	44	4	4	0
	8	44	3	3	0
	9	44	1	2	-1
	10	45	1	1	0
	Total	443	62	62	
Age	**Group**	**No. trees**	**Observed**	**Expected**	**Difference**
Old-growth	1	22	6	5	1
	2	21	1	2	-1
	3	21	1	1	0
	4	22	2	1	1
	5	21	0	1	-1
	6	21	0	1	-1
	7	22	2	0	2
	8	21	0	0	0
	9	21	0	0	0
	10	22	0	0	0
	Total	214	12	12	

Hosmer-Lemeshow statistic = 9.7 (p=0.29) for mature and 9.0 (p=0.35) old-growth models with 8 df.

Appendix H. Top mortality models for each competition index.

Models were selected based on AIC and R^2 values. Competition index (CI) formulas are shown in Table 3.2.

Table H1. Comparison of top Douglas fir mortality models for each competition index.

Stand age	CI no.	CI	Radius	AUC	R^2	AIC	ΔAIC
Immature	CI4	BAL	11	0.915	0.609	1416.53	0
	CI3	Density	13	0.913	0.591	1461.38	44.85
	CI5	Sum DBH	1	0.911	0.587	1471.27	54.74
	CI7	Horiz. Angle Sum	7	0.912	0.587	1471.77	55.23
	CI1	NN Dist.	-	0.911	0.587	1472.24	55.70
	CI6	DBH-Dist. Ratio	1	0.911	0.586	1475.49	58.96
	CI2	NN BA	-	0.910	0.587	1476.09	59.55
Stand age	**CI no.**	**CI**	**Radius**	**AUC**	**R^2**	**AIC**	**ΔAIC**
Mature	CI3	Density	15	0.810	0.329	753.76	0
	CI1	NN Dist.	-	0.800	0.314	765.12	11.37
	CI4	BAL	1	0.799	0.314	765.17	11.41
	CI5	Sum DBH	1	0.799	0.313	765.69	11.94
	CI6	DBH-Dist. Ratio	1	0.799	0.312	766.65	12.90
	CI2	NN BA	-	0.798	0.314	767.43	13.68
	CI7	Horiz. Angle Sum	1	0.798	0.310	767.50	13.74
Stand age	**CI no.**	**CI**	**Radius**	**AUC**	**R^2**	**AIC**	**ΔAIC**
Old-growth	CI6	DBH-Dist. Ratio	1	0.855	0.315	86.23	0
	CI5	Sum DBH	7	0.863	0.242	93.25	7.02
	CI7	Horiz. Angle Sum	7	0.856	0.241	93.33	7.10
	CI3	Density	3	0.858	0.226	94.73	8.50
	CI2	NN BA	-	0.809	0.199	95.43	9.20
	CI4	BAL	2	0.823	0.213	96.00	9.76
	CI1	NN Dist.	-	0.811	0.199	97.33	11.10

Appendix H continued.

Table H2. Comparison of top western hemlock mortality models for each competition index.

Stand age	CI no.	CI	Radius	AUC	R^2	AIC	ΔAIC
Immature	CI5	Sum DBH	14	0.686	0.140	262.40	0
	CI4	BAL	7	0.698	0.130	264.16	1.76
	CI7	Horiz. Angle Sum	14	0.662	0.116	266.52	4.11
	CI3	Density	1	0.655	0.104	268.62	6.21
	CI6	DBH-Dist. Ratio	1	0.656	0.103	268.74	6.34
	CI2	NN BA	-	0.660	0.103	268.78	6.37
	CI1	NN Dist.	-	0.660	0.103	268.79	6.39
Stand age	**CI no.**	**CI**	**Radius**	**AUC**	**R^2**	**AIC**	**ΔAIC**
Mature	CI4	BAL	12	0.698	0.110	186.93	0
	CI5	Sum DBH	12	0.649	0.058	193.99	7.06
	CI3	Density	2	0.604	0.045	195.63	8.70
	CI6	DBH-Dist. Ratio	12	0.612	0.034	197.08	10.15
	CI7	Horiz. Angle Sum	1	0.594	0.027	198.02	11.09
	CI1	NN Dist.	-	0.559	0.025	198.22	11.29
	CI2	NN BA	-	0.568	0.025	198.36	11.43
Stand age	**CI no.**	**CI**	**Radius**	**AUC**	**R^2**	**AIC**	**ΔAIC**
Old-growth	CI5	Sum DBH	13	0.759	0.219	434.02	0
	CI3	Density	1	0.757	0.213	436.36	2.34
	CI7	Horiz. Angle Sum	13	0.756	0.210	437.23	3.22
	CI4	BAL	4	0.753	0.210	437.27	3.25
	CI6	DBH-Dist. Ratio	1	0.748	0.202	440.06	6.04
	CI2	NN BA	-	0.748	0.000	440.21	6.20
	CI1	NN Dist.	-	0.748	0.201	440.37	6.35

Table H3. Comparison of top western redcedar mortality models for each competition index.

Stand age	CI no.	CI	Radius	AUC	R^2	AIC	ΔAIC
Mature	CI3	Density	2	0.733	0.136	335.96	0
	CI4	BAL	3	0.707	0.106	343.94	7.98
	CI6	DBH-Dist. Ratio	10	0.701	0.100	345.48	9.52
	CI5	Sum DBH	3	0.696	0.096	346.50	10.55
	CI7	Horiz. Angle Sum	1	0.683	0.090	348.05	12.09
	CI1	NN Dist.	-	0.684	0.080	350.68	14.73
	CI2	NN BA	-	0.670	0.080	352.82	16.87
Stand age	**CI no.**	**CI**	**Radius**	**AUC**	**R^2**	**AIC**	**ΔAIC**
Old-growth	CI5	Sum DBH	15	0.793	0.173	91.04	0
	CI7	Horiz. Angle Sum	15	0.804	0.164	91.76	0.72
	CI4	BAL	15	0.778	0.156	92.39	1.34
	CI6	DBH-Dist. Ratio	15	0.770	0.126	94.78	3.74
	CI3	Density	6	0.758	0.116	95.58	4.54
	CI1	NN Dist.	-	0.663	0.063	99.68	8.64
	CI2	NN BA	-	0.669	0.063	99.95	8.91